universität wien

DISSERTATION

Titel der Dissertation

Molecular and structural requirements for kinetochore assembly in *Saccharomyces cerevisiae*

Verfasser

Peter Hornung, M.Sc.

Angestrebter akademischer Grad

Doktor der Naturwissenschaften (Dr. rer. nat)

Wien, 2012

Studienkennzahl lt. Studienblatt:	A 091 490
Dissertationsgebiet lt. Studienblatt:	Molekulare Biologie
Betreuer:	Dr. Stefan Westermann

TABLE OF CONTENTS

1 Abstract

All eukaryotic cells have developed complex mechanisms to ensure the transmission of genetic material over many generations. One important module in this elaborated system is the kinetochore, a large multi-protein complex that links the chromosomes to the mitotic spindle. Specialized chromosomal domains termed centromeres direct kinetochore assembly to build up a microtubule attachment site. The building plan of kinetochores is likely universal and the conserved KMN network, including the protein complexes KNL-1, Mis12 and Ndc80, plays a central role in the attachment of the spindle microtubules. A second multi-protein structure is the constitutive centromere associated network (CCAN) that is required to recruit the KMN network.

In this work, I used biochemical reconstitution experiments and genetic analysis to elucidate the protein connectivity of the kinetochore-microtubule interface in *Saccharomyces cerevisiae* (*S. cerevisiae* or budding yeast) revealing a distinct pathway by which the KMN network is linked to the centromere. First, I started with the biochemical reconstitution of the Mtw1 complex, the homolog of the human Mis12 complex and an essential part of the KMN network. The four-protein complex reconstituted from the two stable heterodimers Mtw1-Nnf1 and Dsn1-Nsl1. Direct visualization by electron microscopy revealed an elongated structure with an approximate length of 25 nm. I could demonstrate a direct interaction between the Mtw1 complex and the centromere proximal Spc24-Spc25 subunits of the microtubule binding Ndc80 complex. The Ndc80 complex alone exerted only moderate affinity for microtubules. Strikingly, in the presence of microtubules and the Dam1 complex, an important constituent of the budding yeast kinetochore-microtubule interface, the Ndc80 complex displayed a 10 fold higher microtubule affinity.

A central question is how the Mtw1 complex is recruited to the centromere. Data obtained in human cells and flies suggest a centromere recruitment of the Mis12 complex via the CCAN protein CENP-C. However, it is likely that more than one CCAN subunit anchors the KMN network. The homolog of the human CCAN is the *S. cerevisiae* protein complex Ctf19, but the biochemical functions of individual subunits have largely remained elusive. I have reconstituted a Ctf19 core complex, called COMA (consisting of Ctf19, Okp1, Mcm21, Ame1) and shown that it directly and stoichiometrically associates with the Mtw1 complex *in vitro*. Similar to the four-subunit Mtw1 complex, COMA consists of two stable heterodimers Ame1-Okp1 and Ctf19-Mcm21 and it also associates with the proteins Chl4 and Iml3. COMA directly contacts the Mtw1-Nnf1 heterodimer through a conserved motif present in the extreme N-terminus of the

CENP-U homolog Ame1. This motif is essential for viability and its deletion drastically reduces the levels of both Ame1 and Mtw1 at the kinetochore *in vivo*.

Together these results define a framework of biochemical interactions required to connect centromeric chromatin to microtubules and they identify important molecular determinants for kinetochore assembly.

2 Zusammenfassung

Alle eukaryotischen Zellen haben zur Übertragung des genetischen Materials komplexe Mechanismen entwickelt. Diese gewährleisten die Weitergabe des Genoms von Generation zu Generationen. Ein wichtiger Bestandteil in diesem System ist das Kinetochor. Es ist ein Multi-Protein Komplex, der auf einem speziellen DNA-Abschnitt, dem Centromer, assembliert und als Ansatzstelle für die Mikrotubuli des Spindelapparates dient. Das Centromere initiiert die Anordnung der ersten Proteinkomplexe auf der centromerischen DNA. Nach und nach wird so ein funktionelles Kinetochore aufgebaut. Der Bauplan für ein eukaryotisches Kinetochor ist universell und das KMN Netzwerk, das aus den Protein Komplexes Knl1, Mis12- und Ndc80 besteht, spielt eine zentrale Rolle um die Mikrotubuli an das Kinetochor zu binden. Ein zweites Proteinnetzwerk ist das Constitutive Centromere Associated Network (CCAN), welches zur Rekrutierung des KMN Netzwerkes benötigt wird.

In dieser Arbeit kläre ich teilweise die Protein Konnektivität an der Mikrotubulus-Kinetochor Schnittstelle der Bäckerhefe (*Saccharomyces cerevisiae*) auf und ich zeige auch wie das KMN Netzwerk mit dem Centromer assoziiert ist. Als erstes begann ich mit der biochemischen Rekonstitution des Mtw1 Komplexes, der das Homolog zum Mis12 Komplex darstellt und ein essentieller Bestandteil des KMN Netzwerkes ist. Der Komplex setzt sich aus den zwei stabilen Heterodimeren Mtw1-Nnf1 und Dsn1-Nsl1 zusammen. Die direkte Veranschaulichung des rekombinanten Mtw1 Komplex mit dem Elektronen Mikroskop zeigte eine elongierte Struktur mit einer durchschnittlichen Länge von 25 nm. In weiteren Experimenten konnte ich nachweisen, dass die Interaktion zwischen dem Mikrotubuli Bindekomplex Ndc80 und dem Mtw1 Komplex auch in der Bäckerhefe konserviert ist und diese durch die Centromer proximalen Spc24-Spc25 Untereinheiten des Ndc80 Komplex geschieht. Der Ndc80 Komplex zeigte nur eine mäßige Mikrotubuli Bindungsaktivität. Jedoch unter der Zugabe des weiteren Mikrotubuli-Bindungskomplex Dam1, der ein wichtiger Bestandteil des äußeren Kinetochor ist, erhöhte sich die Ndc80 Komplex Mikrotubuli-Affinität um das zehn fache.

Eine zentrale Frage ist wie der Mtw1 Komplex an das Centromere rekrutiert wird. In humanen Zellen und auch in Fliegen haben Daten suggeriert, dass CENP-C ein CCAN Protein, den Mis12 Komplex rekrutiert. Jedoch ist es wahrscheinlich, dass mehr als eine CCAN Untereinheit das KMN Netzwerk an das Centromere verankert. Das Homolog zum CCAN in der Bäckerhefe ist der Ctf19 Komplex, dessen Funktion zum größten Teil ungeklärt ist. In Bezug dessen habe ich einen Teil des Ctf19 Komplex rekonstituiert, den COMA Komplex. Dieser besteht aus den

Untereinheiten Ctf19, Okp1, Mcm21, Ame1 und wie ich *in vitro* zeigen konnte direkt mit dem Mtw1 Komplex assoziiert. Ähnlich wie für den vier Untereinheiten Komplex Mtw1 unterteilt sich der COMA in zwei Heterodimere Ame1-Okp1 und Ctf19-Mcm21 und desweiteren assoziiert er mit den zwei zusätzlichen Untereinheiten Chl4 und Iml3. COMA kontaktiert direkt das Mtw1-Nnf1 Heterodimer über ein N-terminales Motiv des konservierten Proteins Ame1. Dieses Motiv ist wesentlich für die Viabilität der Bäckerhefe und seine Deletion reduziert drastisch die Level von Ame1 und Mtw1 Protein am Kinetochor *in vivo*. Meine Ergebnisse tragen wichtige Informationen zum generellen Kinetochor Aufbau bei und sie erklären möglicherweise auch die essentielle Funktion von Ame1 und Okp1 in der Bäckerhefe.

3 Introduction

3.1 The cell cycle

3.1.1 Mitosis - a magnificent stage of the cell cycle

Cell division is a hallmark of all living organisms. During this process vital steps are to precisely replicate and transmit the encoding genetic material to the new cell. Failure may lead to cell death, therefore the cell reproduction is under an accurate regulation and control mechanisms to allow the propagation over many generations.

3.1.2 The cell cycle of budding yeast

Saccharomyces cerevisiae is a simple, unicellular eukaryote carrying a fully defined genome. It can proliferate in a haploid state making it a valuable tool to study cell cycle genes with specific mutations without the complications arising from the presence of a second allele. Fundamental processes of the cell cycle are highly conserved among eukaryotes.

The individual steps of cell division are accurately regulated to timely ensure the correct order of stages. Based on the chromosomal events the cell cycle is divided into several stages, which in budding yeast are G_1-, S- and M phase. G_1 interrupts the cell cycle to provide the cell with additional time for growth and organization before it transits into the next cell cycle stage. In the presence of disadvantageous growth conditions the cell decides during G_1 weather it progresses or converts into a non-dividing state, called G_0. G_1 precedes S-phase in which the chromosomes are duplicated via replication. In the following M-Phase, called mitosis, the replicated chromosomes are partitioned between the mother and daughter nuclei. Before the cell cycle reenters into G_1, in the final stage of the cell cycle, termed cytokinesis, the cell divides its cytoplasmic components and two daughter cells emerge (Morgan, 2007).

3.1.3 The role of the kinetochore in Mitosis (M phase)

Mitosis is a process in all eukaryotic cells ensuring that each daughter cell inherits a complete set of chromosomes. In an early event of mitosis, the prophase, the chromosomes begin to

condense and the sister chromatids are securely linked by the cohesin protein complex that later allows a timely coordinated onset of chromosome segregation. Microtubules, a polymeric array of α and β tubulin dimers, emanate from spindle pole bodies and form a bipolar mitotic spindle. In the consecutive metaphase each sister chromatid is attached to the microtubule from opposing spindle poles at a specialized proteinaceous structure, the kinetochore, that assembles on centromeric DNA. Kinetochore-microtubule association develops step-wise. Initially, one of the two sister kinetochores interacts laterally with the microtubule, referred to as a side-on attachment. Subsequently, the association converts into an end-on attachment, meaning it is directly tethered to the tip of the microtubule plus end (Tanaka and Desai, 2008). Once each sister chromatid is attached to the opposite spindle pole in a bipolar orientation, tension can develop across sister kinetochores by the pulling forces of the microtubule. Once all kinetochores achieve biorientation, cohesin is dissolved via proteolytic cleavage of a cohesin subunit, microtubules depolymerize and the sister chromatids are pulled poleward during anaphase. Mitosis ends in telophase with the decondensation of chromosomes and the disassembly of the mitotic spindle. Hence, a functional kinetochore is crucial for faithful chromosome segregation. Defects in the kinetochore structure caused by mutations on its subunits may lead to kinetochore-microtubule detachment.

3.2 The kinetochore

In order to faithfully segregate chromosomes each sister chromatid must be attached to the mitotic spindle. The attachment is mediated by a supramolecular protein assembly, called the kinetochore. The kinetochore is not only a passive site of attachment, it is more a complex molecular machine that actively organizes and regulates a variety of proteins and thereby drives correct partitioning of genetic material between mother and daughter cell. Thus, the kinetochore is a multitasking entity during mitosis. Its primary function is to provide a physical linkage between the centromeric DNA and the spindle microtubule. One intriguing feature of the kinetochore is to spatially embed a dynamic microtubule into its protein meshwork, while remaining stably attached to the microtubule (Rieder and Salmon, 1998). Secondly, it not only accommodates the disassembling microtubule, it also influences its dynamics. Thirdly, it also hosts an elaborated surveillance system that signals to the spindle assembly checkpoint (SAC) to warn against the formation of aberrant kinetochore-microtubule attachments (Musacchio and Salmon, 2007).

Each sister kinetochore of budding yeast binds to one spindle microtubule, whereas kinetochores in higher eukaryotes, such as human, bind to 15-30 microtubules. Despite this higher complexity it is thought that each of the 15-30 KT-MT binding site is a repetition of a single budding yeast attachment unit, hence the underlying foundation in structure and regulation is proposed to be mainly conserved (Joglekar et al., 2008).

Budding yeast kinetochores contain roughly 60 proteins, 39 are organized into seven complexes – Ndc80-, CBF3-, Mtw1-, Spc105-, Ctf19-, Dam1-, CPC complex (Figure 1 B). With the exception of the CBF3- and Dam1 complex all other complexes and also their subcomplexes are conserved from yeast to human (Cheeseman and Desai, 2008; Westermann et al., 2007). A rough categorization divides the complexes of the kinetochore into two large networks: the KMN network (**K**nl1/**M**is12/**N**dc80) and the CCAN (**C**onstitutive **C**entromere **A**ssociated **N**etwork) (Figure 1 A, Table 1). In humans, members of the CCAN constitutively associate to the centromeric DNA throughout the cell cycle thereby forming a foundation for the association of the KMN members (Takeuchi and Fukagawa, 2012). Kinetochore proteins combine two major characteristics for coupling the chromosomes to the mitotic spindle. Firstly, some CCAN members as CENP-C, CENP-T and CENP-W bind directly to DNA (Cohen et al., 2008; Hori et al., 2008a; Sugimoto et al., 1997; Sugimoto et al., 1994). Secondly, on the opposite side some KMN members such as the Ndc80-, Knl1 complex or the outer kinetochore complex Dam1 have an intrinsic microtubule binding activity (Cheeseman et al., 2006; Ciferri et al., 2008; DeLuca et al., 2005; DeLuca et al., 2006; Lampert et al.; Wei et al., 2007; Westermann et al., 2005). Besides the major structural kinetochore complexes, other proteins, such as plus end tacking or motor proteins are also associated with kinetochores but they will not be further outlined.

Figure 1: Schematic outline of the budding yeast kinetochore. A) A general kinetochore building plan of the eukaryotic kinetochore. Kinetochore proteins build two major networks: the CCAN (**C**onstitutive **C**entromere **A**ssociated **N**etwork) and the KMN network (**K**nl1-, **M**is12, **N**dc80 complex). Both networks are mainly conserved from yeast to human. The CCAN is constitutively associated with the centromeric DNA und provides a platform for the assembly of the KMN network. The proteins of the KMN network attach the kinetochore to the microtubules of the mitotic spindle. B) Schematic organization of the budding yeast kinetochore. This illustration only covers the structural complexes, but omits regulatory proteins such as checkpoint proteins or +TIPs. The Dam1- and Ndc80 complexes locate at the kinetochore-microtubule interface and provide the physical linkage to the dynamic microtubule. The linker complex Mis12 connects the outer kinetochore proteins to the inner complexes Ctf19 and/or Mif2 protein. Adapted from Lampert and Westermann (Lampert and Westermann, 2011).

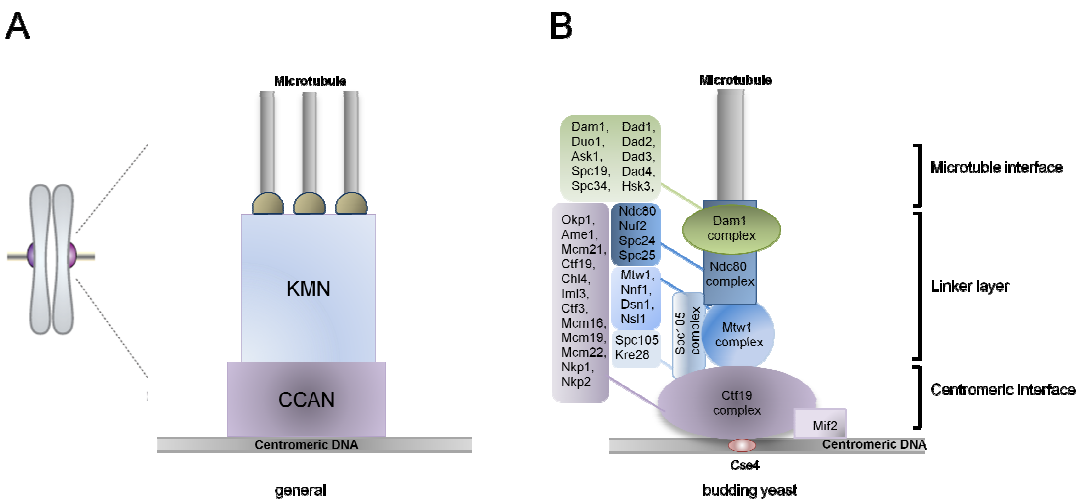

Figure 1

Table 1: Homology relationship between structural proteins of human and budding yeast. Table CCAN/Ctf19 complex**:** Human CCAN subunits are homologous to the budding yeast Ctf19 complex. The grouping of CCAN-/Ctf19 subunits reflects genetically or biochemically defined subcomplexes. As in human, the budding yeast multi-subunit Ctf19 complex can be divided into similar subcomplexes. Adapted from Schleiffer (Schleiffer et al., 2012). Table KMN network: Beside the CCAN all structural kinetochore proteins of the KMN network are conserved based on sequence analysis (Petrovic et al., 2010; Wei et al., 2007; Wei et al., 2006).

CCAN	Ctf19 complex
H. Sapiens	*S. cerevisiae*
CENP-C	Mif2
CENP-R	
CENP-Q	Okp1
CENP-U	Ame1
CENP-P	Ctf19
CENP-O	Mcm21
CENP-L	Mcm19/Iml3
CENP-N	Chl4
CENP-M	
CENP-H	Mcm16
CENP-I	Ctf3
CENP-K	Mcm22
CENP-T	Cnn1
CENP-W	Wip1
CENP-S	Yol086w-A (Mhf1)
CENP-X	Yol160c-A (Mhf2)
	Nkp1
	Nkp2

KMN network	
H. Sapiens	*S. cerevisiae*
Mis12-/Mtw1 complex	
Mis12	Mtw1
Nnf1	Nnf1
Dsn1	Dsn1
Nsl1	Nsl1
Ndc80 Complex	
Ndc80/Hec1	Ndc80
Nuf2	Nuf2
Spc24	Spc24
Spc25	Spc25
Knl1-/Spc105 complex	
Knl1	Spc105
Zwint-1	Kre28/Ydr532C

3.2.1 Specification of kinetochore assembly and inner kinetochore proteins

Kinetochores are assembled on chromosomal loci named centromeres. Based on their arrangement, centromeres are categorized into three classes. First, the point centromeres: each *S. cerevisiae* chromosome has one 125-bp centromere sequence sufficient for chromosome segregation during mitosis and meiosis. This conserved sequence encompasses three centromeric DNA elements, termed CDE I, II and III (Clarke, 1985; Clarke and Carbon, 1985). Second, regional centromeres: in this form of organization, found in humans or in fission yeast, the centromeres span over kilo- or megabases (Cleveland et al., 2003). Those stretches contain repetitive DNA sequences which are considered to be rather epigenetically specified than via their DNA sequence as it is the case in budding yeast. Holocentric centromeres, as a third group, extend along the entire chromosome and can be found e.g. in *Caenorhabditis elegans* (*C. elegans*). An evolutionary conserved feature of all kinetochores is the presence of the specialized histone variant CENP-A (Cse4 in budding yeast). It replaces the canonical histone protein H3 in the centromeric nucleosome (Black and Bassett, 2008). An essential key event in budding yeast kinetochore assembly is the recruitment of the CBF3 complex (Ndc10, Skp1, Ctf13, Cep3) to the centromeric region CDEIII. The recruitment of all other budding yeast kinetochore proteins depends on its centromere localization (Lechner and Carbon, 1991).

3.2.2 CENP-C/Mif2

The presence of CENP-C proteins at the centromere is in all organisms required for viability. In *C. elegans* and *D. melanogaster* CENP-C is the only CCAN protein that has been identified, demonstrating the importance of this protein. The human CENP-A associates with the conserved CCAN subunit CENP-C (Carroll et al., 2010), the homolog of budding yeast Mif2. The centromere localization of Mif2 depends on Cse4 and CBF3 (Meluh and Koshland, 1997; Ortiz et al., 1999; Westermann et al., 2003). In humans, the amino-terminal twenty amino acids of CENP-C associate with the Mis12 complex *in vitro* (Screpanti et al., 2011), and targeting the N-terminus of *D. melanogaster* CENP-C to an ectopic site, recruits all KMN members (Knl1-, Mis12-, Ndc80 complex) (Przewloka et al., 2011). Structural analysis of Mif2 shows a cupin fold domain at the C-terminus responsible for dimerization. The presence of an AT-hook DNA binding element can explain the association with the A:T rich centromere region *in vitro* (Cohen et al., 2008). Interestingly, based on a fluorescence localization study Mif2 is necessary to recruit Ctf19 complex proteins such as the COMA complex and also the Mtw1 complex (Cohen

et al., 2008). This indicates that Mif2 acts in the same recruitment pathway as Mtw1c and COMA or it directly associates with them. Strikingly, in affinity purifications from yeast extracts Mif2 copurifies with two subsets of proteins. The first group corresponds to the centromeric histone proteins H2A, H2B, Cse4, H4, and the second to members of the Mtw1 complex. The Mtw1 complex copurifies besides Mif2 with outer kinetochore proteins of the Ndc80 complex (Westermann et al., 2003). These data suggest a centromere proximal localization of Mif2 compared to the KMN members and an evolutionary conserved function of CENP-C/Mif2 in acting as a linker between the inner and the outer kinetochore.

3.2.3 CCAN/Ctf19 complex

Equal chromosome distribution into daughter cells requires a permanent and solid scaffold on the centromeric DNA onto which other kinetochore proteins can assemble. Biochemical and proteomic approaches revealed a network of approximately 16 proteins in vertebrates that is comprehensively called the constitutive centromere associated network (CCAN), although not all members localize to the centromere throughout the cell cycle, (CENP-C, CENP-H, CENP-I, CENP-K, CENP-L, CENP-M, CENP-N, CENP-O, CENP-P, CENP-Q, CENP-R, CENP-U/50, CENP-S, CENP-X, CENP-T and CENP-W) (Foltz et al., 2006; Hori et al., 2008b; Okada et al., 2006) (see also Table 1) .

Systematic depletion of one kinetochore protein and subsequent analysis of the recruitment of other proteins to the kinetochore have shed light on the assembly hierarchy and localization dependency at the vertebrate kinetochore. This has also allowed a categorization of CENPs into five distinct subclasses known as CENP-C, CENP-O/P/Q/R/U, CENP-T/W, CENPS/X and CENP-H/I/K (Amano et al., 2009; Hori et al., 2008a; Okada et al., 2006). CENP-A is the most upstream protein in the assembly hierarchy since in its absence other kinetochore proteins fail to localize (Liu et al., 2006; Regnier et al., 2005). In CENP-A mutants the CENP-H/-I localization is abolished meaning that the CENP-H/-I complex is downstream of CENP-A in kinetochore assembly. Whereas in CENP-H/-I depleted cells CENP-T/W were still visible at kinetochores indicating that CENPH/-I lies upstream (Hori et al., 2008a). In biochemical experiments CENP-N has been identified to associate with the CENP-A nucleosome and its depletion reduced CENP-A localization showing that the assembly hierarchies are not always strictly unidirectional (Carroll et al., 2009).

Some CCAN subunits have also been implicated in the direct contact between centromeric DNA and the microtubule plus end and thus may have roles in regulating chromosome oscillations (Amaro et al., 2010).

Most CCAN subunits are conserved in the form of the budding yeast Ctf19 complex. A recent bioinformatic and biochemical approach revealed new unrecognized Ctf19 complex subunits and most of the 12 subunits are conserved (De Wulf et al., 2003; McAinsh et al., 2006; Schleiffer et al., 2012; Westermann et al., 2003). Furthermore, analogous to humans, the homologous proteins of *S. cerevisiae* are probably organized into similar subcomplexes.

The heterotetrameric COMA complex is an inner kinetochore component that is required for stable kinetochore-microtubule attachments and for the maintenance of the spindle assembly checkpoint (Knockleby and Vogel, 2009). It contains four subunits **C**tf19, **O**kp1, **M**cm21, **A**me1, of which only Ame1 and Okp1 are required for yeast viability. In contrast, none of the chicken homologous proteins CENP-P/-Q/-O/-U is essential (Hori et al., 2008b). Furthermore, biochemical analysis proposed that the COMA components subdivide into two heterodimeric complexes Ame1-Okp1 and Ctf19-Mcm21 (De Wulf et al., 2003). In *ctf19Δ* and *mcm21Δ* cells the Ame1-GFP and Okp1-GFP signals are not reduced at kinetochores (De Wulf et al., 2003). The nonessential Ctf19-Mcm21 subunits may act as auxiliary factors in COMA assembly and for accurate chromosome segregation and genomic stability (Hyland et al., 1999; Poddar et al., 1999). Previous experiments implied Ame1 as a critical subunit in recruiting COMA to the kinetochore. In an *ame1-4* temperature sensitive (ts) mutant none of the COMA subunits remained localized at the kinetochore. In contrast, in an *okp1-5* ts mutant, Ctf19 and Mcm21 are mislocalized, but Ame1 remains associated with kinetochores suggesting Ame1 as the most critical COMA subunit (Knockleby and Vogel, 2009).

Also the localization of Sli15 and Bub3, which are components of the spindle checkpoint, are disrupted in *ame1-4* cells. This is consistent with the finding, that both *ame1-4* and *okp1-5* strains arrest in G2/M phase and in single step affinity purifications Sli15 and Bub3 were also physically linked to Ame1 and Okp1 (Knockleby and Vogel, 2009; Matson et al.; Pot et al., 2005).

Chl4 and Iml3, the homolog of CENP-N/-L, showed a pairwise interaction in a yeast two hybrid assay and their localization depends on the COMA subunit Ctf19, whereas reciprocally Ctf19 is independent of Chl4 and Iml3 suggesting COMA interact with Chl4 and Iml3 (Ghosh et al., 2001; Pot et al., 2003).

Recently, localization dependencies implied Chl4 as a prerequisite for the localization of Wip1 an interaction partner of the conserved centromere binding protein Cnn1/CENP-T. Cnn1 contains a histone fold domain at the C-terminus and acts as direct recruiter of the microtubule binding complex Ndc80 with an N-terminal binding motif (Schleiffer et al., 2012).

Despite these insights, the CCAN still remains one of the more mysterious complexes at the kinetochore and a functional assignment for most subunits is still missing.

3.2.4 The KMN network and the outer kinetochore

The connection of the kinetochore to the microtubule is a key feature and it must be stable enough to transmit the forces that are generated during chromosome segregation. Previous work demonstrated that the energy required for chromosome movement relies on the ability of kinetochores to remain attached to the disassembling microtubules during anaphase. The experimental approach was conducted in a defined *in vitro* environment without ATP that excludes the possibility of motor based motility (Coue et al., 1991; Koshland et al., 1988). Also inhibition of the kinetochore motors CENP-E and cytoplasmic Dynein do not significantly eliminate the chromosome-microtubule interaction (Howell et al., 2001; Putkey et al., 2002). Hence, the kinetochore-microtubule interface has drawn much attention during the last decade and especially three distinct protein complexes, that are thought to form the core microtubule attachment site, have been characterized. The protein assembly is known as the KMN network derived from the metazoan complexes **K**nl1-, **M**is12-, and **N**dc80 complex. Tandem affinity purification from worms, flies, human and yeast identified those evolutionary conserved proteins as an essential part of the outer kinetochore (Cheeseman et al., 2006; Cheeseman et al., 2004; De Wulf et al., 2003; DeLuca et al., 2005; Desai et al., 2003; Nekrasov et al., 2003; Przewloka et al., 2007; Westermann et al., 2003). Preventing kinetochore localization of one of the KMN members results in chromosome segregation defects and either in a partial or complete detachment of the kinetochore from the microtubules (Cheeseman et al., 2008; DeLuca et al., 2005; Kline et al., 2006). *In vitro* reconstitution of the *C. elegans* KMN network demonstrated that the Ndc80 complex and Knl1 are low affinity microtubule binders. However, the entire network synergistically enhances the microtubule binding activity of the individual complexes suggesting that they form a microtubule binding interface of central importance (Cheeseman et al., 2006). Recently, fluorescence based measurements have estimated the presence of about eight to twenty copies of the KMN network per kinetochore-microtubule attachment site. This

number is thought to be conserved between point and regional centromeres (Joglekar et al., 2008; Joglekar et al., 2006; Lawrimore et al., 2011).

Furthermore, members of the budding yeast outer kinetochore include many additional proteins such as the minus- or plus end directed motors Kar3 and Cin8, the plus end tracking proteins Bim1, Bik1, Stu2, other microtubule associated proteins and the Dam1 complex. The latter drew much attention as a kinetochore-microtubule coupler and it plays a critical role for chromosome segregation in yeast.

3.2.5 Ndc80 complex

Extensive structural and biochemical analysis makes the Ndc80 complex one of the best studied kinetochore constituents. It is a heterotetrameric protein complex consisting of the subunits Ndc80, Nuf2, Spc24 and Spc25. Each subunit has a globular domain connected to a coiled-coil region allowing firstly the heterodimerization between Ndc80-Nuf2 and Spc24-Spc25 subunits and secondly, the tetramerization of the two heterodimers into the Ndc80 complex (Figure 2 A). The resulting full length complex has a dumbbell-like appearance with a length of about 57 nm *in vitro* (Wei et al., 2005). Both the Ndc80 and Nuf2 globular domains contain a Calponin homology domain mediating the microtubule binding activity. Both, human and yeast Ndc80 contains an unstructured, highly positively charged N-terminal tail of 80 and 116 residues, respectively. Deletion of this tail led to a lower affinity for microtubules *in vitro* and it has been suggested to mediate Ndc80-Ndc80 complex oligomerization on the microtubule lattice (Alushin et al., 2010; Ciferri et al., 2008; Wei et al., 2007). Deletion of the human Ndc80 tail leads to severe instability of the kinetochore-microtubule attachment *in vivo* (Guimaraes et al., 2008), while in contrast a tail deletion in budding yeast did not affect viability (Kemmler et al., 2009). The Spc24-Spc25 head orients centromere-proximal and is presumably responsible for the interaction with the Mis12 complex (Cheeseman et al., 2006).

Fluorescence nanometer-scale mapping of kinetochore constituents revealed a decreased length of the Ndc80 complex from 54 nm in metaphase to 34 nm in late anaphase, probably due to intramolecular conformation changes that occur after loss of tension (Joglekar et al., 2009) (

Figure **2** B). This flexibility of the Ndc80 complex can be explained by an evolutionary conserved region that forms a loop in the Ndc80-Nuf2 coiled-coil region introducing a flexible joint into the rod like structure (Wang et al., 2008). A flexible kink might also be more favorable for force transduction, because it slowly rather than abruptly builds up tension compared to a stiff fibril

coupler. Recently, a study implicated the Ndc80 loop region in the interaction with the Dam1 complex. In a yeast two hybrid assay a partial deletion of the conserved loop region significantly reduced the interaction to Dam1. The Dam1 complex is loaded onto KTs when end on attachment is achieved (Tanaka et al., 2007). In Ndc80 loop mutant cells an efficient conversion from lateral to end-on attachment was rare suggesting that the loop is required for an association with Dam1 complex to achieve proper end on attachment (Maure et al., 2011).

Electron microscope image reconstruction, showing the Ndc80 complex bound to microtubule, revealed a minimal contact point between the Ndc80 subunit and the interface of two adjacent tubulin monomers. This interaction is sensitive to the conformational state of tubulin, thus the curving of protofilaments, as it occurs during microtubule disassembly, would suffice for a biased diffusion of Ndc80 complex along the lattice (Alushin et al., 2010).

The Ndc80 complex has also been implicated in SAC activation. *Spc24-2* and *spc25-7* temperature sensitive alleles failed to segregate chromosomes at the restrictive temperature and the DNA remained in the mother cell. Nocodazole is a drug that disassembles microtubules and activates the SAC in healthy cells. Treatment of *Spc24-2* and *spc25-7* with nocodazole led to a similar phenotype than a deletion of the SAC protein Mad2 indicating a SAC impairment.

Consistently, *ndc80-1* mutant cells carrying a degradable Nuf2 subunit, rereplicated their DNA and did not arrest in metaphase. Overall, this demonstrates that the Ndc80 complex is important for checkpoint function (Janke et al., 2001; McCleland et al., 2003).

In this context, it has been shown that the Ndc80 complex is targeted by the Ipl1 and Mps1 kinases that are part of the surveillance system for correcting malformed kinetochore-microtubule attachments (Akiyoshi et al., 2009; Kemmler et al., 2009).

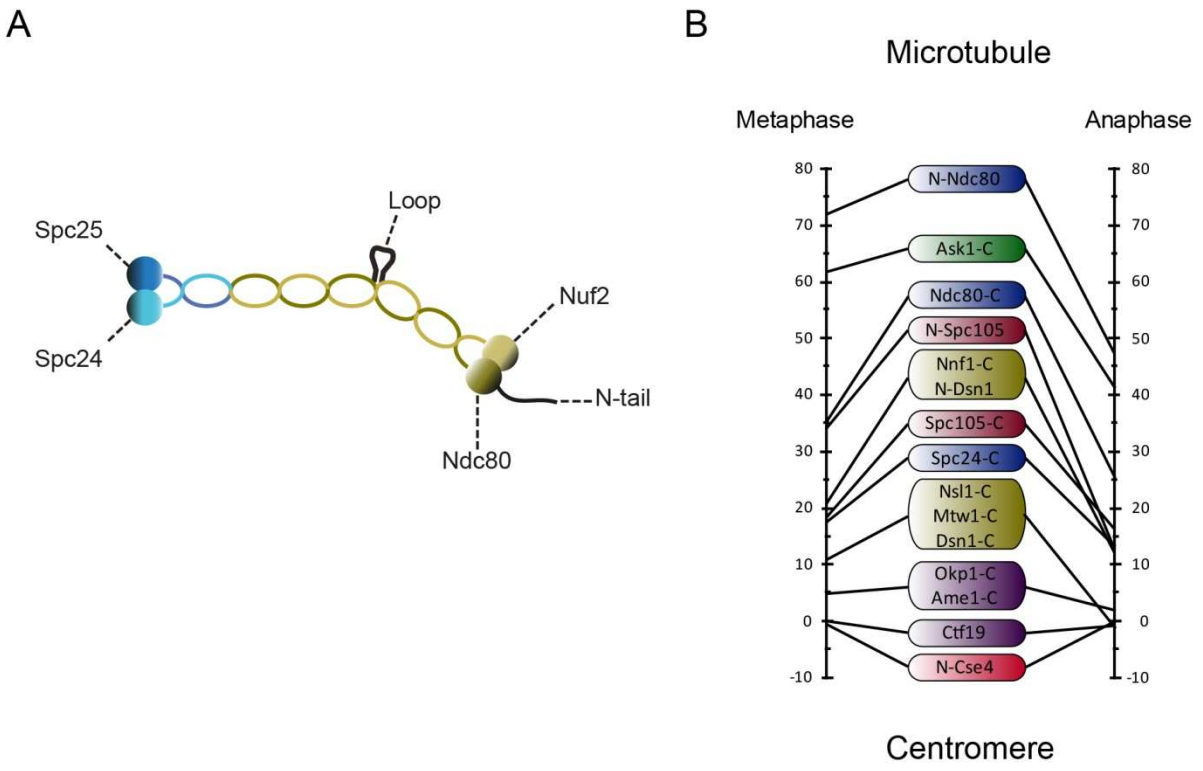

Figure 2: Architecture of the Ndc80 complex and kinetochore protein localization. A) From the microtubule binding head of budding yeast Ndc80 a 116 amino-acid long N-terminal extension protrudes. A Coiled-coil region mediates the dimerization of Ndc80-Nuf2 heads and it is interrupted by an insertion giving flexibility to the N-terminal head. The C-terminal coiled-coil domains of Ndc80-Nuf2 tetramerize with the N-terminal parts of Spc24-Spc25. B) Average localization of kinetochore proteins along the budding yeast kinetochore axis in nanometer resolution. The proteins were ordered according to a one- dimensional map along the axis in metaphase and anaphase. Strikingly, the kinetochore length is shortened in anaphase when tension is lost. This length reduction comes mainly from the Ndc80 complex. N- and C-termini refer to as N-, C-. Adapted from Joglekar (Joglekar et al., 2009).

3.2.6 Mis12/Mtw1 complex

The Mtw1 complex - also named the MIND complex - consists of four essential subunits: Mtw1, Nnf1, Dsn1 and Nsl1. Cells carrying a temperature-sensitive (ts) *mtw1-1* allele arrested in metaphase and they activate the spindle assembly checkpoint in an Ipl1 dependent manner indicating a defect in biorientation (Pinsky et al., 2003). Ts alleles of NNF1 displayed a reduced stability for minichromosomes and mitotic spindle defects (Euskirchen, 2002). Depletion of Mtw1 subunits in human, worm and flies by RNAi led to similar aberrant defects in spindle morphology, chromosome segregation and kinetochore biorientation (Cheeseman et al., 2004; Kline et al., 2006; McAinsh et al., 2006; Przewloka et al., 2007).

FRAP experiments of human cells showed high turnover of Mis12 during interphase, whereas Mis12 became stably associated with the kinetochore in metaphase indicating a structural role of the Mis12 proteins that physically contributes to a stable kinetochore-microtubule interface (Hemmerich, 2008).

In a combined approach of affinity purification and mass spectrometry the centromere associated protein Mif2 copurified with the H3 histone variant Cse4 and all constituents of the Mtw1 complex. Strikingly, the Mtw1 complex copurifies with the outer kinetochore protein Ndc80, the inner protein Mif2 and with the members of the Ctf19 complex suggesting that the Mtw1 complex is more centromere distal than Mif2, but more centromere proximal than Ndc80 (De Wulf et al., 2003; Nekrasov et al., 2003; Westermann et al., 2003)

Interestingly, in human and flies the centromeric heterochromatin binding protein HP1 has been identified to physically bind to the Mis12 complex and HP1 RNAi disrupts Mis12 kinetochore localization (Obuse et al., 2004; Przewloka et al., 2007). *In vitro* reconstitution experiments identified a motif in the Mis12 complex that binds HP1 in a manner that is competitive with binding to the Ndc80 complex (Petrovic et al., 2010). Thus the HP1 protein might recruit Mis12 complex to the centromere and become later replaced by the Ndc80 complex.

Super resolution light microscopy revealed that the N-terminus of Dsn1 and the C-terminus of Nnf1 localize in close vicinity to the Spc24 and Spc105 carboxyterminal domains during metaphase and anaphase. Subunits of the Ctf19 complex located in close proximity to the Mtw1 complex (Figure 2A) (Joglekar et al., 2009). The experiments suggest that the Mis12-/Mtw1 complex acts as a bidirectional linker for outer and inner kinetochore proteins.

3.2.7 Spc105-/Knl1 complex

The human protein Knl1 stably associates with Zwint and the same is true for the budding yeast homologs Spc105 and Kre28. Biochemical characterization of Spc105 and Kre28 revealed that two Kre28 molecules associate with one Spc105 molecule. The frictional coefficient suggested an elongated shape similar to the Ndc80 complex. Both proteins are essential for budding yeast viability. Spc105 ts cells are compromised in recruiting microtubule associated proteins (MAPs) such as Bim1, Bik1, Slk19 and motors such as Cin8 and Kar3. Similar effects are observable for mutants *ndc80-1* and *mtw1-1* suggesting a collaboration between these complexes (Pagliuca et al., 2009). *C. elegans* Knl1 and budding yeast Spc105 bind with lower affinity to taxol-stabilized microtubules compared to Ndc80 or Dam1. Very recently, several studies have demonstrated

the critical role of Spc105 for Bub1 recruitment. Spc105 mutants cells that were unable to recruit Bub1 lacked a functional checkpoint (London et al., 2012). Also the human Knl1/Blinkin is required for the recruitment of checkpoint proteins Bub1 and BubR1 (Kiyomitsu et al., 2007; Petrovic et al., 2010).

3.2.8 Dam1 complex

The essential heterodecameric Dam1 complex (Dam1, Ask1, Hsk3, Dad1, Dad2, Dad3, Dad4, Duo1, Spc19, Spc34) is evolutionary restricted to fungi. Early studies with Dam1 ts mutants demonstrated its requirement to establish and maintain biorientation of sister kinetochores and it was implicated in having a critical role in maintaining anaphase spindle integrity. For instance, the *spc34-3* allele fails to maintain biorientation suggesting that the Dam1 complex is also necessary for KT-microtubule attachments after establishment of biorientation (Janke et al., 2002). Consistently, other Dam1 ts alleles also led to high rates of chromosome missegregation (Cheeseman et al., 2001; Janke et al., 2002; Li et al., 2002).

Importantly, the Dam1 complex is also required for the transition from side-on to end-on microtubule attachment of kinetochores (Tanaka et al., 2005).

Dam1 localizes to the kinetochore in a microtubule and Ndc80 dependent manner and its function is regulated by the Ipl1 kinase *in vivo* (Cheeseman et al., 2002; Li et al., 2002). Studies suggest that upon biorientation, when tension is established, the Dam1 complex becomes dephosphorylated and the attachment is stabilized (Keating et al., 2009).

A possible association between the Ndc80 complex and the Dam1 complex was suggested based on yeast two hybrid studies (Wong et al., 2007). A recent study showed that cells that contained a mutation in a conserved loop region of the Ndc80 complex insufficiently form end on attachments, suggesting that this loop contributes to the association between Dam1- and Ndc80 complex (Maure et al., 2011).

The entire Dam1 complex is able to bind with high affinity to microtubules *in vitro* encircling them through ring formation (Miranda et al., 2005; Westermann et al., 2005) (Figure 3). A ring module that allows force conversion from a deploymerising microtubule end into chromosome movement would be an efficient mechanism to couple the kinetochore to the dynamic microtubule. Several biophysical experiments support this model (Asbury et al., 2006; Westermann et al., 2006). Evidence for the ring model *in vivo,* however, is so far lacking. In

addition to the Dam1 complex, the fibrillar, elongated shape of the Ndc80 complex could act as a perfect coupler towards the inner kinetochore.

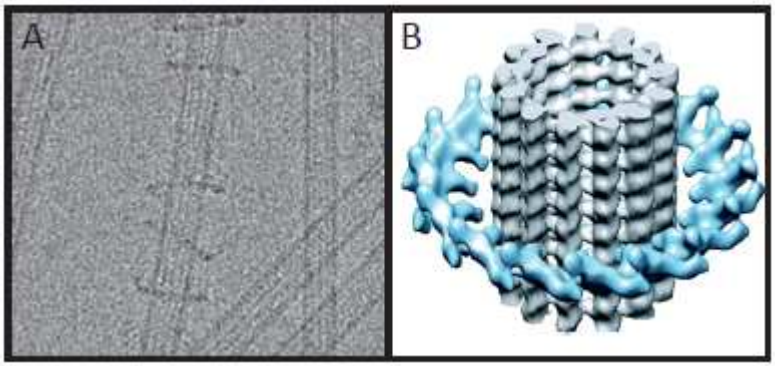

Figure 3: Microtubule decoration and topology of the Dam1 complex. A) Cryo-EM demonstrating ring formation of the Dam1 complex. B) Reconstruction of the Dam1 ring on microtubule. Adapted from Nogales and Ramey (Nogales and Ramey, 2009; Ramey et al., 2011)

3.3 Spindle assembly checkpoint

The spindle assembly checkpoint (SAC) distinguishes correct from incorrect mitotic spindle attachments and allows the cell to proceed with anaphase only when correct kinetochore-microtubule connections have been established. This surveillance mechanism is important, because high fidelity chromosome segregation requires stable kinetochore-microtubule attachments that withstand the forces of the disassembling microtubule during anaphase.

In all eukaryotes, two major protein networks ensure the SAC. Firstly, the chromosomal passenger complex (CPC) including the budding yeast proteins Ipl1 (in human Aurora B), Sli15 (INCENP), Bir1 (Survivin) and Nbl1 (Borealin) and the mitotic checkpoint complex (MCC) Mad2, Mad3, Bub1, Bub3 and Cdc20. The CPC component Ipl1 phosphorylates different outer kinetochore substrates such as the Ndc80 and Dam1 complexes thereby preventing the stabilization of incorrect attachments. It neutralizes the positively charged N-terminal tail of Ndc80 by adding negative phosphate groups and reducing the microtubule affinity (Ciferri et al., 2008; Guimaraes et al., 2008) or it lowers the association between Ndc80 and the phosphorylated Dam1 complex *in vitro* (Lampert et al., 2010). It is thought that Ipl1 can distinguish correct from incorrect attachments by a spatial mechanism. The CPC localizes at the centromere through interactions with inner kinetochore proteins. When a correct attachment is achieved tension is applied across the sister kinetochores and the distance between the

centromere and the microtubule increases. This also stretches the kinetochore making distant substrates unreachable for Ipl1 (Liu et al., 2009; Maresca and Salmon, 2009; Tanaka et al., 2002; Uchida et al., 2009). Opposing phosphatases, such as PP1, reduce the phosphorylation state thereby stabilizing the kinetochore microtubule attachments.

MCC proteins are recruited to unattached kinetochore-microtubule attachments that do not establish enough tension and they negatively regulate Cdc20, a coactivator of the E3 ubiquitin ligase anaphase promoting complex (APC). Once the SAC is satisfied, Cdc20 is released and it activates the APC, that mediates the degradation of its key substrates Pds1 (securin) and cyclin B. Pds1 forms an inhibitory complex with the protease Esp1 (separase) that cleaves the cohesin complex at the Scc1 subunit, thus dissolving the linkage between the sister chromatids. Destruction of Pds1 releases Esp1 and this in turn leads to cohesin cleavage and allows sister chromatid segregation (Buschhorn and Peters, 2006; Ciosk et al., 1998). Kinetochore proteins provide a platform for the recruitment of SAC proteins. Hence a functional kinetochore structure is necessary for SAC function. The likely kinetochore receptors for SAC proteins were found in the KMN network such as Spc105- (Knl1) and the Ndc80 complex (DeLuca et al., 2003; Kiyomitsu et al., 2007; London et al., 2012).

3.4 Aim of this work

Over the last decade much effort was invested in the elucidation of the kinetochore composition. Biochemical isolation of proteins from cell extract unraveled step by step the protein composition of the kinetochore and their associated partners leading to the notion that single proteins are organized into distinct complexes, which in turn are part of larger building blocks. Genetic, biochemical and microscopy approaches assigned a relative mutual arrangement of kinetochore complexes with high accuracy giving us a good knowledge of the protein position within the DNA- microtubule bridge. Nevertheless, a currently challenging question is to define the topology of the kinetochore on a molecular and structural level by elucidating the interfaces between proteins and protein complexes.

Working in a defined *in vitro* environment, with biochemically reconstituted kinetochore complexes, is optimal to study intrinsic properties of a molecule and its structure. Since similar analyses are conducted in different species, functional and topological assignments can be compared across organisms. Since biochemical reconstitution experiments in *C. elegans* have revealed that the Ndc80 complex functions together with the conserved Mis12-/Mtw1 complex

and the Knl1-/Spc105 protein in a multi-protein assembly, called the KMN network, several questions have emerged from this finding:

i) Are the structural and biochemical features of the KMN network conserved among evolutionary diverged eukaryotes?

ii) Does the KMN network independently form the core microtubule binding site or does it cooperate with the Dam1 complex in budding yeast?

iii) How is the KMN network anchored towards the inner kinetochore?

In this report I describe my work on the Ndc80-, Dam1-, Mtw1- and Ctf19 complexes. I aim to partially reconstitute the molecular connectivity of the kinetochore *in vitro*, beginning at the microtubule interface, to unravel step-by-step the associations between kinetochore complexes towards the centromere. Furthermore, I analyse structural and functional properties of these molecules. To this end, I use recombinant proteins/protein complexes expressed in heterologous systems.

4 Results

4.1 Reconstitution of the Mtw1 complex

The four subunits of the Mtw1 complex (Mtw1c) (Mtw1, Nnf1, Dsn1 and Nsl1) were coexpressed under the control of a T7 promoter in the *Escherichia coli* (*E. coli*) expression strain BL21 (DE3). Affinity purification from an *E. coli* lysate with a hexahistidine (6x-His) tag on the Nnf1-C (C-terminus) subunit followed by size exclusion chromatography (SEC) showed that the complex eluted as a single species (Figure 4 A). SEC separates molecules based on size and shape. Considering the theoretical molecular mass of 148 kDa the Mtw1c eluted in an unusually low volume from the SEC with a Stokes radius of 74.3 Å. The Svedberg coefficient of 6.4 S was determined by glycerol gradient centrifugation. By applying the formula of Siegel and Monty, I could determine the molecular mass of the complex to 183 kDa (Siegel and Monty, 1966). In addition, quantifying the intensity of the Coomassie-stained bands on a SDS-PAGE revealed a 1:1:1:1 stoichiometry of the four subunits. The frictional coefficient (f/f_0) of 2.0, which gives an indication of the overall size and shape of a protein, suggests a moderate to highly elongated molecule. These values of the recombinant molecular mass are in close agreement with the ones obtained for the native Mtw1c (De Wulf et al., 2003), meaning its biophysical properties closely matches the counterpart *in vivo* (Table 2).

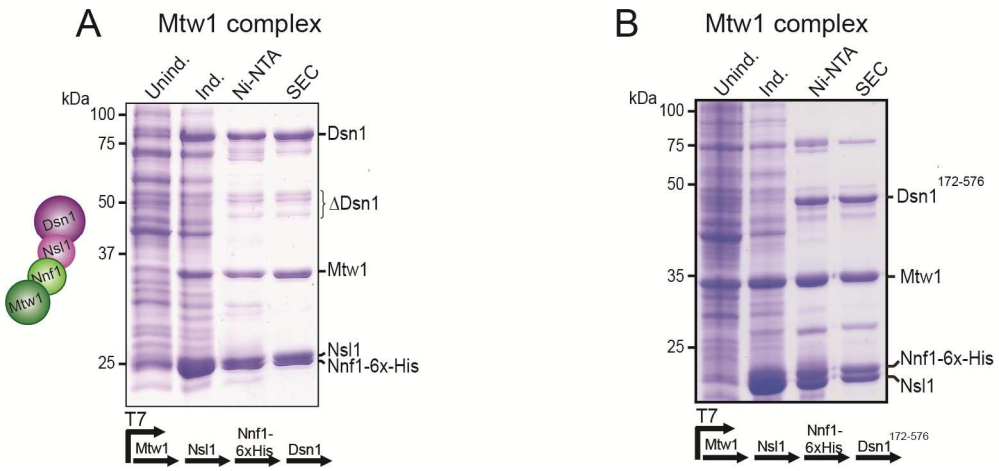

Figure 4: Recombinant expression of the Mtw1 complex A) Purification strategy of the Mtw1c. The Coomassie-stained SDS-PAGE demonstrates the consecutive steps in the purification protocol: Cell extract before (Unind.) and after (Ind.) induction with IPTG (isopropyl β-D-1-thiogalactopyranoside), affinity purified eluate from the nickel-nitrilotriacetic acid (Ni-NTA) beads and in the last lane a protein fraction from the SEC. Note, that the Dsn1 subunit was prone to degradation. B) Expression and purification of an Mtw1c with an N-terminal deleted Dsn1$^{172-576}$ subunit.

Table 2: Hydrodynamic properties of the Mtw1 complex

Construct	Predicted molecular mass (kD)	Analysed molecular mass (kD)	Sedimentation coefficient (10^{-13}s)	Stokes radius (Å)	Predicted stoichiometry	Frictional coefficient
Mtw1C Nnf1-6xHis	148	183.3	6.4	73.2	1:1:1:1	2.0

The Dsn1 subunit has a tendency to degrade during expression and purification yielding several truncations. N-terminal sequencing of the major truncation products revealed that the first 170 amino acids of the N-terminus were prone to be proteolytically removed. The expression of an N-terminally shortened version of the Dsn1 subunit, that lacks the first 171 amino-acids, with the full length NNF1-6xHis, NSL1 and MTW1 genes resulted in a stable Mtw1c (Figure 4 B).

The N-terminus of Dsn1 is predicted to be unstructured and the previous experiment shows that it is dispensable for Mtw1 complex formation *in vitro*. In an *in vivo* assay I tested if the first 171 amino acids have an essential function in the cell. To this end, a haploid Dsn1 deletion strain contained a centromeric plasmid (CEN) with the wild-type Dsn1^{WT} and a second CEN- plasmid with either the Dsn1^{WT} allele or the N-terminally truncated Dsn1$^{172-576}$. 5-fluoroorotic acid selects against the URA plasmid, thereby eliminating the Dsn1^{WT} copy leaving behind either Dsn1^{WT} as control or Dsn1$^{172-576}$. The latter supported wild-type growth and thus the N-terminus of Dsn1 does not have an essential function *in vivo* (Figure 5).

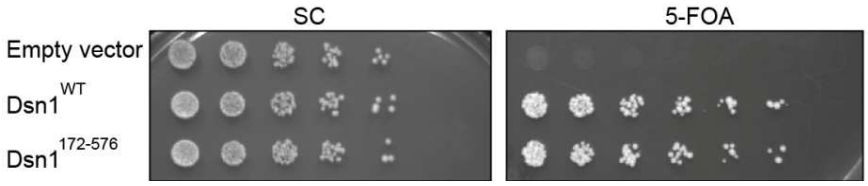

Figure 5: The N-terminal extension of Dsn1 is dispensable *in vivo*. Dsn1$^{172-576}$ shows the same growth as Dsn1^{WT} on 5-FOA plates demonstrating the dispensability of the first 171 Dsn1 amino-acids.

In a later approach I purified the Mtw1c via an N-terminal Dsn1 (N-Dsn1) 6xHis tag for isolating only full-length Dsn1. Instead of a SEC an anion exchange chromatography was applied which better removed the *E. coli* Hsp70 chaperone (purification strategy is not shown).

4.2 Reconstitution of the Mtw1 complex from two stable heterodimers

Hydrodynamic analysis of kinetochore proteins in yeast extracts suggested the presence of single species of the Ndc80c and Dam1c *in vivo*. In contrast, Mtw1c analysis argued for three distinct subpopulations (De Wulf et al., 2003). To test the existence of Mtw1 subcomplexes *in vitro*, I expressed different combinations of Mtw1c genes in *E. coli* and I was able to isolate two distinct heterodimeric subcomplexes: Mtw1-Nnf1 (MN) and Dsn1-Nsl1 (DN) (Figure 6 A+B). I next addressed the question whether the full length complex reconstitutes from the two stable heterodimers by applying them onto SEC. All four Mtw1c subunits coeluted in a single peak, identical with the full length expressed Mtw1c (Figure 6 C+D).

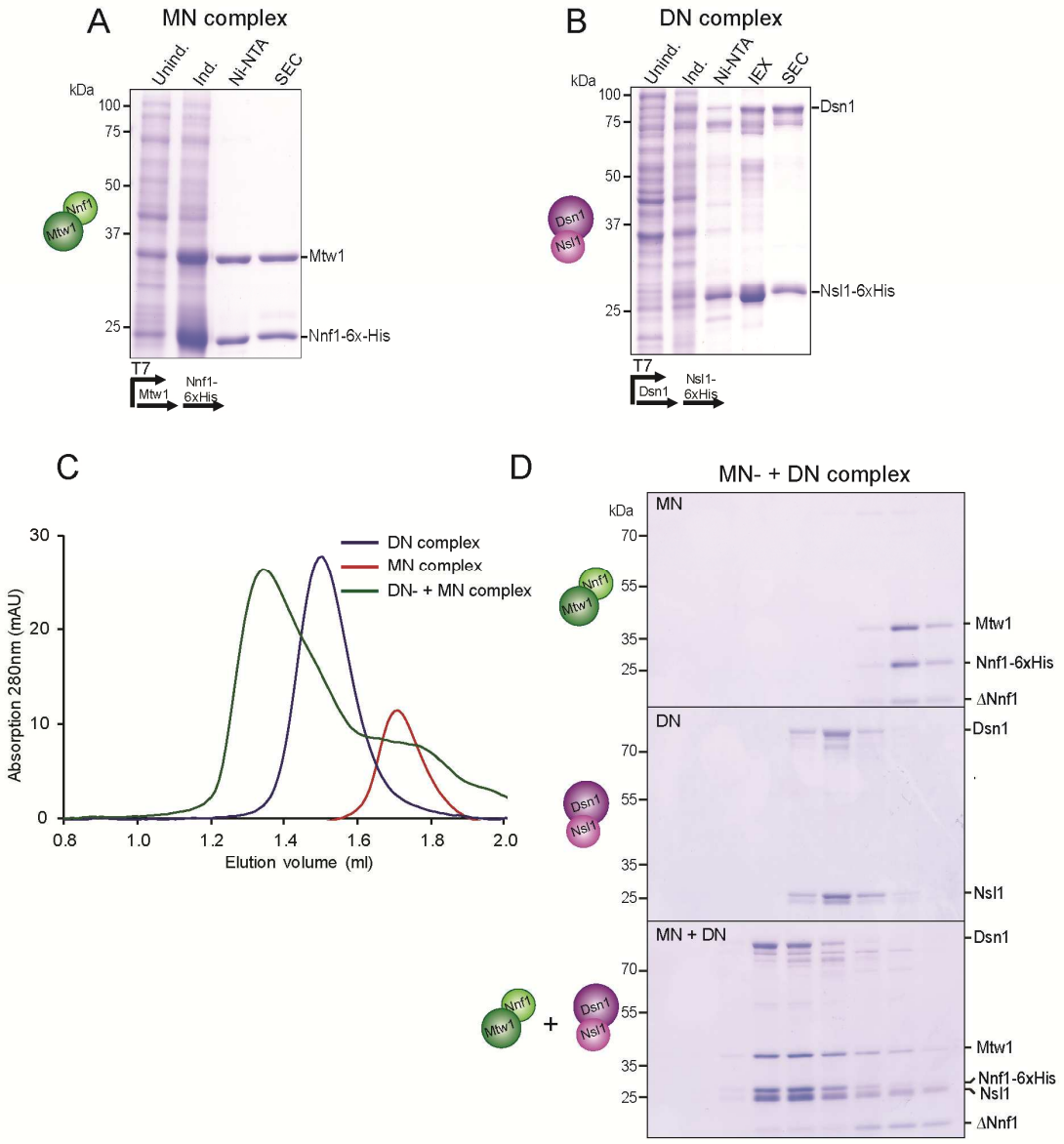

Figure 6

Figure 6: Reconstitution of the Mtw1 complex. A+B) Expression and purification of a stable Mtw1-Nnf1 (MN) and Dsn1-Nsl1 (DN) heterodimer, IEX indicates anion-exchange chromatography. C) Chromatography traces of Dsn1-Nsl1 and Mtw1-Nnf1 complexes alone or combined (8µM each) resulting in a reconstituted Mtw1c. D) Chromatography fractions were separated on a SDS-PAGE and stained with Coomassie.

4.3 Electron microscopy analysis of the Mtw1 complex

Besides the functional dissection of kinetochore proteins, structural characterization of molecules may contribute to assign a shape-function relation. In collaboration with Eva Nogales, Gregory M. Alushin and Gabriel C. Lander we used negative-stain single-particle analysis by electron microscopy (EM) to analyze the structural properties of the Mtw1c. While the images contained several heterogeneous aggregates and small fragments, monomeric full length complexes could be manually picked based on their size and 2D class images were generated (Figure 7 A+B+D). The complex showed a bilobed structure of 25 nm in length. One of the two globular domains consistently appeared larger, with 7 nm in diameter and the second globular domain present in the structure is approximately 4.7 nm. The thin density that connects the two globular domains is roughly 9 nm long. This distance might correspond to the length of the predicted coiled-coil region of the Mtw1 and Nnf1 subunits (Figure 7 C). The larger head domain displayed conformational variability and appeared in some images as a hook-like structure with an open conformation (Figure 7 B, white arrow head). The multiple shape and size variability may reflect the presence of N-terminal degradation in the Dsn1 subunit.

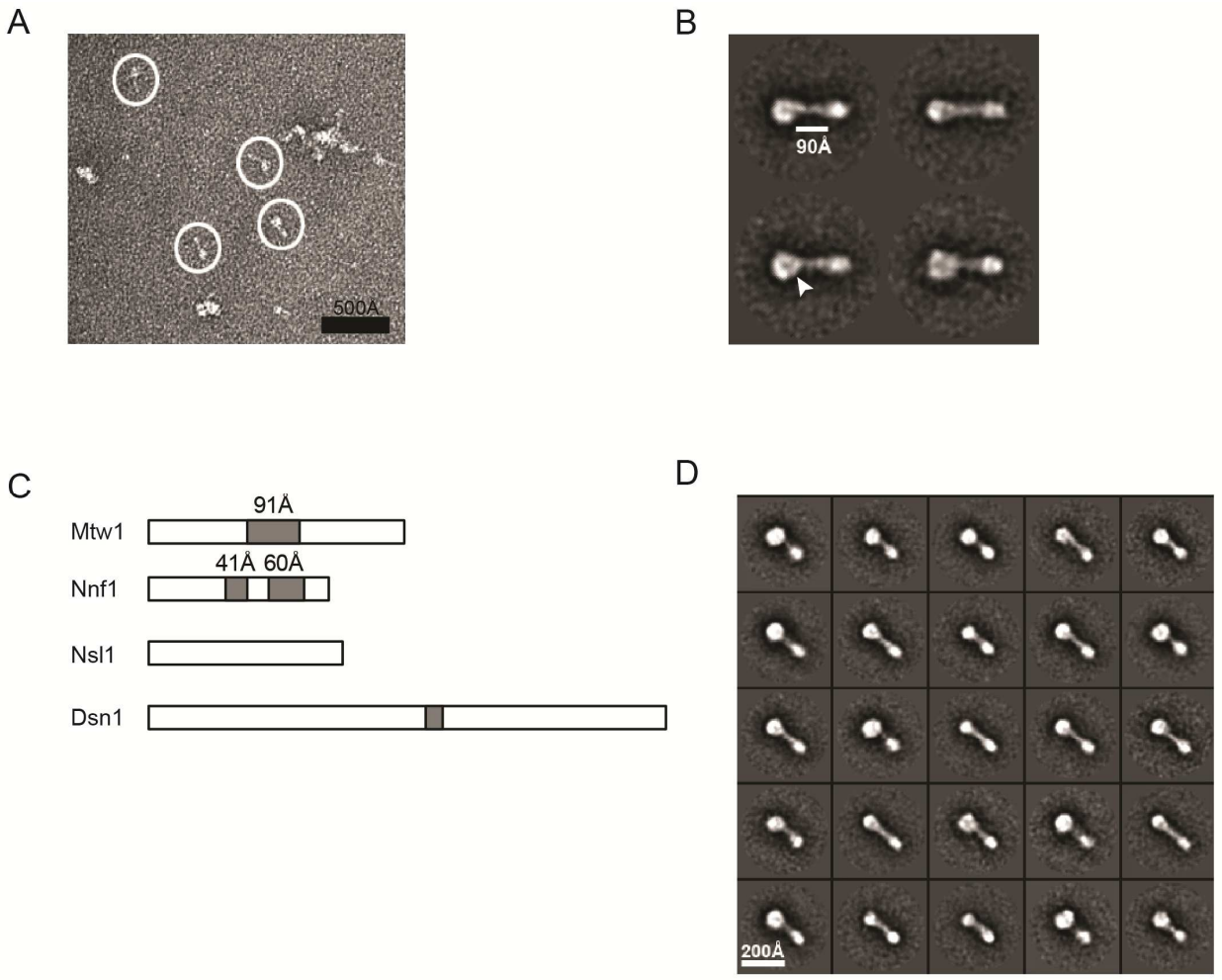

Figure 7: EM analysis of the recombinant Mtw1 complex. A) EM image of the negatively stained Mtw1c. The white circles correspond to particles taken for the 2D class averages analysis. B) A selection of two 2D class images illustrating the overall assembly of the Mtw1c and the conformational variety. The complex is composed of two globular domains with different sizes that are connected by a thin density. The larger domain shows multiple conformations. C) Coiled-coil predictions for the Mtw1c subunits. Grey regions indicate a coiled-coil region with greater 50% probability. D) Complementary 2D class images for the evaluation of the overall complex structure. All complexes share a bilobed structure with much heterogeneity in the size of the larger globular domain.

4.4 The Mtw1 complex directly binds to the Ndc80 complex via the Spc24-25 centromere-proximal head

Previous work has shown that the *C. elegans* Mtw1c homolog, the Mis12c, associates with the microtubule binding complex Ndc80 and the Knl1 protein to form the KMN network (Cheeseman et al., 2006). I next addressed the question whether the budding yeast recombinant Mtw1c is able to associate with the Ndc80c. To this end, I expressed the Spc24-Spc25 and the Ndc80-Nuf2 heterodimers individually and reconstituted the full length Ndc80c using SEC (Figure 8 A).

Subsequently, I examined whether the Mtw1c associates with the Ndc80c by SEC. The observation of a fast eluting species indicated complex formation between the Ndc80c and Mtw1c (Figure 8 C). Densitometry of Ndc80c and Mtw1c subunits based on the Coomassie-stained bands suggested a 1:1 stoichiometry of the two complexes (Figure 8 B). The Ndc80c-Mtw1c ratio is in agreement with quantitative fluorescence microscopy measurements that estimate identical and conserved numbers of Ndc80c and Mtw1c per kinetochore-microtubule attachment (Joglekar et al., 2008; Johnston et al., 2010; Lawrimore et al., 2011). Thus, the budding yeast Mtw1 and Ndc80 complexes can associate in the absence of Spc105. In contrast, the *C. elegans* Ndc80c and Mis12c association requires the presence of the Knl1 protein *in vitro* (Cheeseman et al., 2006). In all organisms the formation of the Ndc80c and Mtw1c interaction is essential for kinetochore function, whereas evolutionary differences in the underlying molecular binding mechanisms may exist.

The third member for the formation of the entire KMN network is the metazoan protein Knl1, whose budding yeast homolog is Spc105. Despite extensive efforts to express the Spc105 protein I was unable to purify full length Spc105 from bacteria or from insect cells. The C-terminus of human KNL-1 was shown to bind to Mis12 complex (Petrovic et al., 2010). In an analogous experiment, I could purify a 200 amino-acid C-terminal fragment of the Spc105 fused to GST from bacteria but no complex formation was observed between Mtw1c and GST-Spc105 C-terminus by SEC or by coexpression in bacteria (results not shown). Also mixing all three KMN members did not result in ternary complex formation (results not shown).

The two globular domains of the Ndc80c mediate different functions. The Ndc80-Nuf2 head displays microtubule binding activity, while the Spc24-Spc25 head projects towards the centromere and it is thought to couple the Ndc80c to the rest of the kinetochore. Therefore I tested if the Spc24-Spc25 head is sufficient to provide the association to the Mtw1c by SEC. The Spc24-Spc25 heterodimer coeluted with the Mtw1c, however with a much lower efficiency as the full-length Ndc80c (Figure 8 D+E). This means either that the interaction requires additional structural parts of the Ndc80-Nuf2 complex or the Spc24-Spc25 complex undergoes a conformational change in the context of the full Ndc80c, thereby making the Mtw1c binding site more accessible. In support of these biochemical experiments, high resolution mapping of the kinetochore placed the Spc24-Spc25 head into close vicinity of the Mtw1c within the centromere-microtubule axis (Joglekar et al., 2009).

I conclude that the Ndc80c directly associates with the Mtw1c via its centromere-proximal Spc24-Spc25 head.

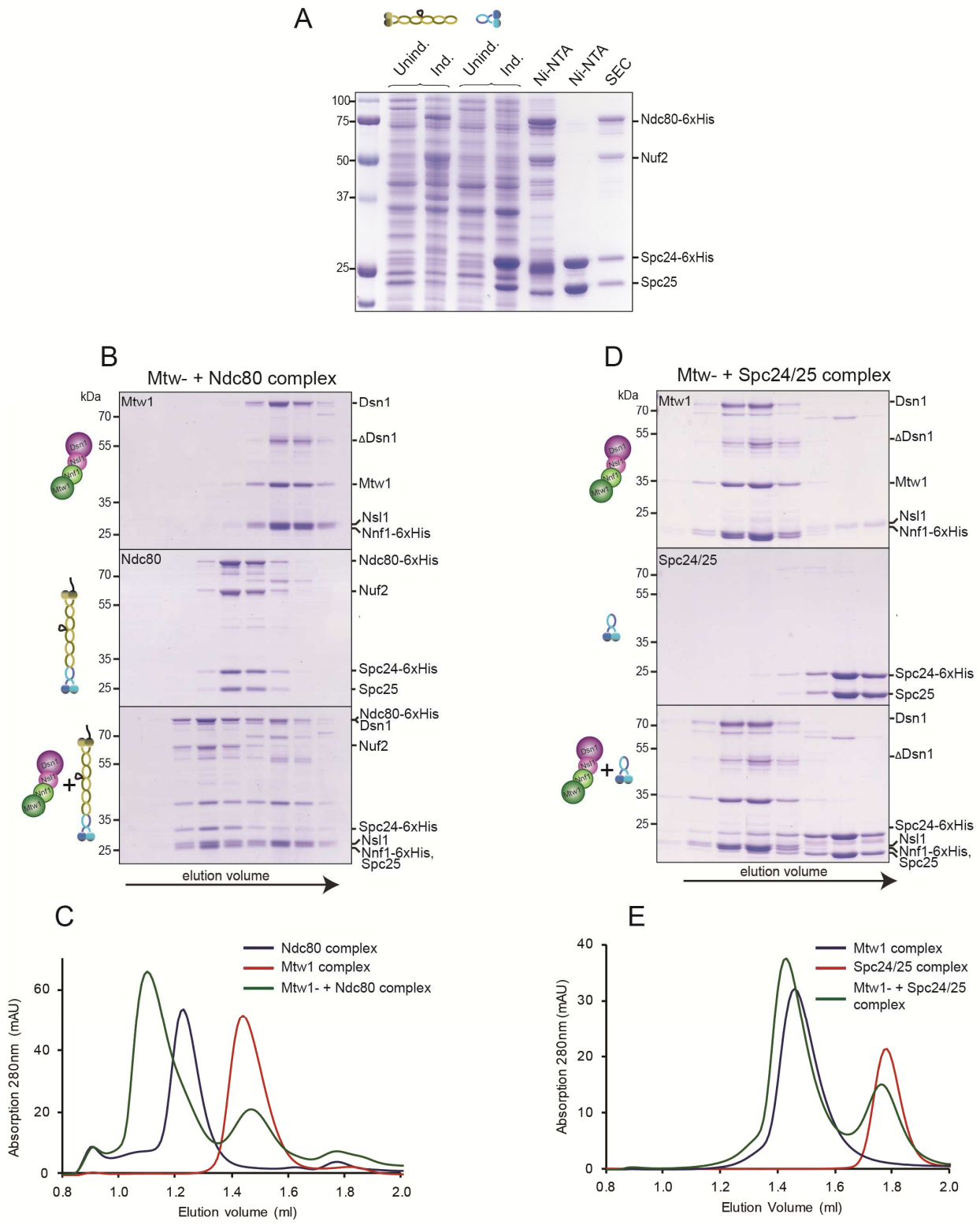
A
Unind.
Ind.
Unind.
Ind.
Ni-NTA
Ni-NTA
SEC
100
75
50
37
25
Ndc80-6xHis
Nuf2
Spc24-6xHis
Spc25
B
Mtw- + Ndc80 complex
kDa
Mtw1
Dsn1
ΔDsn1
Mtw1
Nsl1
Nnf1-6xHis
Ndc80
Ndc80-6xHis
Nuf2
Spc24-6xHis
Spc25
Ndc80-6xHis
Dsn1
Nuf2
Spc24-6xHis
Nsl1
Nnf1-6xHis,
Spc25
elution volume
D
Mtw- + Spc24/25 complex
kDa
Mtw1
Dsn1
ΔDsn1
Mtw1
Nsl1
Nnf1-6xHis
Spc24/25
Spc24-6xHis
Spc25
Dsn1
ΔDsn1
Spc24-6xHis
Nsl1
Nnf1-6xHis,
Spc25
elution volume
C
Ndc80 complex
Mtw1 complex
Mtw1- + Ndc80 complex
Absorption 280nm (mAU)
Elution volume (ml)
E
Mtw1 complex
Spc24/25 complex
Mtw1- + Spc24/25 complex
Absorption 280nm (mAU)
Elution Volume (ml)

Figure 8

Figure 8: Ndc80 complex expression and its interaction with the Mtw1 complex. A) Expression and purification strategy of the Ndc80c. Firstly, the strategy included the separate expression of the two heterodimeric subcomplexes Ndc80-Nuf2 and Spc24-Spc25. Secondly, by combining the two subcomplexes on a SEC the full Ndc80 complex was reconstituted. B) Coomassie stained fractions from the corresponding SEC in C showing that the Mtw1c and the Ndc80c elute in a single peak in a 1:1 stoichiometry (9µM). C) SEC profile from the individually analysed Mtw1c and Ndc80c and their combination. D) Coomassie-stained SDS-PAGE from Mtw1c and Spc24-25c (6µM). E) SEC traces corresponding to D. The Spc24-Spc25 head does not stoichiometrically interact with the Mtw1c. Conclusively, the Mtw1c associates directly with the Ndc80c via the Spc24-Spc25 centromere proximal head.

To biochemically characterize the function of the Mtw1c, I performed a microtubule cosedimentation assay. In agreement with experiments conducted with the *C. elegans* Mis12c, the budding yeast Mtw1c does not have an intrinsic microtubule binding activity *in vitro*. Consistently, upon addition of the Ndc80c the Mtw1c copelleted with the Ndc80c while not influencing the intrinsic Ndc80c microtubule binding properties (Figure 9).

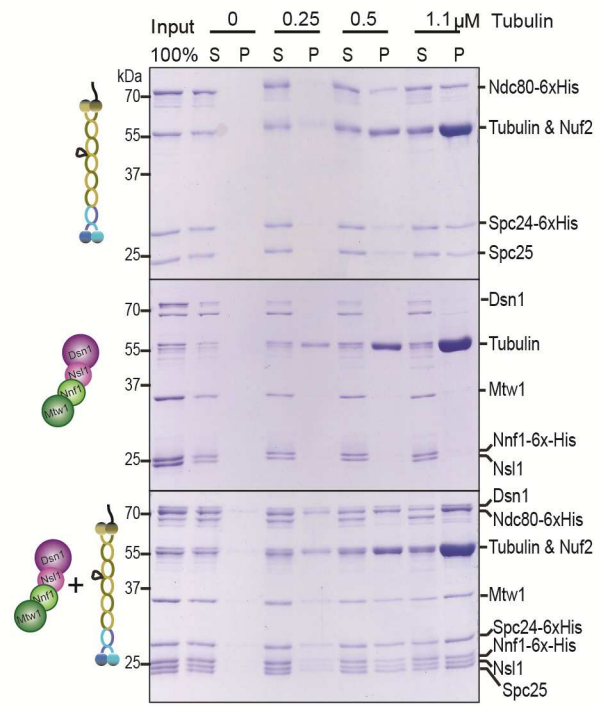

Figure 9: Microtubule copelleting assay with the Ndc80- and the Mtw1 complex. The complexes were either individually or together subjected to cosedimentation with taxol stabilized microtubules. Abbreviation: S – supernatant; P – pellet of the centrifugation. The Ndc80c copellets with taxol stabilized microtubules, while the Mtw1c alone remains in the supernatant. In combination, the Mtw1c is with the Ndc80c in the pellet.

4.5 The Ndc80 complex interacts with the Dam1 complex in the presence of microtubules

Previous reports have demonstrated the microtubule binding properties of the worm, human and yeast Ndc80c *in vitro* (Cheeseman et al., 2006; Ciferri et al., 2008; Wei et al., 2007). Microtubule cosedimentation assays of human and *C. elegans* Ndc80c suggested a high affinity for microtubules (Ciferri et al., 2008). I sought to analyze the microtubule binding properties of the *S. cerevisiae* Ndc80c fused to EGFP more carefully.

Microtubule cosedimentation experiments performed at different salt concentrations uncovered a strong salt sensitivity of Ndc80c microtubule binding. A decrease of the NaCl concentration from 100 to 25 mM lowered the apparent dissociation constant (K_D) by one order of magnitude. At 100 mM NaCl the K_D was 1.27±0.27 µM decreasing to 0.107 ± 0.27 µM at 25mM NaCl (Figure 10 A). The result demonstrates that the microtubule binding activity of the budding yeast Ndc80c is moderate to weak under physiological salt concentrations. The low affinity was surprising because the Ndc80c was implicated as a microtubule binding protein of high importance for the kinetochore. Therefore I assumed a high affinity for microtubules. In budding yeast the Dam1c plays a critical role for chromosome segregation, it acts as a plus end tracker on depolymerizing microtubules and it is thought that the Dam1c transmits the forces from the depolymerizing microtubule to other kinetochore proteins through their interaction (Asbury et al., 2006; Cheeseman et al., 2001; Janke et al., 2002; Li et al., 2002; Westermann et al., 2006).

Next, I addressed whether the presence of the strong microtubule binding complex Dam1 alters the Ndc80c affinity for microtubules in a cosedimentation assay at 100 mM NaCl. Strikingly, upon inclusion of equimolar Dam1c in the assay the K_D of the Ndc80c decreased seven fold compared to Ndc80c alone (Figure 10 B). Consistently, a Coomassie stained SDS-PAGE visualized a substantially increased amount of Ndc80c in the pellet of the cosedimentation assay when the Dam1c was present (Figure 10 C). Therefore, I asked whether the Ndc80c also interacts with the Dam1c in solution using SEC. However, no stable complex formation was observed in solution (Figure 10 D+E).

These results indicate that the microtubule binding affinity of the Ndc80c is enhanced by the Dam1c in budding yeast and furthermore the interaction between the two complexes requires the presence of microtubules.

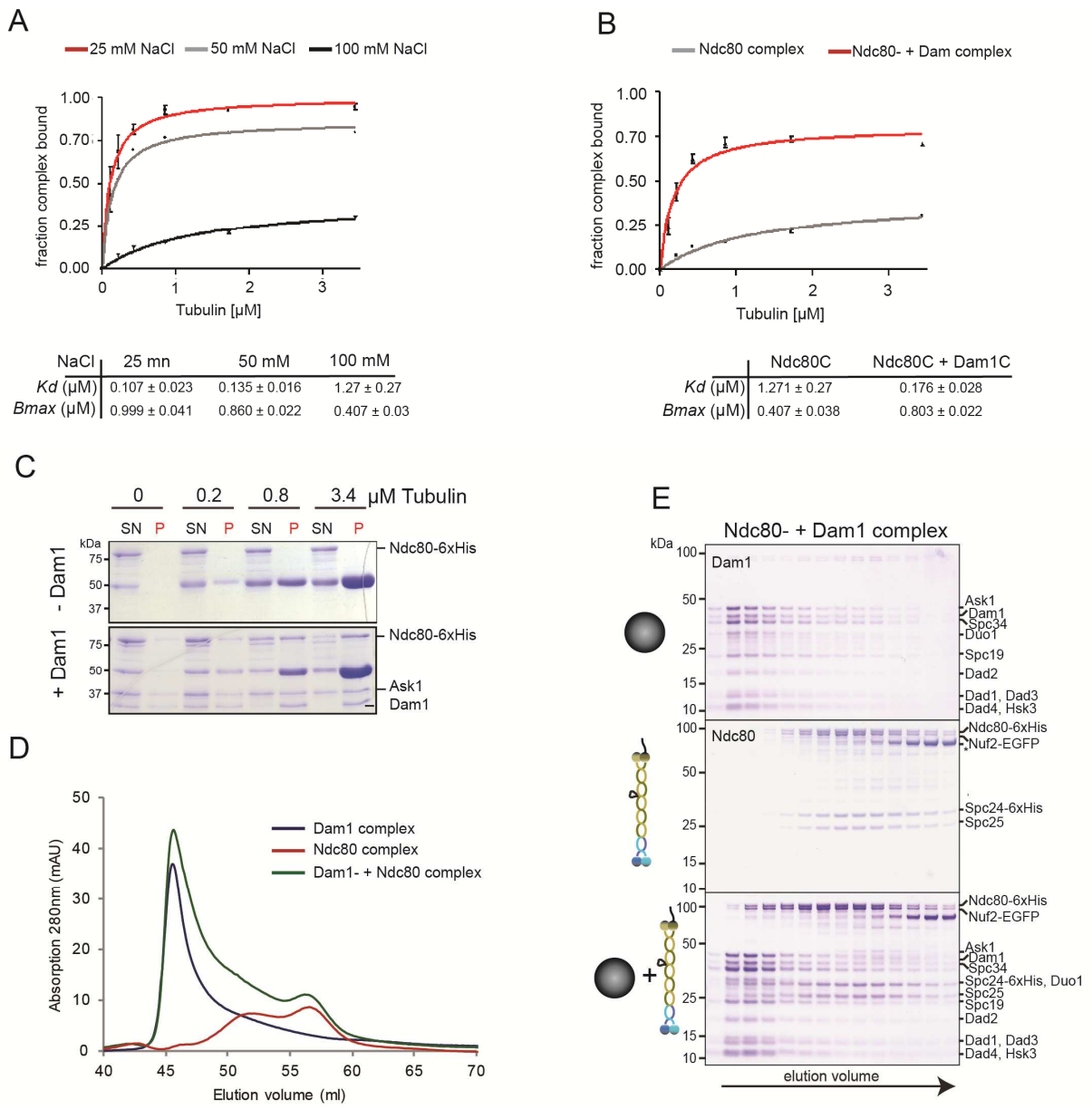

NaCl	25 mn	50 mM	100 mM
Kd (µM)	0.107 ± 0.023	0.135 ± 0.016	1.27 ± 0.27
Bmax (µM)	0.999 ± 0.041	0.860 ± 0.022	0.407 ± 0.03

	Ndc80C	Ndc80C + Dam1C
Kd (µM)	1.271 ± 0.27	0.176 ± 0.028
Bmax (µM)	0.407 ± 0.038	0.803 ± 0.022

Figure 10: The microtubule affinity of the Ndc80 complex increases under low salt and upon addition of the Dam1 complex. A) In a microtubule cosedimentation assay the Ndc80c-EGFP was fluorescently quantified in the presence of 25, 50 and 100 mM salt (NaCl). The binding affinity curve was generated from three independent experiments. Error bars represent standard deviation and the table below summarizes the *Kd* and *Bmax* values of the binding curve. B) Fluorescence quantification of a Ndc80c-EGFP microtubule cosedimentation assay. The Ndc80c-EGFP *Kd* for microtubule binding was determined in the absence and presence of equimolar amounts of the Dam1c and the Ndc80c in 100 mM NaCl. The Binding curves were generated from three independent experiments, presented with standard error bars and a table of *Kd* and *Bmax*. C) Coomassie stained SDS-PAGE of a microtubule cosedimentation assay with the Ndc80c and Dam1c in 100mM Salt. The amount of Ndc80c in the pellet increases in the presence of the Dam1c. Abbreviation: S – supernatant; P – pellet of the centrifugation. D) Combining the Dam1c and Ndc80c on SEC. Absorbance traces at 280 nm of the individual and combined complexes. E) Identical protein fractions from SEC on a Coomassie stained SDS-PAGE, showing that the Ndc80c and Dam1c do not interact in solution.

4.6 *In vitro* reconstitution of CCAN members

In a mature kinetochore, the microtubule-binding interface needs to be connected to centromeric chromatin. Besides building up a fundamental structure on the centromeric DNA little is known about the specific functions of individual CCAN proteins. The identification of the contact point between the KMN network and the CCAN is therefore of great interest.

The twelve subunit Ctf19 complex (Ctf19c) is subdivided into several stable subcomplexes and it represents the functional homolog of the CCAN (De Wulf et al., 2003; Schleiffer et al., 2012). In budding yeast only two Ctf19c proteins are essential for viability, namely Ame1 and Okp1. With the help of diploma student Michael Maier I started a partial reconstitution of the Ctf19c and analysed its composition. First, we reconstituted a core subcomplex of the Ctf19c consisting of **C**tf19, **O**kp1, **M**cm21 and **A**me1, called the COMA complex, by coexpression in *E. coli*. After coexpression and purification via a 6xHis tag on the Ame1 subunit, four bands were resolved on a 20 cm long 10% SDS-PAGE and the corresponding proteins were assigned by mass spectrometry (Figure 11 A).

Previous analysis of epitope-tagged COMA subunits in yeast extracts have suggested the presence of an Ame1-Okp1 and a Ctf19-Mcm21 subcomplex (De Wulf et al., 2003). Taking into account metazoan CCAN-subcompositions, genetic interactions studies and homology relationships between CCAN and Ctf19c, we derived a possible existence of a Chl4-Iml3 subcomplex. We were able to purify three stable heterodimers: the AO complex (Ame1-Okp1), the CM complex (Ctf19-Mcm21) and the CI complex (Chl4-Iml3) (Figure 11 B-D). Coexpression of the COMA with the CI complex in bacteria led to an isolation of the stable hexameric complex COMA-CI coeluting from SEC (Figure 11 E). Estimating the band intensity on Coomassie-stained SDS-PAGEs indicated the presence of stoichiometrical ratios between the COMA-CI, COMA, AO and CI subunits. In contrast, the Ctf19-Mcm21 ratio seemed to be 2:1 (Figure 11 A-E).

The metazoan CCAN includes also the essential protein CENP-C. I was able to recombinantly purify the *S. cerevisiae* CENP-C homolog Mif2 from bacteria (Figure 11 F).

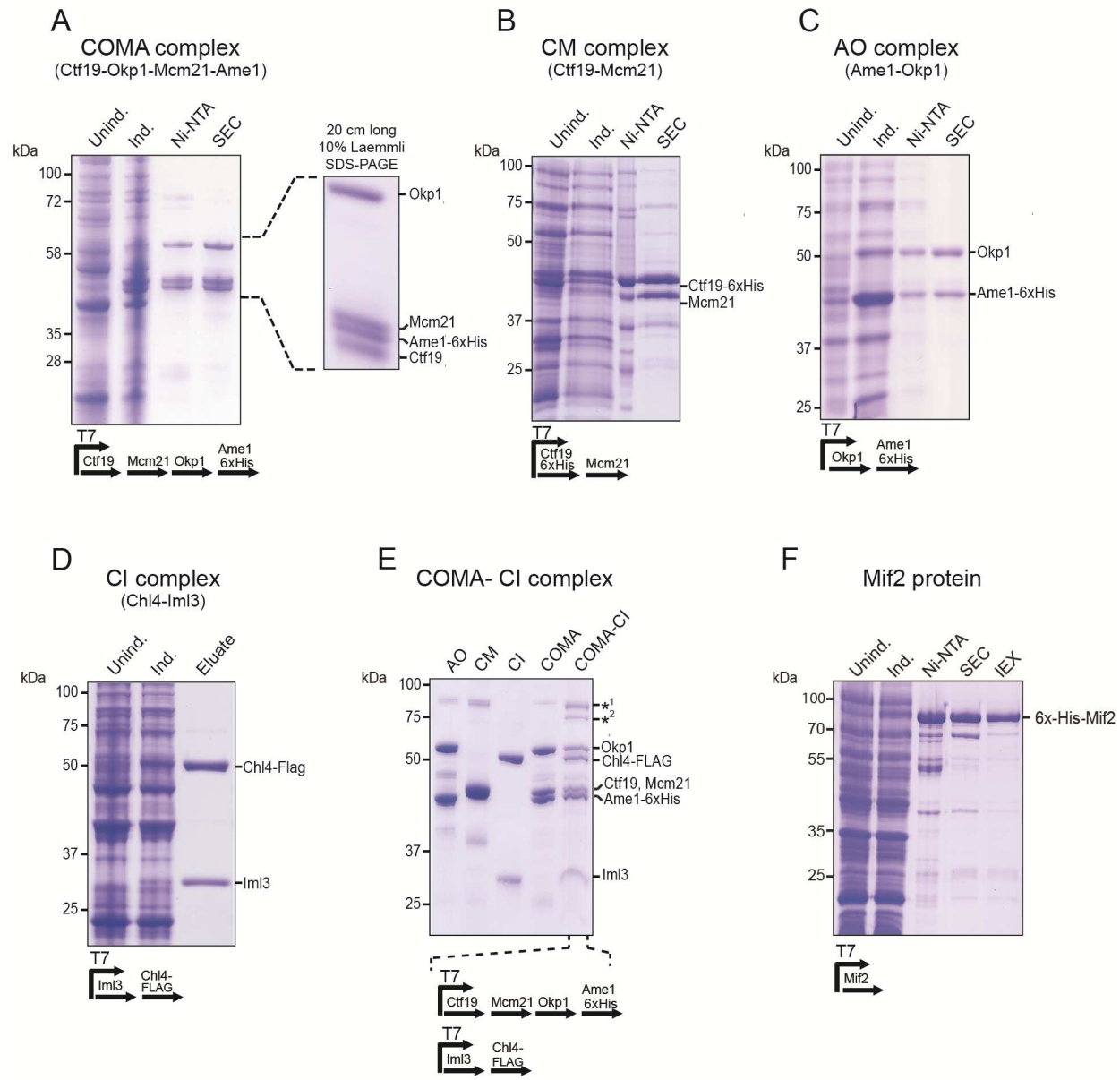

Figure 11: Reconstitution of CCAN components in *E. coli*. A-F) Expression and purification strategies for different Ctf19 subcomplexes and the Mif2 protein on Coomassie stained SDS-PAGEs. Unind, Ind indicates before and after induction with IPTG. After elutions from the affinity beads denotes Ni-NTA. **A**) COMA (Ctf19, Okp1, Mcm21, Ame1). The four subunits were resolved on a 20 cm long SDS-PAGE; **B**) CM (Ctf19, Mcm21), a COMA subcomplex; **C**) a second COMA subcomplex, called AO complex (Ame1, Okp1); **D**) CI complex (Chl4, Iml3); **E**) COMA and CI complex were coexpressed from separate T7 promoters in bacteria and purified via FLAG M2 beads. This indicates that COMA and CI form a larger assembly. Asterisk 1 and 2 probably indicate *E. coli* Hsp70 chaperone. **F**) Purification strategy of the Mif2 protein.

4.7 The Mtw1 complex associates with the Ctf19 complex to establish a connection towards the inner kinetochore

Fluorescence colocalisation studies of kinetochore proteins placed the Mis12/Mtw1 complex in close proximity to the kinetochore-centromere interface (Joglekar et al., 2009). In humans the conserved CCAN component CENP-C associates directly via a conserved N-terminal motif to the Mis12c (Screpanti et al., 2011), and a similar CENP-C-Mis12 interaction has been reported in flies (Przewloka et al., 2011). In *S. cerevisiae* the point of contact between KMN and CCAN is still unknown. Affinity purification of epitope-tagged Mtw1c from yeast extracts copurified all members of the Ctf19c and also the protein Mif2. However, extensive tests failed to detect any interaction of recombinant Mtw1c and bacterially expressed Mif2 using pull-down assays and SEC (data not shown).

A second potential link of Mtw1c to the centromere was the core Ctf19c, the COMA. Therefore I performed pull down assays with COMA and the Mtw1c. In parallel I tested the kinetochore complexes Dam1 and Ndc80 for COMA binding (Figure 12 A+B). To this end, different amounts of FLAG tagged COMA was incubated with affinity beads and with recombinant Mtw1c, Ndc80c, or Dam1c. After washing, bound proteins were eluted with FLAG peptide. While the Ndc80c and Dam1c did not coelute with COMA, the Mtw1c interacted with COMA in a concentration dependent manner.

To verify the result I performed a reciprocal experiment in which Ni-NTA beads contained different amounts of 6xhistidine tagged Mtw1c, Ndc80c or Dam1c, whereas COMA was added at a constant concentration. Interaction with COMA was only detectable in the Mtw1c pull down experiment (Figure 12 B).

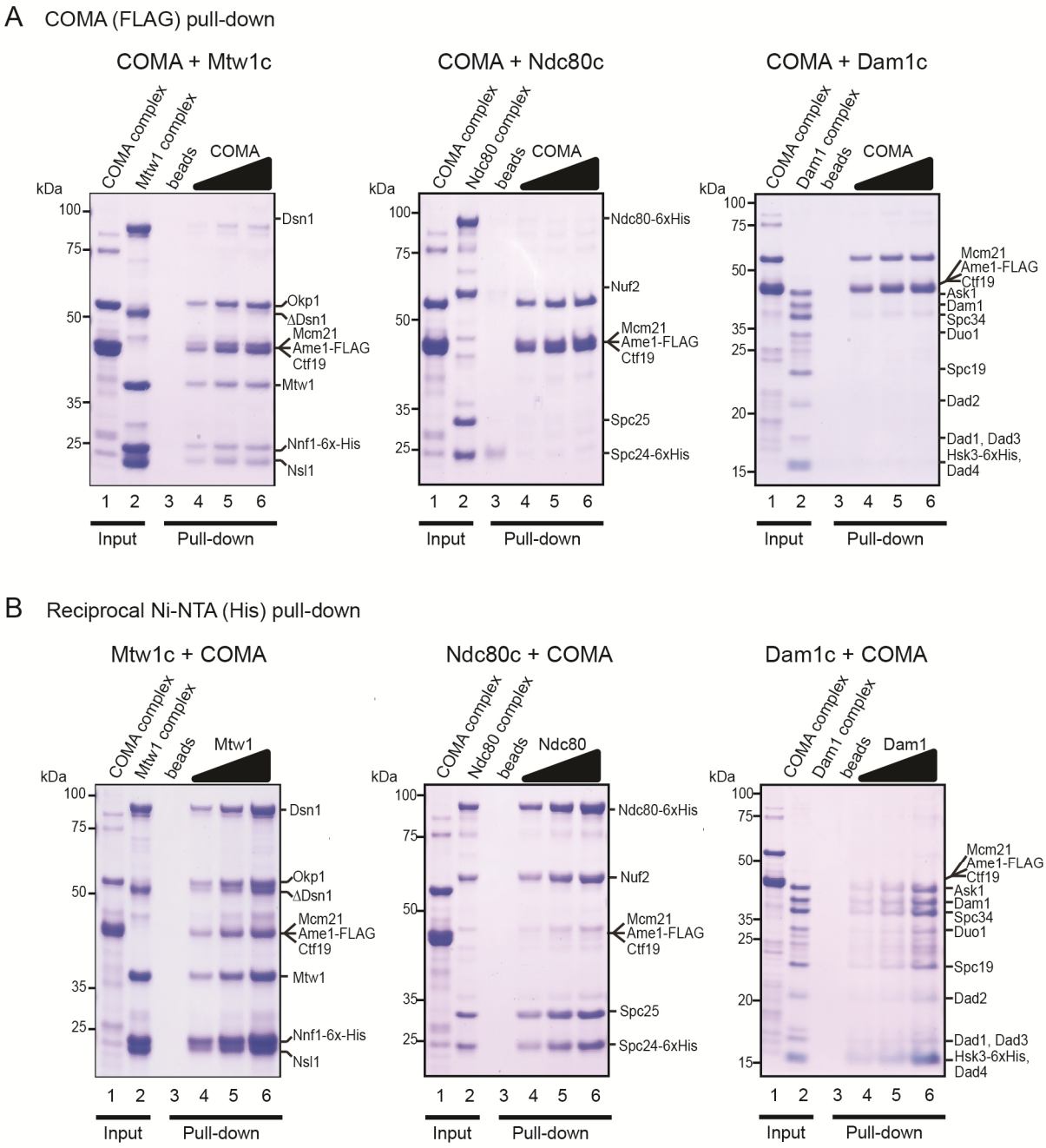

Figure 12: COMA interacts with the Mtw1 complex but not with the Ndc80- and Dam1 complexes. A) Affinity pull down assays with FLAG tagged COMA and 6xhistidine tagged Mtw1c, Ndc80c, Dam1c. Lane 1) Input COMA; lane 2) Input Mtw1c, Ndc80c or Dam1c. Lane 3) In a control experiment M2 beads were only incubated with the respective 6xhistidine tagged complexes Mtw1, Ndc80 or Dam1. Lane 4-6) Anti-FLAG M2 beads were incubated with increasing molarities of COMA and a constant molarity of Mtw1c, Ndc80c and Dam1c. Beads were washed and proteins were eluted with Flag peptide. Note, that only the COMA coelutes with Mtw1c. B) Reciprocal experiment to (A) by using Ni-NTA beads. Different amounts of Mtw1c, Ndc80c and Dam1c were incubated with constant amount of COMA complex. Denotations of lanes are identical as in (A). Proteins were eluted with imidazole from Ni-NTA beads. Consistently, the experiments showed only the association of the COMA with the Mtw1c but not with the Dam1c or the Ndc80c.

A more stringent method to test physical interactions is SEC. Therefore, I analysed the interaction further by SEC, showing Mtw1c and COMA also coeluted even under these conditions (Figure 13 A+B).

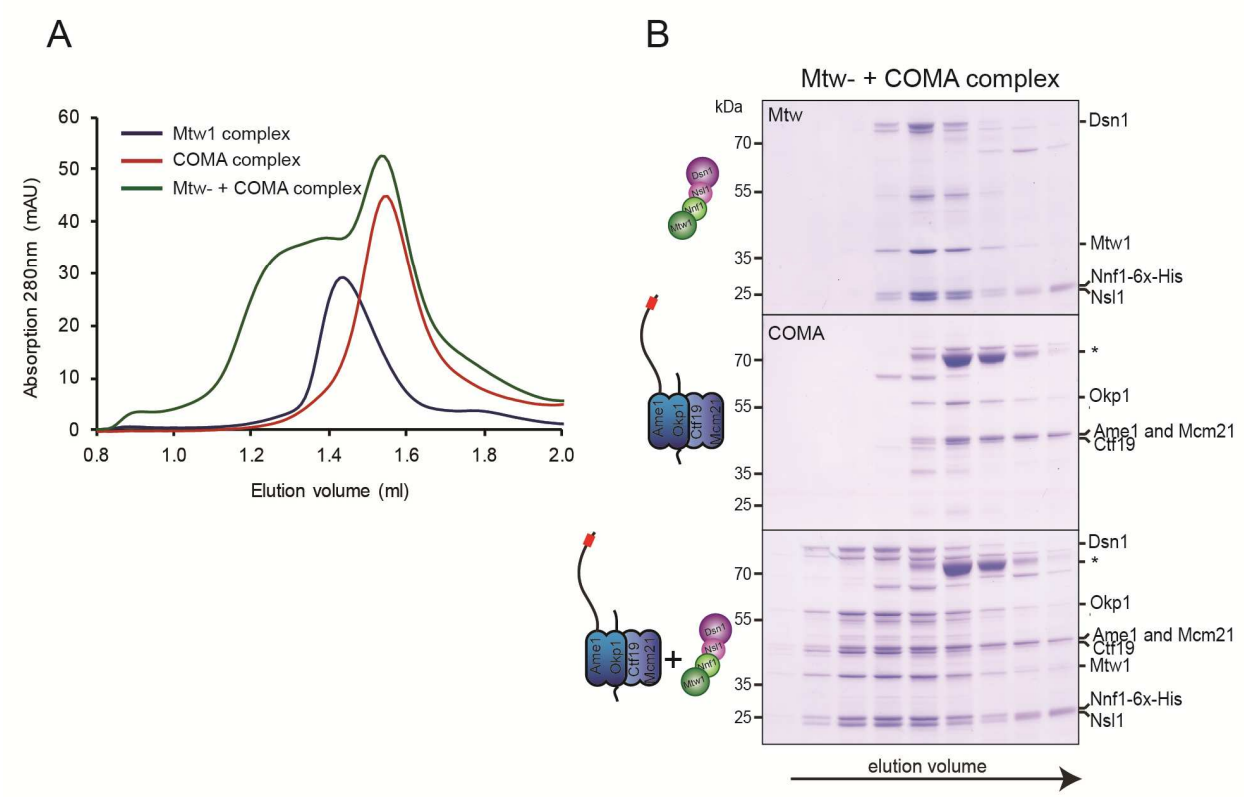

Figure 13: SEC of the COMA-Mtw1c interaction. A) Individual SEC runs of Mtw1c, COMA and in combination (5µM). B) Respective fraction from the individual SEC runs on Coomassie stained SDS-PAGEs. Asterisk indicate *E. coli* Hsp70 chaperone

The existence of the two Mtw1 subcomplexes Mtw1-Nnf1 (MN) and Dsn1-Nsl1 (DN) allowed me to constrain the Mtw1c-COMA contact point to one of the two subcomplexes. I separately tested the MN and DN complexes for the association with COMA in a pull down assay. This clearly identified MN as a more efficient binding partner, whereas DNc barely bound COMA (Figure 14).

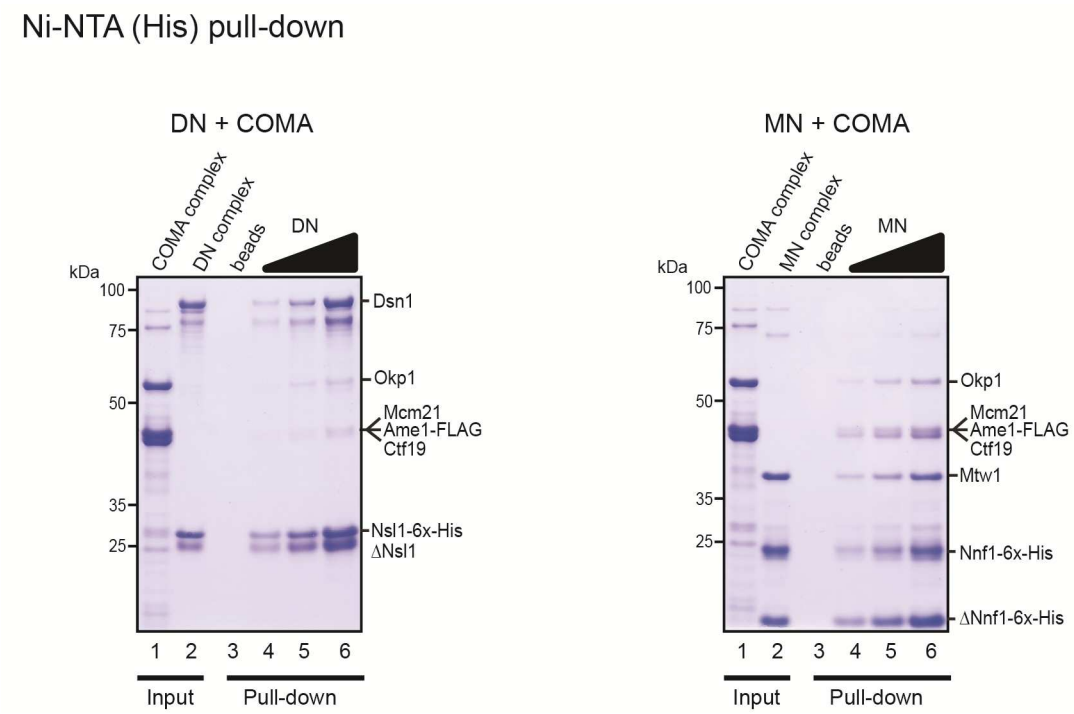

Figure 14: COMA interacts with the Mtw1 complex subunits Mtw1 and Nnf1. C) Pull down experiments were performed as in Figure 12 B. C) By using Ni-NTA beads 6xhistidine tagged MNc and DNc were combined with FLAG tagged COMA and eluted with imidazole. Note that COMA is mainly pulled down with the MN complex.

4.8 Direct binding of the AO complex to the Mtw1 complex

The previous experiments have indicated that COMA is composed of two stable subcomplexes Ame1-Okp1 (AOc) and Ctf19-Mcm21 (CMc) that can be separately expressed and purified from bacteria (Figure 11 B + C). These two stable subcomplexes could be used to reveal which subunits are responsible for Mtw1c binding. Therefore I asked whether one of the two COMA subcomplexes is sufficient to bind to the Mtw1c by analyzing the interaction of the Mtw1c with either the AOc or the CMc during SEC. Indeed, the Mtw1c and AOc physically associated and formed a higher molecular weight complex, containing all six subunits in apparently equal stoichiometry (Figure 15 A+B). In contrast, no binary complex emerged with the Mtw1c and the CMc (Figure 15 C+D). This indicates that the AOc, representing the two essential subunits, is responsible for physically linking COMA with the Mtw1c. This may explain the essential role of Ame1 and Okp1 at the kinetochore.

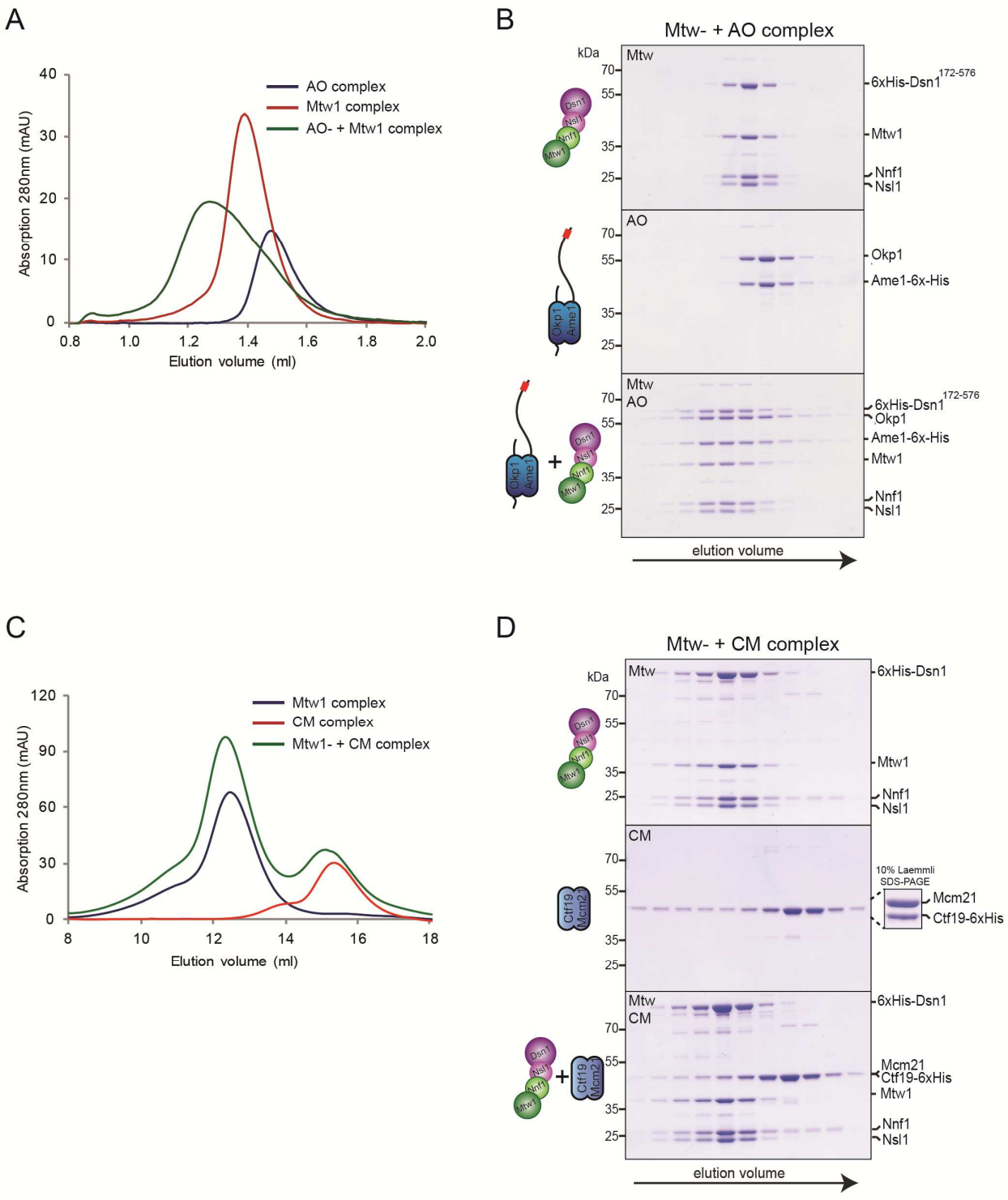

Figure 15: The Ame1-Okp1 heterodimer provides the centromeric link to the Mtw1 complex. A) SEC analysis shows that the Mtw1c and the AOc form a higher molecular weight species when mixed stoichiometrically compared to the individual complexes (8µM). This indicates the formation of a stable Mtw1c-AO binary complex. B) Coomassie-stained SDS-PAGE from consecutive SEC elution fractions shown in A. C) SEC elution profile from the Mtw1c, the CMc and their stoichiometric combination (14 µM). D) SDS-PAGE analysis from the elution profile shown in C. Note that CMc was unable to associate with the Mtw1c.

4.9 The Ame1 subunit directly binds the MN complex

Pull down experiments demonstrated the preferred association of COMA to the MNc and analytical SEC showed that the AOc binds directly to the Mtw1c, revealing that the COMA-Mtw1c interaction is mediated by the MN and AO subcomplexes.

To further dissect the COMA-Mtw1 interface, I coexpressed the MNc-6xHis with a FLAG tagged version of Ame1 or Okp1 and asked which of the individual COMA subunits are able to bind to MNc. In previous attempts I observed, that single subunits of COMA were barely soluble when expressed alone in bacteria, while coexpression with their complex partners strongly increased solubility. Strikingly, after co-expression and purification via a Flag-tag on Ame1, I stoichiometrically copurified the MNc indicating that the Ame1 subunit provides the direct link between COMA and the Mtw1c (Figure 16). In contrast, Okp1-FLAG did not associate with the MNc-6xHis. These results suggest a direct contact of the MNc subunits with the kinetochore-centromere interface. Interestingly, in a human colocalization study Nnf1 was placed most centromere proximal among all Mtw1c subunits (Wan et al., 2009).

In summary, I first identified the interaction between COMA and the Mtw1c. Second, I showed that the MNc and AOc are necessary for their interaction and third, the Ame1 subunit is sufficient to bind to the MNc.

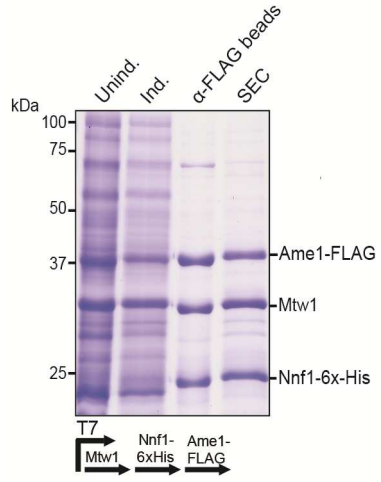

Figure 16: The Ame1 subunit directly associates with the MN complex. All three subunits were coexpressed from the pST39 vector. Unind. indicates before and Ind. after induction with IPTG. α-FLAG M2 Affinity beads (Sigma) were used to purify the Ame1-FLAG subunit while the MNc was copurified. Proteins were eluted with 3xFLAG peptide. The ternary complex also stably eluted from SEC.

4.10 The AO- and the Ndc80 complex bind the Mtw1 complex noncompetitively

The KMN network has to be stably integrated into the centromere associated network in order to allow force transmission from the disassembling microtubule to the chromosome. In the next analysis I asked whether the AOc binding to the Mtw1c was compatible with the Mtw1c-Ndc80c association. COMA was unable to bind to Ndc80c on its own (Figure 12 A), however in the presence of the Mtw1c a ternary complex was formed. In this experiment I used the AOc instead of COMA due to simplification. The AOc-Mtw1c-Ndc80c interaction appears stoichiometric. This result suggests that the AOc-Mtw1c association is compatible with the Mtw1c-Ndc80c interaction.

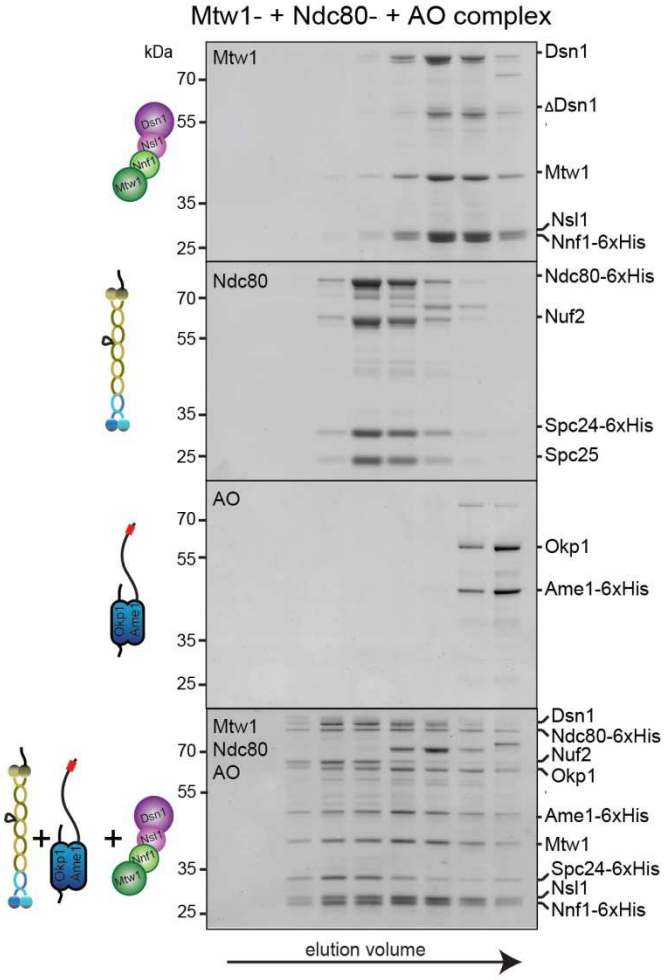

Figure 17: The AO-Mtw1 complex interaction is compatible with the Mtw1-Ndc80 complex interaction. Consecutive elution fractions from SEC on Coomassie-stained SDS-PAGEs. The ternary multi-complex formation of AOc-Mtw1c-Ndc80c is indicated by a shift. All 10 subunits coeluted stoichiometrically.

4.11 The AO complex binds to DNA

CCAN members are considered to generate a platform on the centromeric DNA for kinetochore assembly, thus some proteins contain intrinsic DNA binding properties (Takeuchi and Fukagawa, 2012). The human proteins CENP-W and CENP-T form together a DNA binding complex and also the Mif2 protein, the budding yeast homolog of CENP-C, associates with DNA *in vitro* (Cohen et al., 2008; Hori et al., 2008a).

During the COMA, AO-, CI- and CM complex purification we observed the association of bacterial DNA with the complexes. Therefore, I initially tested whether AO possesses a DNA binding ability. Centromeric (Cen) DNA fragments derived from yeast chromosome V (230 bp in length) or salmon sperm (SS) DNA, sheared by sonication to approximately 250 bp, were incubated with the AOc and analysed under nondenaturating conditions with an electrophoretic mobility shift assay (EMSA). The agarose gel was stained with Ethidium bromide and later with Coomassie to analyse the co-migration of DNA and proteins. I observed a shift of both CEN-DNA and SS-DNA to a higher migrating species upon incubation with AOc demonstrating the DNA binding properties (Figure 18). The ability to bind the random SS-DNA indicates that AOc probably does not specifically recognize CEN-DNA.

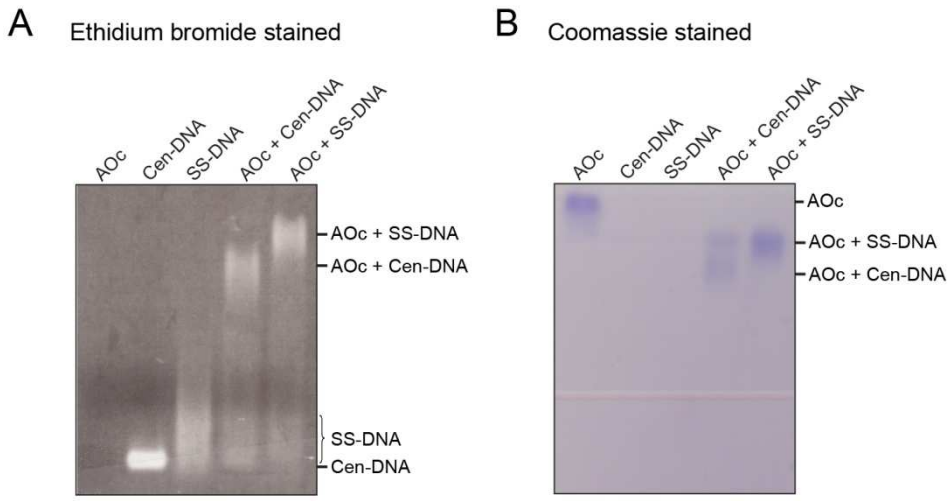

Figure 18: AO complex binds to DNA. A) 200 ng of centromeric DNA (Cen-DNA) or salmon sperm DNA (SS-DNA) were analyzed on an agarose gel individually or in combination with 0.8 µM AOc. Afterwards the gel was stained with Ethidume-bromide. In the presence of AOc the Cen-DNA as well as the SS-DNA migrated slower indicating the formation of an AOc-DNA complex. B) Agarose gel shown in A was stained with Coomassie. Compared to the AOc alone, AOc with DNA migrated faster.

4.12 Identification of a conserved N-terminal motif in Ame1

Very recently, advanced bioinformatic analysis has demonstrated the homology relationship between centromere associated proteins of *S. cerevisiae* and higher eukaryotes (Schleiffer et al., 2012). This analysis has shown that Ame1 and Okp1 are the budding yeast homologs of human CENP-U and CENP-Q, respectively. Both proteins contain an evolutionary conserved C-terminal or central domain, which is required for their heterodimerization (Francesca Malvezzi, personal communication) and they additionally have unstructured tail domains whose function is unknown (Schleiffer et al., 2012) (Figure 19 A).

Using the motif search program MEME a short conserved motif was detected at the extreme N-terminus of Ame1. A similar motif is present in Mis17, the Ame1 homolog of *S. pombe*, but its conservation in human CENP-U is at this point unclear. The 15 amino acid long motif is predicted to fold into an α-helix with several conserved positively charged residues followed by a conserved glycine residue (Figure 19 A+B).

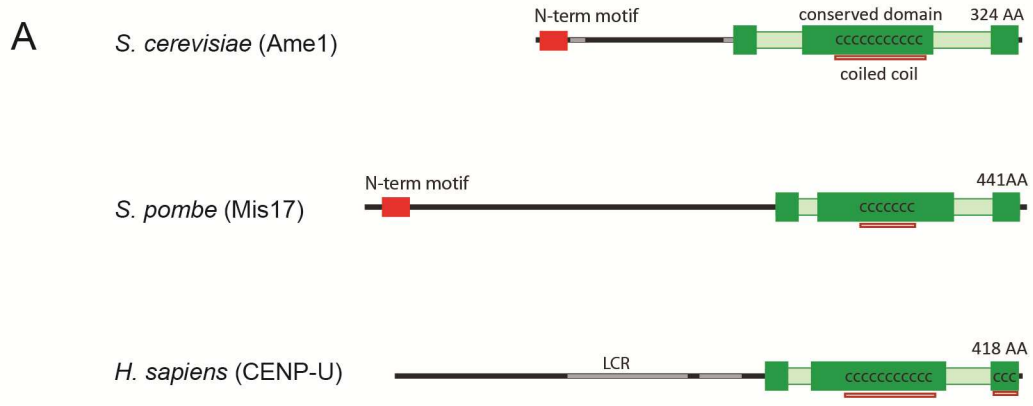

Figure 19

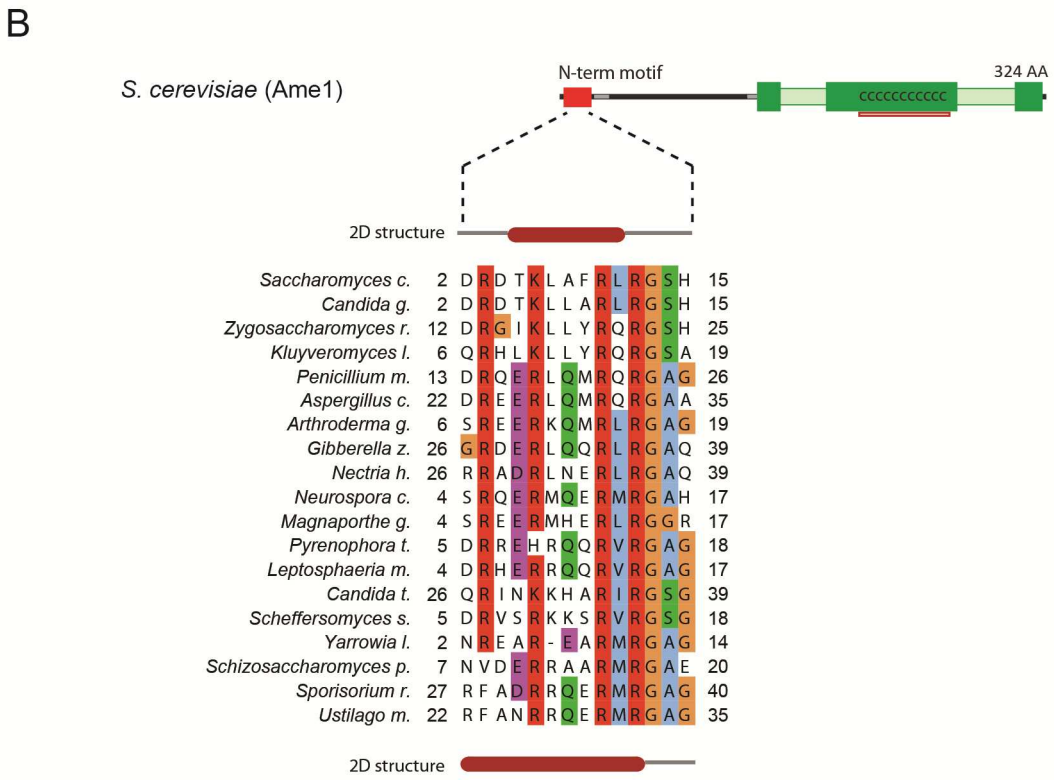

Figure 19: The Ame1 N-terminus contains a conserved motif. A) Ame1, Mis17 and CENP-U are homologous proteins and have a similar architecture. Mis17 and Ame1 display a short motif at the extreme N-terminus (red) and all three homologs have a conserved C-terminal domain (green). Polar regions of low complexity are in grey. The coiled-coil regions are labeled with a red bar. Illustration is adapted from Schleiffer et al. (Schleiffer et al., 2012). B) Multiple sequence alignment of conserved N-terminal motifs in fungal Ame1 homologs. Note that besides the glycine the majority of highly conserved residues are positively charged amino acids. Secondary structure predictions suggested an 2D structure of an α-helix present in the motif of S. cerevisiae (top) and *U. maydis* (bottom).

4.13 The N-terminal motif of Ame1 is required for Mtw1 complex binding

I speculated that this N-terminal motif may be involved in the binding to the Mtw1c. To test this hypothesis I deleted the first 15 residues of Ame1 and tested whether the AOc still associates with MNc on a SEC. In contrast to the wild type complex, the AOc lacking the 15 conserved residues of Ame1 failed to stably associate with the Mtw1c (Figure 20 A-D).

These results imply that the motif is indeed necessary for a stable association between COMA and the Mtw1c *in vitro*.

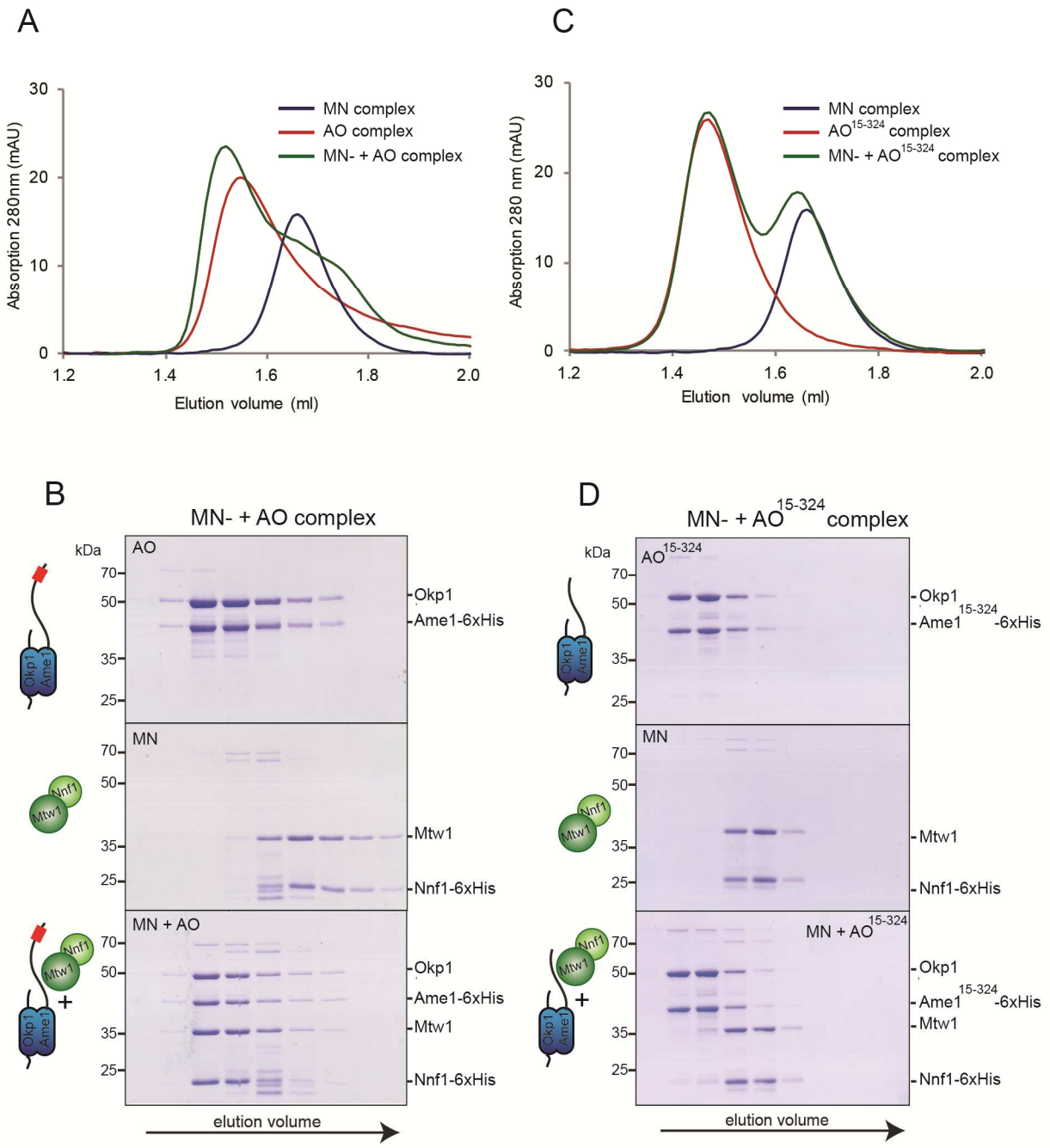

Figure 20: Deletion of the N-terminal Ame1 motif abolishes the interaction with the Mtw1 complex. A+B) SEC elution profile and the corresponding SDS-PAGE analysis of the MNc and the full length AOc. Mixing AO and MN result in stoichiometric binary complex. C+D) Identical analysis as in A+B with the exception that Ame1 lacks the 15 N-terminal residues (Ame1$^{15-324}$). Ame1$^{15-324}$ is unable to stably bind to the MNc. Note that it seems that the AO$^{15-324}$ has still some remaining capability for MN binding, since small amount of the MNc is shifted towards an earlier elution volume.

4.14 The Ame1 motif is essential for *S. cerevisiae* viability

Collectively, the biochemically data pointed to the AO heterodimer being a crucial binding partner for Mtw1c thus linking a centromere associated protein to the KMN network. In particular, the Ame1 subunit alone was sufficient for Mtw1c binding and a conserved motif at the extreme N-terminus of Ame1 was absolutely necessary to provide a strong association *in vitro*.

Depletion of Mtw1c/Mis12c subunits in budding yeast and human resulted in a recruitment defect for the outer kinetochore complexes Ndc80 and Dam1 and the mutants failed to establish biorientation (Kline et al., 2006; Scharfenberger et al., 2003). I assumed that a defective kinetochore recruitment of the Mtw1c, in mutants with a compromised Mtw1c-AOc interaction, would lead to a severe growth phenotype.

To test this, I employed a conditional approach using the anchor-away (AA) technique for kinetochore proteins (Haruki et al., 2008). This technique takes advantage of the closed mitosis in budding yeast by anchoring away proteins from the nucleus into the cytoplasm. Thus, the anchored protein cannot exert its normal function anymore. Wild-type or mutant alleles of the respective protein that cannot be anchored away are then used to analyze phenotypes. In a haploid strain the endogenous copy of Ame1 was fused to the human mTOR domain (FRB) which heterodimerizes with the ribosomal anchor (RPL13A-FKBP12) in the presence of Rapamycin thereby transiting Ame1-FRB from the nucleus into the cytoplasm (Figure 21 A).

Ame1 is an essential gene and consequently the AA strain carrying the Ame1-FRB fusion protein was inviable in the presence of Rapamycin. Importantly, growth was restored by the expression of wild type Ame1^{WT} from an extrachromosomal centromeric plasmid. In contrast, cells expressing an Ame1 mutant lacking the first 15 amino-acids failed to rescue the lethality in the presence of Rapamycin (Figure 21 B).

With strains carrying stably integrated Ame^{WT}-6xFLAG and Ame1$^{15-324}$-6xFLAG in the URA3 locus under control of the endogenous Ame1 promoter I confirmed similar expression levels of wild-type and mutant protein (Figure 21 C).

Tetrad dissection of stably integrated Ame^{WT} or Ame1$^{15-324}$ in a heterozygous Ame1 knock out strain further verified the lethality of spores harboring Δame1/Ame1$^{15-324}$ alleles (Figure 21 D). In contrast spores with the genotype of *Δame1*/Ame^{WT} recovered growth.

Thus, the biochemically characterized AOc-Mtw1c interaction is critical *in vivo*. Its abolishment yields a lethal phenotype and these findings demonstrate the essential role for the N-terminal Ame1 motif in budding yeast.

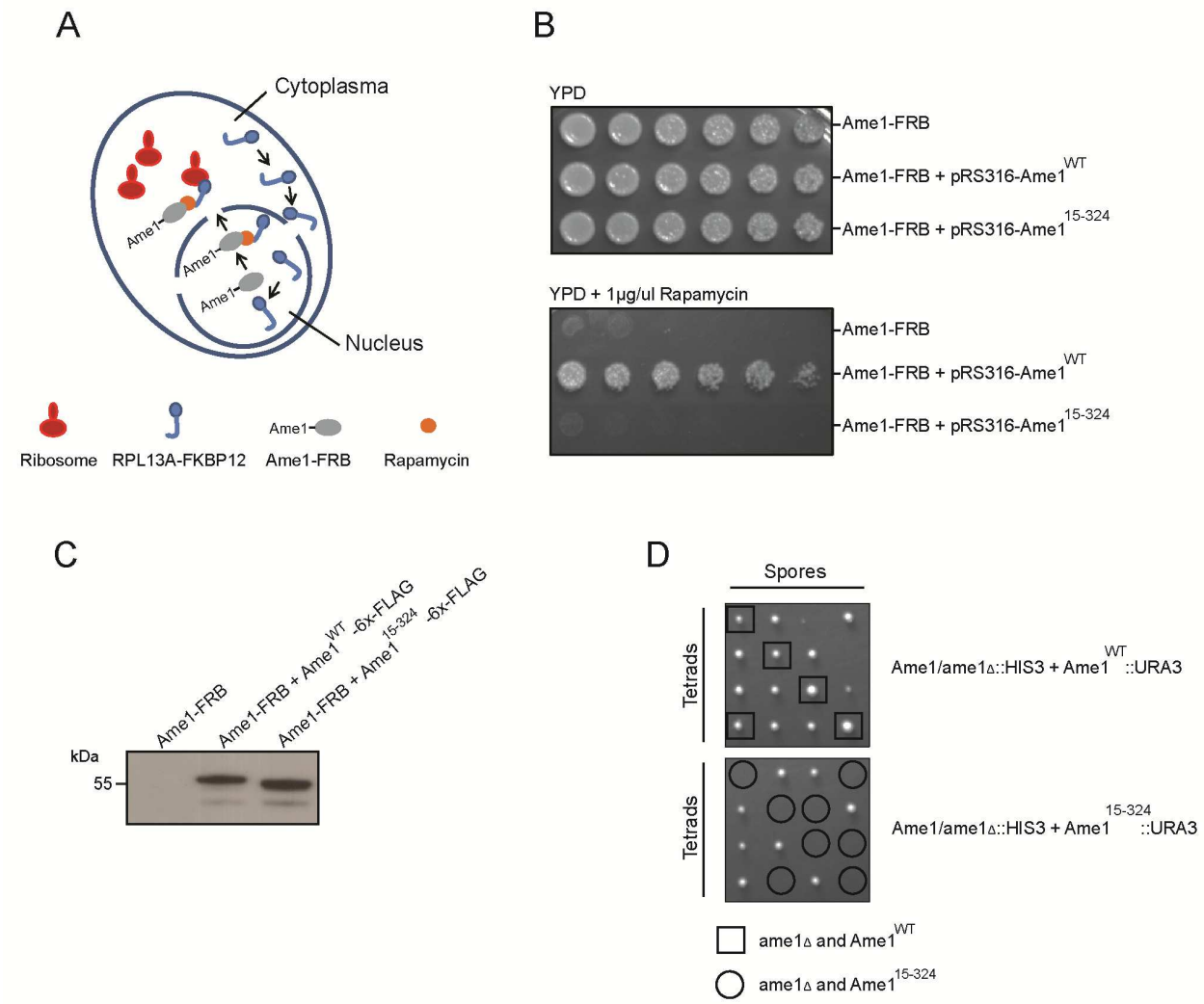

Figure 21: The Ame1 N-terminal motif is essential for viability in budding yeast. A) Schematic illustration of the anchor away (AA) technique. The ribosomal anchor protein RPL13A is fused to FKBP12. The RPL13A-FKBP12 shuttles in and out of the nucleus. The endogenous Ame1 protein is fused to a FRB domain that associates with the FKBP12 domain upon Rapamycin addition. The complex is subsequently transported into the cytoplasm, where it anchors to ribosomes, leaving back the mutant allele of Ame1 or Ame1^{WT} as control. Adapted from Haruki et al. (Haruki et al., 2008). B) Spot assay of the AA background strain containing Ame1-FRB, Ame1-FRB with either Ame1^{WT} or Ame1$^{15-324}$, expressed from a centromeric plasmid. Ame1^{WT} restores growth in the presence of Rapamycin whereas Ame$^{15-324}$ is lethal. This assay was also conducted with stably integrated Ame1^{WT} or Ame1$^{15-324}$ copy expressed from the endogenous promoter showing identical results. C) Western blot analysis of whole cell extracts testing for the expression of stably integrated Ame1^{WT} or Ame1$^{15-324}$ alleles. D) Tetrad dissection of a heterozygous *Δame1* strain with a stably integrated Ame1^{WT} (upper) or Ame1$^{15-324}$ (lower) allele. Viable *Δame1*/Ame1^{WT} spores are highlighted with a square. The *Δame1*/Ame1$^{15-324}$ spores, highlighted by a circle, failed to grow indicating that the deletion of the first 15 amino-acids is lethal.

In order to investigate the contribution of individual amino acids within the motif, I systematically mutated conserved arginine (R) residues R3, R10, R12 to either alanine (A) or aspartic acid (D). By using the AA technique Ame^{WT}, Ame1$^{15-324}$ or the respective single mutants were analysed. While the Ame1 R3D mutation did not affect viability, introducing a negative charge at position 10 or 12 was lethal similar to the complete lack of the Ame1 N-terminal motif (Ame1$^{15-324}$). However, the exchange to the neutral amino-acid alanine at positions 10 and 12 restored wild-type growth (Figure 22). This highlights the importance of the conserved arginine residues R10 and R12 for Mtw1c binding suggesting that these residues participate at the interacting interface.

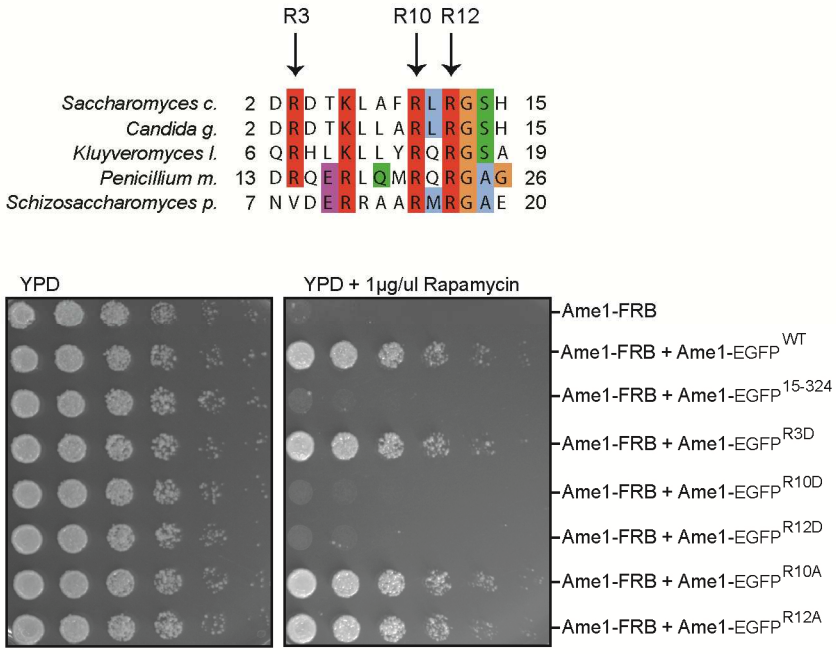

Figure 22: The conserved arginine residues in the Ame1 motif are essential for viability. (Top) Multiple sequence alignment of the N-terminal Ame1 motif showed in Figure 19. Arrows indicate which residues were selected for the introduction of point mutations. (Bottom) AA spot assay with strains carrying single point mutations in the Ame1 motif. R3, R10 or R12 were replaced with a negative (aspartic acid - D) or a neutral (alanine – A) charge. Strains rescued with Ame^{WT} restored growth in the presence of Rapamycin. Similarly to the Ame$^{15-324}$ the point mutations in residues R10D and R12D were lethal. Both R10A and R12A mutation restored wild type growth as well as the R3D mutant.

4.15 A short N-terminal Ame1 fragment is sufficient to bind to the Mtw1 complex

By deleting the N-terminal 15 residues of Ame1 I showed that this motif is necessary for a stable Mtw1c association *in vitro*. In a reciprocal experiment I addressed whether the motif alone is

sufficient for binding to the Mtw1c or whether other structural features of the AOc contribute to the binding.

To this end, I tested the recombinant fragments Ame1$^{1-30}$ and Ame1$^{1-114}$ which were N-terminally fused to Glutathione-S-transferase (GST) for binding to the Mtw1c by SEC. The SEC elution profiles exhibited an unusually low elution volume starting close after the void volume when Mtw1c and GST-Ame1$^{1-30}$ or GST-Ame1$^{1-114}$ were mixed. I observed the formation of a high molecular weight complex and the first fractions contained both Mtw1c and GST-Ame1$^{1-114}$ or GST-Ame1$^{1-30}$, whereas no complex was formed with GST alone. While the Mtw1c-GST-Ame1$^{1-114}$ complex displayed a 1:1 stoichiometry, the GST-Ame1$^{1-30}$ bands appeared diffuse thus the stoichiometry was difficult to estimate (Figure 23 A+B). The unusually high molecular weight despite the relative small contribution of the two short segments (30 to 114 amino-acids) may be explained by the GST dimerization. One GST Ame1$^{1-30}$ or GST-Ame1$^{1-114}$ dimer might be able to bind two elongated Mtw1c resulting in a molecular mass of 350 kDa with a highly extended conformation.

In summary, these observations suggest that the N-terminal Ame1 motif is necessary and sufficient for binding to the Mtw1c.

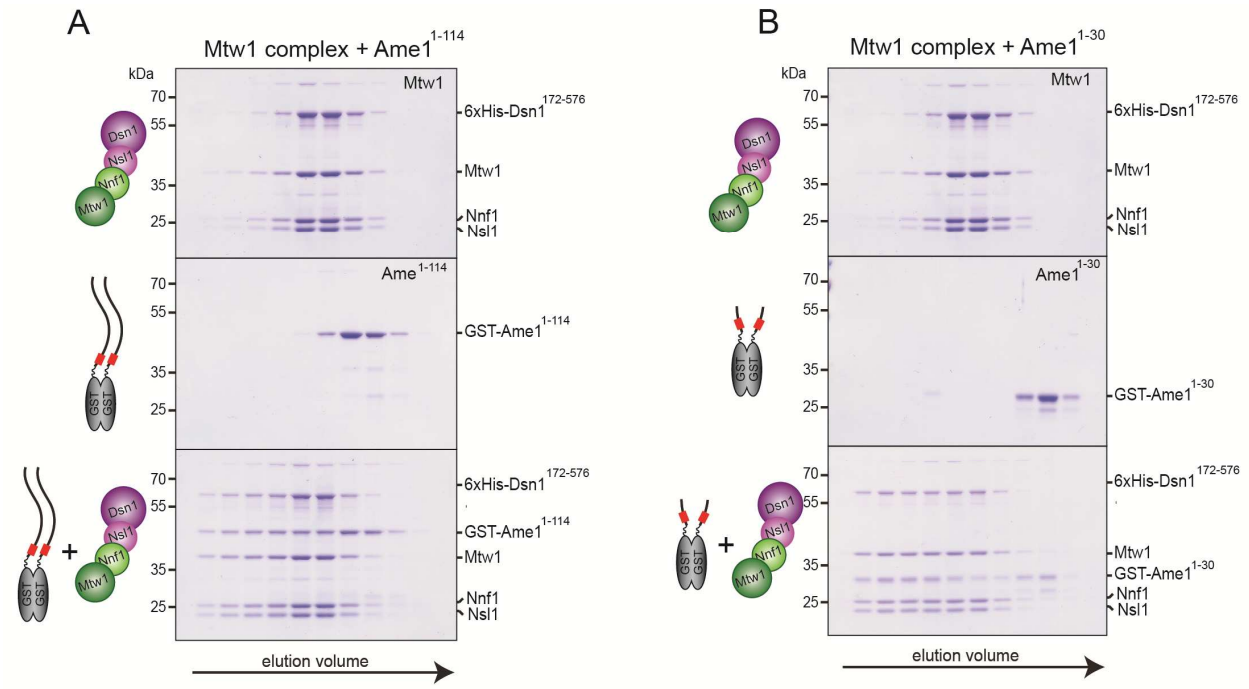

Figure 23: The N-terminal Ame1 motif is sufficient to bind to the Mtw1 complex. Successive elution fractions on Coomassie-stained SDS-PAGEs from SEC analysis. A) Mtw1c + GST-Ame$^{1-114}$; B) Mtw1c + GST-Ame$^{1-30}$. When mixed approximately in equimolar amounts (10µM) Mtw1c and Ame$^{1-30}$ or Ame$^{1-114}$ coeluted.

4.16 Analysis of Ame1 phenotypes *in vivo* using the anchor-away technique

Biochemical data indicate the inefficiency of the Ame1 mutant lacking the N-terminal motif in binding to the Mtw1c. Additionally, conditional assays *in vivo* demonstrated that the Ame1 motif has an essential role for budding yeast viability. Mtw1c is a linker of high importance especially for the assembly of the outer kinetochore. Defects in Mtw1c recruitment to kinetochores result in biorientation errors due to a reduced amount of Ndc80c and Dam1c (Kline et al., 2006; Scharfenberger et al., 2003). Furthermore, since spindle assembly checkpoint (SAC) receptors were found in the KMN network, the outer kinetochore components are necessary for the recruitment of SAC proteins (DeLuca et al., 2003; Kiyomitsu et al., 2011; London et al., 2012). I reasoned that eliminating the Ame1 N-terminal motif might lead to a severe disruption of the kinetochore structure thus resulting in lethality.

To analyze the terminal phenotype of Ame1 mutant cells, I took advantage of the anchor away (AA) strain carrying an Ame1-FRB- and either an Ame^{WT}- or $Ame^{15\text{-}324}$ allele. Cells were arrested in G1 with alpha-factor and synchronously released into Rapamycin containing medium. While Ame^{WT} cells cycled normally in the presence of Rapamycin, $Ame^{15\text{-}324}$ mutants displayed an accumulation of morphologically large budded cells (Figure 24 A). Interestingly, at later timepoints a fraction of the Ame1 mutant cells or those lacking any rescue allele started to re-bud without completing cytokinesis.

To monitor the activity of the SAC, I followed the levels of Pds1 (securin) by western blotting. SAC activation leads to the stabilization of Pds1 level, thus a decrease of the Pds1 level means either that the cells cycle normally or the SAC is defective. After release of G1 arrested cells into Rapamycin, the Pds1 level of the mutant $Ame^{15\text{-}324}$ cycled similar to Ame^{WT} cells indicating the SAC is not activated (Figure 24 B).

From these initial experiments I tentatively conclude that Ame1 mutant cells do not maintain a mitotic checkpoint arrest. One explanation for this phenotype might be an erroneous outer kinetochore assembly which leads to recruitment defects of checkpoint proteins.

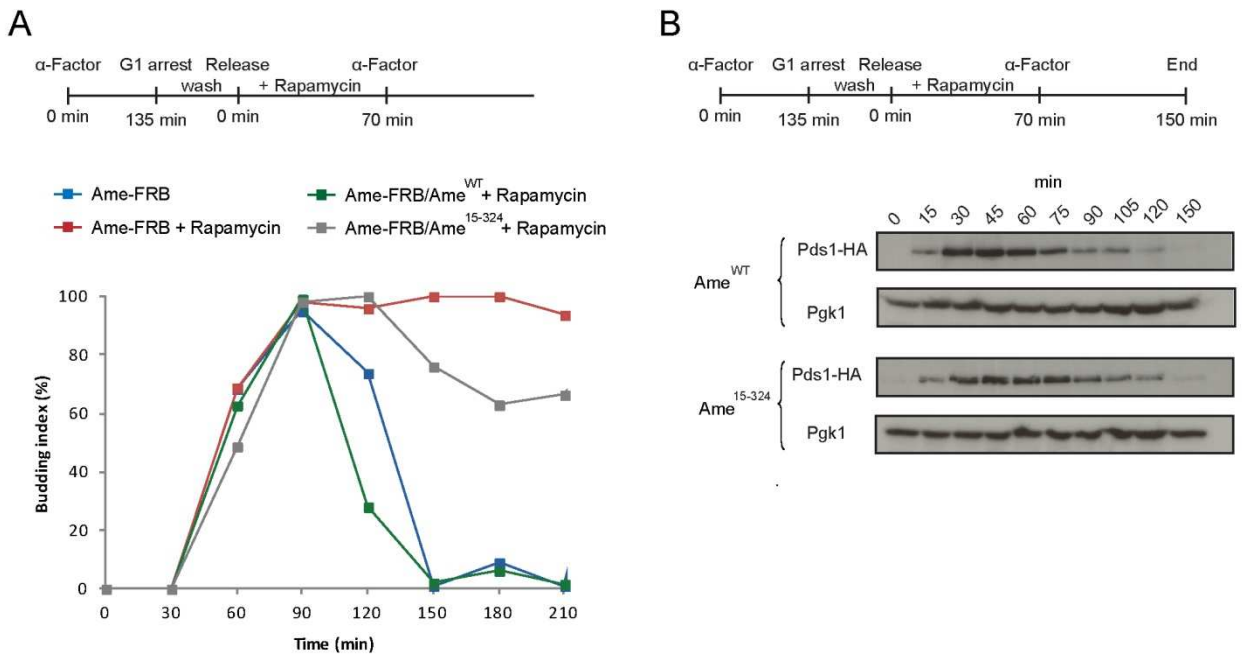

Figure 24: Cells deleted of the N-terminal Ame1 motif show abnormal cell cycle progression and have a defective spindle assembly checkpoint: A) Top - experimental outline. Bottom - cell cycle progression of the Ame1 mutant strain. Cells were arrested in G1 with α-factor and released into Rapamycin containing medium. They were counted for unbudded and large budded cells. 70 min after release new α-factor was added to prevent cells from completing a second cell cycle. Ame-FRB cells completely remained large budded whereas Ame1$^{15-324}$ mutants mainly arrested large budded. Ame^{WT} cycled comparable to control cells (Ame1-FRB without Rapamycin). B) Top - experimental outline. Bottom - western blot analysis of HA tagged Pds1 levels in AA strains carrying either wild-type Ame^{Wt}-6xFLAG or mutant Ame$^{15-324}$-6xFLAG alleles. Whole cell lysates were prepared at the indicated time points and immunoblotted with anti-HA or with the Pgk1 antibody as a loading control.

4.17 The N-terminal interaction motif is important for the kinetochore localization of both Ame1 and the Mtw1 complex

Next, I investigated the localization of Ame1 mutants and respective consequences on the recruitment of other kinetochore components *in vivo*. For this purpose I again made use of the AA technique and generated Ame1-FRB strains that allowed simultaneous imaging of Ame^{WT} or Ame$^{15-324}$ fused to EGFP with either Mtw1- or Mif2-mCherry. All fusion proteins were stably integrated into the genome either at the URA3 (Ame^{WT}-, Ame$^{15-324}$-EGFP) or at the endogenous locus (Mtw1-, Mif2-mCherry). One hour after addition of Rapamycin to logarithmically growing cultures, cells were processed for live cell microscopy (Figure 25 A). The Ame1$^{15-324}$ mutant protein failed to localize to kinetochores at normal levels. Fluorescence quantification revealed a 73% reduction in signal intensity for Ame$^{15-324}$-EGFP compared to normalized Ame1^{WT}-EGFP (Figure 25 C). Strikingly, in the Ame1 mutant cells the Mtw1 signal at kinetochores was

diminished to a proportional extent of 68% compared to the wild-type Mtw1-mCherry signal (Figure 25 C). I also found that the Mif2-mCherrry kinetochore localization was also affected by the deletion of the Ame1 motif, but to a lower extent, with an average fluorescence signal reduction of 29% (Figure 25 B+C).

These observations suggest that the Ame1-Mtw1 complex interaction is critical for proper kinetochore assembly *in vivo*. Its disruption prevents the association of the AOc with kinetochores at a normal level and it also leads to a strongly reduced level of Mtw1c. This severe disruption of kinetochore structure can explain the lethal phenotype of the Ame1$^{15\text{-}324}$ mutant. My observation suggests that the Ame1 subunit critically depends on the Mtw1c for its localization and vice versa. Several studies revealed the hierarchical assembly of kinetochore proteins from the centromere to the microtubules. This result might demonstrate an example of localization interdependency between the CCAN members and the KMN network.

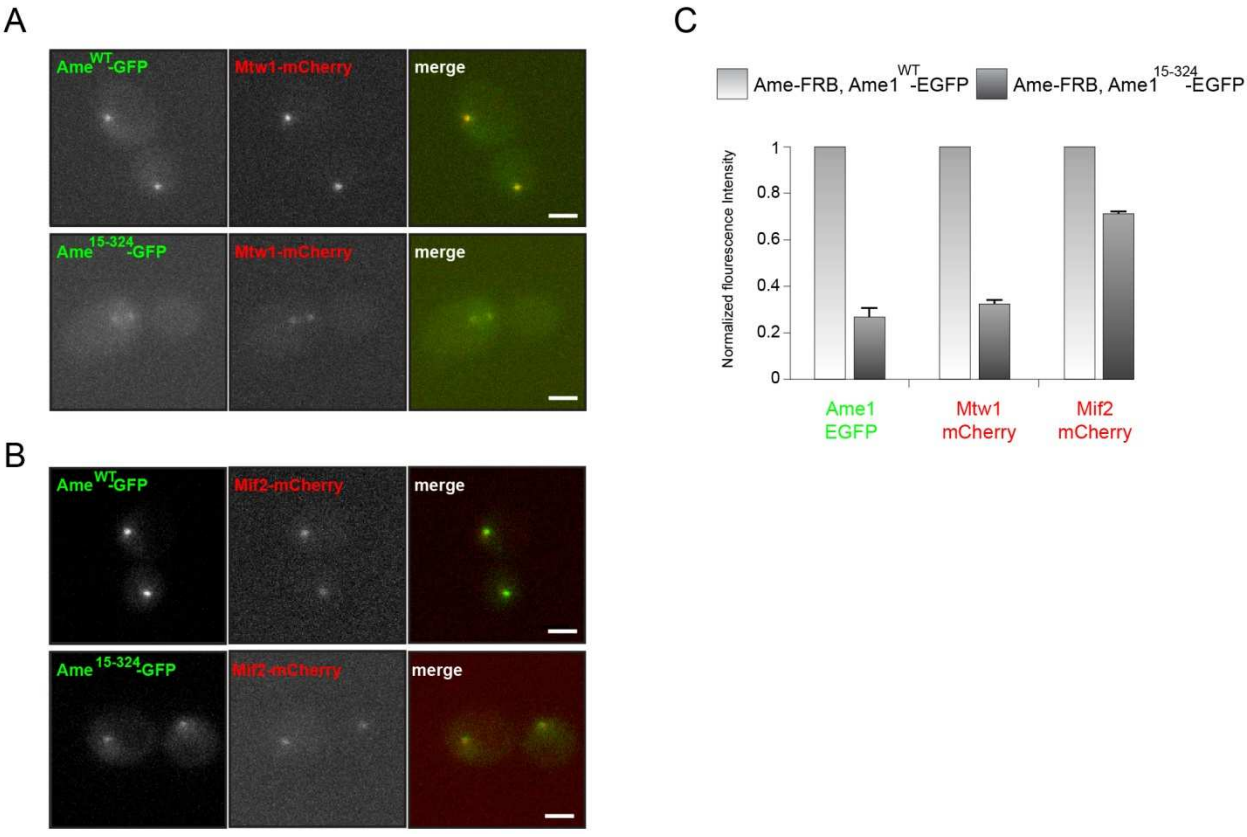

Figure 25: The Ame1 motif is important for Ame1p, Mtw1p and Mif2p kinetochore localization. A+B) Live cell microscopy in an AA background strain carrying an Ame-FRB and stably integrated alleles of Ame^{WT}-EGFP or Ame$^{15\text{-}324}$-EGFP combined with either Mtw1-mCherry or Mif2-mCherry. Scale bar 2 µm. C) Quantification of measured fluorescence intensity. The fluorescence signals of approximately 100 kinetochores were quantified and averaged. EGFP or mCherry signals from cells carrying the Ame1 wild-type allele were used for normalization and compared to the signal obtained from the Ame1$^{15\text{-}324}$ mutant allele.

5 Discussion

5.1 The Mtw1 complex and its conserved association with the Ndc80 complex

One main aim of this work was the reconstitution and characterization of the Mtw1c. In parallel, two additional groups also described a biochemical and structural analysis of the budding yeast and the human Mtw1/Mis12c. All studies revealed a similar elongated structure of the Mis12c/Mtw1c of about 20-25 nm in length by Electron microscopy. The budding yeast Mtw1c appears as a dumbbell like structure in which one globular head is smaller and the larger lobe in some images seems to adopt a hook-like structure. The appearance may slightly differ between human and budding yeast but it might also depend on the homogeneity of the sample and the image processing. The human Mis12c appears more as a straight rod with a globular or hook-like structure at one end (Hornung et al., 2011; Maskell et al., 2010; Petrovic et al., 2010; Screpanti et al., 2011).

The human and yeast Mis12c/Mtw1c share similarity in the existence of identical subcomplexes, Mtw1-Nnf1 and Dsn1-Nsl1, and they function as bidirectional linkers that associate with inner and outer kinetochore proteins. The complete organization of the Mtw1 complex remains unclear but according to our understanding is the Mtw1-Nnf1 dimer responsible for the interaction with inner kinetochore proteins while the Dsn1-Nsl1 subunits are involved in the Ndc80c association. The molecular mechanism of how the association occurs between the Mis12c/Mtw1c with the Ndc80c differs in both organisms. In humans a short motif in the Nsl1 subunit is necessary for high affinity Ndc80c binding. In contrast, in budding yeast the Ndc80c contacts the Mtw1c via a short motif in the carboxyterminus of the Dsn1 subunit (Malvezzi et al., unpublished data). The human as well as the budding yeast Mis12c/Mtw1c interacts with the Ndc80c in the absence of the Knl1/Spc105 protein, whereas in *C. elegans* the association requires the presence of Knl1 (Cheeseman et al., 2006; Hornung et al., 2011; Maskell et al., 2010; Petrovic et al., 2010; Screpanti et al., 2011). Overall, this demonstrates a universal organization of the KMN network, however it also reflects the emergence of slightly different structural requirements for KMN network assembly in evolution.

5.2 The Dam1 complex connects via the Ndc80 complex to the rest of the kinetochore

The Dam1c is evolutionary restricted to fungi and plays a central role in chromosome segregation in budding yeast. I found that the Ndc80c associates with the Dam1c in a microtubule dependent manner *in vitro* (Lampert, Hornung et al., 2010). This shows how the Dam1c connects to the rest of the kinetochore and secondly it illustrates how molecules from the centromeric- and the microtubular side both contribute to the formation of a mature kinetochore-microtubule interface. While the KMN network assembly is evolutionary conserved and the Dam1c not, the way how a stable kinetochore-microtubule attachment is formed may differ between organisms.

Evidence for a Ndc80c-Dam1c cooperation can also be found in literature. In temperature sensitive *ndc80-1* mutants, the kinetochore fails to interact with microtubules (Janke et al., 2001; Wigge and Kilmartin, 2001). When *ndc80-1* cells are shifted to the restrictive temperature, kinetochore localization of the Dam1c is abolished while spindle localization persists (Janke et al., 2002). This indicates that the Dam1c depends on the Ndc80c and on the presence of microtubules for its kinetochore localization. Furthermore, two complementary previous studies indicate the cooperative function of the Dam1c and Ndc80c. The first study describes that human Ndc80 mutant lacking the unstructured N-terminal tail fail to establish kinetochore-microtubule attachments (Guimaraes et al., 2008). In contrast, budding yeast cells lacking the Ndc80 N-tail grow comparably to wild type cells (Kemmler et al., 2009). This suggests, due to the Dam1c contribution, the N-terminal Ndc80 tail may be dispensable for a strong kinetochore microtubule attachment in budding yeast.

No clear Dam1c homolog has been identified in higher eukaryotes but several additional microtubule binding proteins, such as CENP-E or the Ska complex are present that may act as a functional counterpart (McEwen et al., 2001; Welburn et al., 2009). Why does budding yeast have the Dam1c? A theoretical reason would be that metazoans approximately attach 30 microtubules to one kinetochore, whereas budding yeast has to deal with the challenge of attaching one microtubule per kinetochore. Faithful genetic transmission strictly depends on a stable attachment of all kinetochores to the mitotic spindle. A single-microtubule attachment may require additional security that may be contributed through the Dam1c. A second, quantitative reason may have become apparent during this study. Under physiological salt concentrations the human Ndc80c bound to microtubule with an apparent dissociation constant of *Kd* 0.040 µM (Ciferri et al., 2008), whereas the budding yeast Ndc80c displayed a 30 fold

lower *Kd* of 1.2 µM. In the presence of the Dam1c the microtubule-binding affinity of yeast Ndc80c was approximately equal to the human counterpart. This shows that the generation of a high affinity kinetochore-microtubule attachment requires an additional protein in budding yeast and this may explain the collaboration of the Ndc80c and Dam1c.

On the other side, the recently identified Ska complex in metazoans is of special interest and may function as a Dam1c homolog. Its association with the kinetochore depends on the KMN network and Ska subunit depletion results in a destabilization of kinetochore-microtubule attachments (Chan et al., 2012; Gaitanos et al., 2009). Furthermore, similar to Dam1c, the Ska complex is also able to track deploymerizing microtubules (Welburn et al., 2009). Overall, this suggests that additional molecules for coupling the kinetochore to microtubules are required in metazoans.

5.3 Kinetochore proteins and their DNA binding properties

Several kinetochore proteins contain an intrinsic DNA binding ability, however not all proteins bind specifically to centromeric DNA. The Cbf3 complex contains two DNA binding proteins Ndc10 and Cep3, but only Cep3 specifically recognizes a sequence in the CDEIII region (Cho and Harrison, 2012; Perriches and Singleton, 2012). Mif2 specifically binds to an AT rich sequence at the centromere whereas the vertebrate CENP-T/-W seems to have again nonspecific DNA binding properties (Nishino et al., 2012).

In the present work I have demonstrated in preliminary experiments the nonspecific DNA binding of the Ame1-Okp1 heterodimer. Furthermore I also observed binding to *E. coli* DNA during the purification of the heterodimers Ctf19-Mcm21 and Chl4-Iml3 indicating that several CCAN members have DNA binding capability. This finding supports the idea that CCAN components form a platform on the centromere on that the KMN network assembles. A remaining question is how they achieve their specification to the centromeric DNA. Probably, a nonspecific DNA contact becomes specific through an interaction with other kinetochore proteins as Cep3 guides Ndc10 to the CDEIII region.

5.4 Both centromeric protein complexes CENP-C and AO may recruit the KMN network

CENP-C (Mif2) is a kinetochore constituent in all organisms, while other CCAN components are absent in *C. elegans* and *D. melanogaster.* This places CENP-C as a component of central

importance. CENP-C has been reported for being closely located to the potential binding partner CENP-A (Cse4) (Ando et al., 2002; Cheeseman et al., 2004; Guse et al., 2011; Westermann et al., 2003). Biochemical analysis in flies and humans showed the direct association of CENP-C's N-terminus to the Mis12c (Mtw1c) (Przewloka et al., 2011; Screpanti et al., 2011). However, the human N-terminal motifs are not conserved in budding yeast and moreover the N-terminus of Mif2 is dispensable for viability (Cohen et al., 2008). An additional interesting feature of the Mif2 dimer is its ability to bind centromeric DNA with the C-terminus (Cohen et al., 2008). Besides all *in vivo* data strongly pointing towards an association of Mif2 and Mtw1c, I was unable to detect any interaction between the recombinant complexes *in vitro*. One reason may be a non functional Mif2 protein when expressed in bacteria. Future experiments with endogenous Mif2 purified from yeast extracts may shed light on their interaction.

A recent fluorescence quantification analysis measured in average twelve Mtw1c and three to four Mif2 and Ctf19 copies per kinetochore (Lawrimore et al., 2011). According to their copy number, Mif2 and also the COMA subunit Ctf19 are substoichiometric with respect to the KMN network. Hence, the recruitment of twelve copies of the Mtw1c to the centromere may require more than one centromere receptor.

Strikingly, my results identify the heterodimer Ame1-Okp1 as a new and essential centromere receptor for the KMN network. This finding may explain the unique status of Ame1 and Okp1 in budding yeast, which are together with Mif2 the only essential CCAN subunits. Future experiments will have to address to which extent the Ame1-Okp1 homologs CENP-U and CENP-Q perform an analogous function.

The molecular mechanism of how CENP-C associates with Mis12c resembles the AOc-Mtw1c interaction defined in this study. CENP-C contains a 20 amino acid motif at the extreme N-terminus that is predicted to fold into an α-helix. Single point mutations in this motif severely diminished the interaction to the Mis12c *in vitro*. Overexpression of an N-terminal CENP-C fragment had a dominant negative effect on the outer kinetochore assembly *in vivo*, while dislocalization was not observed in fragment with two mutations (Screpanti et al., 2011). In *D. melanogaster* the interaction is mediated through the Mis12 subunit Nnf1. In comparison, the Ame1 protein contains a positively charged α-helical motif within the first 15 amino acids. Deletion of the motif or insertion of point mutations, converting positively into negatively charged residues led to the complete loss of the Mtw1c interaction *in vitro* and to lethality *in vivo*. As a last similarity Ame1 also targets the Mtw1-Nnf1 heterodimer.

In respect to this work important remaining questions are whether Mif2 and AOc simultaneously bind the Mtw1c or whether these are mutually exclusive interactions that represent two parallel pathways of Mtw1c recruitment to the centromere.

5.5 Multiple pathways connect the outer kinetochore to the centromere

Ndc80 depleted cells do not from a metaphase plate, whereas cell depleted of individual CCAN members show a milder phenotype (Liu et al., 2003; McCleland et al., 2003; Zhang et al., 2012). This suggests that there are several connection pathways emerging from the centromere to the microtubule-binding interface.

In vertebrate cells two distinct pathways have been identified that target the outer kinetochore complex Ndc80c. One recruits Ndc80 complex via CENP-C (Mif2) and the second through the histone fold proteins CENP-T/-W/-S/-X (Cnn1/Wip1/Mhf1/Mhf2) (Gascoigne et al., 2011; Hori et al., 2008a; Schleiffer et al., 2012). CENP-T/W/S/X may form a nucleosome-like structure, that wraps DNA at human centromeres that do not contain specific sequences (Gascoigne and Cheeseman, 2012; Nishino et al., 2012; Takeuchi and Fukagawa, 2012). Thus, besides the presence of the CENP-A containing nucleosome in all eukaryotes, the CENP-T/W/S/X complex would be an additional specialized nucleosome. The extended N-terminus of Cnn1 (CENP-T) directly associates with the Ndc80c subunits Spc25-Spc24 via a short hydrophobic α-helical domain (Gascoigne et al., 2011; Schleiffer et al., 2012) & (Malvezzi, unpublished).

Some common structural features of CCAN subunits are beginning to emerge: the CENP-T (Cnn1), CENP-C and now also Ame1 proteins all contain an extended, largely unstructured N-termini harboring short interaction motifs. The question arises as to why CCAN components contain these elongated N-terminal structures with binding motifs. A possibility is to introduce flexibility into the kinetochore conformation. But why kinetochores need to be flexible? There are probably several points as to why kinetochore conformation has to be flexible rather than stiff. During chromosome segregation kinetochores have to adapt to horizontal forces that are generated along the microtubule axis, while keeping the vertical axis, along the chromosome, fairly stable. For instance, in metaphase the horizontal force of the pulling microtubule stretches the kinetochore that is later relaxed in anaphase. A flexible conformation within the horizontal axis of the kinetochore allows transmitting the forces in a gentler manner than abruptly as in a rigid assembly. Furthermore, a dynamic load-bearing attachment, such as the microtubule-kinetochore-chromosome unit, requires flexible elements that allow sufficient free movement during chromosome segregation.

Multiple contact points on the horizontal chromosome axis first distribute the pulling forces on the chromosome. Second, they also generate a platform on the chromosomes that maintains the fairly perpendicular arrangement between the chromosome and microtubule thereby preventing extreme chromosome rotation.

The error correction mechanism of kinetochores has to distinguish between correct and incorrect attachments. The molecular basis of how such a correction system works may underlie an elastic kinetochore. It is thought that Ipl1 senses correct from incorrect attachments by a spatial mechanism. The CPC, that includes Ipl1, localizes at the centromere. When the kinetochore attaches to the microtubule, tension is applied and the kinetochore stretches, making substrates in the outer kinetochore unreachable (Liu et al., 2009; Uchida et al., 2009). For such a correction mechanism elastical protein structures are necessary.

The precise role of the elongated N-termini with respect to kinetochore function has to be dissected in future. Do the N-termini contain additional segments that contribute to the interaction? What happens when the N-termini are shortened while keeping the interaction motif? Can recruitment pathways be bypassed by replacing motifs among kinetochore proteins while keeping the kinetochore functional? For instance, can the Mtw1 recruitment be bypassed by replacing the Ame1 motif with the Cnn1 motif?

5.6 Reciprocal dependencies between inner and outer kinetochore complexes

The analysis of localization dependencies of kinetochore proteins after depleting other kinetochore proteins has revealed a rough assembly pathway from the centromere towards the microtubule (Cheeseman et al., 2008; Hori et al., 2008a). The KMN members depend on the presence of the CCAN proteins while in turn the CCAN requires the CENP-A containing nucleosome. The assembly hierarchy is not always unidirectional and there are discrepancies between different cell types and techniques. In a simplified descriptive manner the kinetochore mainly directs its assembly from the inner to the outer kinetochore proteins. However, kinetochores are complex structures and proteins from both sites, centromeric and microtubular, may bilaterally contribute to their localization meaning their dependency is not always unidirectional. For example, Mis12 depletion affects CENP-A and CENP-H localization in human cells (Kline et al., 2006). A previous study demonstrated that Nsl1 depletion not only interfered with the microtubular Dam1 localization, but it also affects the centromere localization of Okp1 and Mcm21 (Scharfenberger et al., 2003). Furthermore, there is also an assembly hierarchy within one layer/network. Depletion of one CCAN subunits results in a loss of another

(Cheeseman et al., 2008). Overall, these studies indicate the dependency between inner and outer kinetochore proteins and their depletion often leads to a general kinetochore defect.

In agreement with these previous results, I observed a dependency that was directed from the KMN network towards the CCAN. The disruption of the AOc-Mtw1c interaction delocalized both proteins from the kinetochore to a similar extent suggesting that Ame1 requires the Mtw1c for its kinetochore localization and vice versa. Interestingly, also the apparent DNA binding activity of the AOc is not sufficient for KT localization *in vivo*. Furthermore the delocalization of the AOc affected also, albeit to a lesser extent, the localization of the CCAN component Mif2 and likely also the assembly of the outer kinetochore. Overall, my results suggest that single point mutations within a motif of just 15 amino acids had catastrophic effects on the general kinetochore assembly.

5.7 Illustrative summary of this work

My investigations into the budding yeast kinetochore architecture have uncovered general and also new organization principles from the microtubule-attachment point towards the centromere. Based on my findings combined with the latest literature, I suggest following scheme of the budding yeast kinetochore (Figure 26). The Dam1 complex tracks the plus ends of growing and shrinking microtubule (Lampert et al.; Westermann et al., 2006). In a microtubule dependent manner the Dam1c and the Ndc80c engage thereby connecting the Dam1c to the rest of the kinetochore (Lampert, Hornung, 2010) enhancing the association of Ndc80c with microtubules. The exact molecular mechanism how the association occurs is under investigation and probably involves a loop insertion close to the Ndc80 CH-domain (Lampert et al., unpublished). The centromere proximal globular domains of Spc24-Spc25 directly associate with the Mtw1c through a conserved motif in the Dsn1 subunit (Hornung et al., 2011) & (Malvezzi, unpublished). The Mtw1c subunits Mtw1-Nnf1 form a stable heterodimer that is probably oriented towards the centromere and it directly interacts with the unstructured N-terminus of the Ame1 protein. The first fifteen amino acids of Ame1 harbor a short motif that is absolutely necessary for a strong Mtw1c binding.

The conserved Ame1 protein (homolog of human CENP-U) forms a heterodimer with Okp1 (CENP-Q), that in turn assembles into a hexameric complex with Ctf19-Mcm21 and Chl4-Iml3, called COMA-CI. Ame-Okp1 and likely also also other subunits of COMA-CI have an intrinsic DNA-binding activity, contributing to the formation of an interface with centromeric DNA. The recently discovered histone fold proteins Cnn1 and Wip1 bypass the Mtw1c recruitment

pathway and directly associate via a hydrophobic N-terminal motif with the globular Spc25-Spc24 domains (Schleiffer et al., 2012). Interestingly, Cnn1 and Dsn1 have related motifs that compete for the same binding site on the Ndc80c (Malvezzi, unpublished). Thus, budding yeast harbors at least two distinct recruitment pathways for the Ndc80c. Firstly, the Mtw1c receptor pathway via Ame1 and secondly the Cnn1 receptor pathway. How the Mif2 homodimer contributes to the KMN network recruitment in budding yeast still remains elusive.

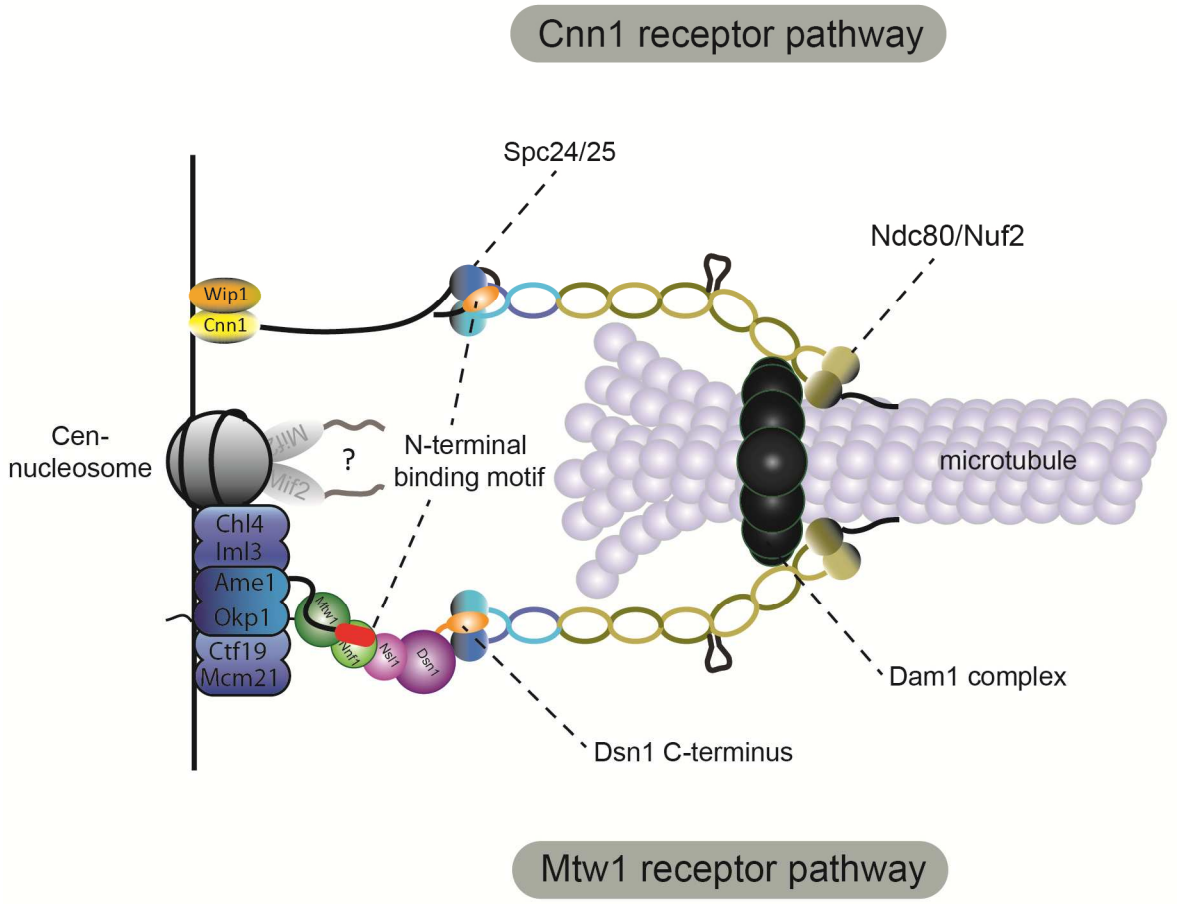

Figure 26: Molecular architecture of the *S. cerevisiae* kinetochore. This illustration summarizes the results presented in this work. A detailed explanation is described in the paragraph 5.7. N-terminus of Cnn1 and the C-terminus of Dsn1 have related binding motif (orange). Ame1 contains also an N-temrinal binding motif (red). Note, the Mif2 interaction has not been assigned - indicated with a question mark.

5.8 Towards a reconstitution of a eukaryotic kinetochore

Kinetochores are complex machineries with multiple functions. During the last three decades most of the kinetochore proteins have been identified, and approximately 200-500 individual proteins are present per kinetochore in budding yeast (Akiyoshi and Biggins, 2012; Joglekar et al., 2006; Lawrimore et al., 2011). However, our understanding of how these numerous proteins are arranged into a functional kinetochore is rudimentary.

There are several approaches to study kinetochore structure and function. In the simplest approach one could try to study an intact kinetochore in the cell, using for example electron tomography. This approach has been very successful for the investigation of nuclear pore complexes (Akey and Radermacher, 1993; Stoffler et al., 2003), but for kinetochores the structural insights have been limited (Dong et al., 2007). In a top-down approach native kinetochores are purified from cells helping to understand their function as a larger entity (Akiyoshi et al., 2010). This type of approach has been very successful for the investigation of ribosomes, which have even been crystallized after purification from cells. For kinetochores this approach is challenging, because they are clearly less abundant and less stable than ribosomes. *In vitro* reconstitution of recombinant kinetochore complexes stands for a bottom up approach. It represents a key technique to biochemically and structurally elucidate the function of individual kinetochore proteins. In a second step, reconstitutions of larger modules, such as the KMN network or CCAN, are essential to understand the synergistic role of several combined kinetochore proteins. The ultimate goal in kinetochore research is to assembly an entire kinetochore *in vitro*. A defined system with pure components will allow us to answer question that are difficult to address *in vivo*.

Recently, a study isolated all major core kinetochore components via a single tag at the Dsn1 subunit with the top-down approach (Akiyoshi et al., 2010). Applying this strategy may retain some of the kinetochore integrity, which may be difficult to achieve by the bottom-up approach. However, both systems are powerful tools for unraveling specific protein function and regulation mechanisms. Furthermore, they also enable us to answer questions such as, how does a kinetochore couple to dynamic microtubule? What are the stoichiometries of individual kinetochore proteins and how are they geometrical arrangement? How does the underlying chromatin sequence specify the kinetochore assembly? How do post translational modifications (PTMs) alter the kinetochore assembly and function? Knowledge about posttranslational modifications will be important to assemble kinetochore modules from recombinant proteins. The *in vitro* reconstitution will progress the structural and architectural understanding of

kinetochores, it will identify important interfaces and define structural requirements for kinetochore assembly.

So far, we have already gained first insights into the function of individual kinetochore proteins and their architecture. Improvements in sample preparation and advancement of methods will lead to a higher resolution map of the kinetochore contributing to our understanding of how a kinetochore functions. However, we have just started to discover their nature.

6 Material and methods

6.1 Cloning

The primers for 6xHis-Mif2 included NcoI/XhoI restriction sites compatible for cloning into the expression vector pet28a (Novagen). The N-terminal GST fusion GST-Ame1$^{1-114}$ and GST-Ame1$^{1-30}$ were cloned into the BamHI/XhoI restriction sites of the expression vector pGEX-6P-1 (GE-Healthcare). Details for the cloning of other kinetochore genes that were expressed in this work are listed in Table 3 and Table 4.

Table 3: Cloning of genes into pST39 cassettes. The table describes which restriction enzymes were used and in which of the four cassettes the genes were cloned. Mcm21 was amplified from yeast cDNA due to the presence of an intron.

	Mtw1c	**MNc**	**DNc**	**COMA**	**AOc**	**CMc**
Cassette 1	Mtw1 NdeI/BamHI	Mtw1 NdeI/BamHI		Ctf19 NdeI/BamHI		Ctf19-6xHis NdeI/BamHI
Cassette 2	Nsl1 NdeI/BamHI		Nsl1-6xHis NdeI/BamHI	Mcm21 NdeI/BamHI		Mcm21 NdeI/BamHI
Cassette 3	Nnf1 NdeI/BamHI	Nnf1-6xHis NdeI/BamHI	Nnf1 NdeI/BamHI	Okp1 NheI/KpnI	Okp1 NheI/KpnI	
Cassette 4	6xHis-Dsn1 NdeI/HindIII		Dsn1 NdeI/HindIII	Ame1-6xHis/-FLAG	Ame1-6xHis NdeI/KpnI	

Table 4: Cloning of genes into duet vectors (Novagen). The table describes which restriction enzymes were used and in which of the two cassettes the genes were cloned.

Proteins	**Ndc80-Nuf2 complex**	**Spc24-Spc25 complex**	**Chl4-Iml3 complex**
Vectors	pACYC Duet-1	pET Duet-1	p-COLA Duet-1
Cassette 1	Ndc80-6xHis NcoI/BamHI	Spc24-6xHis NcoI/BamHI	Iml3 NcoI/BamHI
Cassette 2	Nuf2 NdeI/KpnI	Spc25 NdeI/KpnI	Chl4-FLAG NdeI/KpnI

6.2 Protein expression and purification

6.2.1 General expression and purification conditions

Unless indicated otherwise the following conditions are valid for all protein expressions performed in this work. Cells were grown at 37℃ until OD_{600} of 0.6 and subsequently induced with 0.2 mM isopropyl-β-D-thiogalactopyranoside (IPTG). Expressions were conducted ON at 18℃ with the exception of the MNc (0.5 mM IPTG, 4h at 37℃). Expression of Mtw1c, MNc, DNc, Ndc80-Nuf2 and Spc24-Spc25 were performed in BL21 (DE3) (Novagen). COMA, AOc, CMc, Mif2 were expressed in Rosetta 2(pLys) (DE3) cells (Novagen). Lysis-, wash- and elution buffers as well as chromatography steps varied for the different protein complexes and are described in the individual sections. Sonication of bacteria was performed in the presence of protease inhibitors (Roche) and PMSF. The 6xhistidine fusion proteins were isolated with Ni-NTA agarose beads (Qiagen), whereas M2 affinity agarose (Sigma) was used for FLAG tagged proteins. Incubation with affinity beads was performed in batch format in a 50 ml Falcon tube for 1h at 4℃.

6.2.2 Mtw1 complex

Two versions of the Mtw1 complex were used in the study: the first was tagged with 6xHis at the C-terminus of Nnf1 and the second, newer, version was N-terminally tagged with 6xHis at the Dsn1 subunit. For expression conditions of the first version and DNc, MNc see Hornung et al (Hornung et al., 2011). Lysis buffer for Mtw1c was 50 mM Tris-HCL pH 7.5, 500 mM NaCl, 30mM imidazole, 10% Glycerol, 0.5% Tween20 as described in (Maskell et al., 2010). Elution was performed with 30 mM Tris pH 8.5, 80 mM NaCl, 250 mM imidazole. Subsequently, proteins were directly loaded onto anion exchange chromatography (MonoQ5/50 GL column (GE Healthcare). The chromatography was performed with a step gradient consisting of buffer 30 mM Tris HCl pH 8.5, 5% Glycerol from (A) 80 mM to (B) 1M NaCl using a flow rate of 1ml/min. The first step includes three CV with 20% of buffer B. The conductivity has to be kept under 26 mS/cm. After 15 CV the protein is eluted within 2 CV by increasing buffer B to 50%.

6.2.3 DN- and MN complex purification

Purification was performed as for Mtw1 complex. Additionally, after the IEX a SEC was conducted with buffer 30 mM HEPES pH 7.5, 150 mM NaCl, 5% Glycerol.

6.2.4 COMA purification

Pellets were resuspended in lysis buffer 30mM HEPES pH 7.5, 30 mM imidazole, 5 mM $CaCl_2$, 1 mM DTT, 150 mM NaCl. To remove the *E. Coli* DNA that was bound to COMA, beads were washed six times 10 min minutes at 4℃ while rotati ng with wash buffer consisting of 30mM HEPES pH 7.5, 30 mM imidazole, 5 mM $CaCl_2$, 1 mM DTT, 600 mM NaCl. COMA-6xHis was eluted with 30 mM HEPES pH 7.5, 300 mM imidazole, 5 mM $CaCl_2$, 1 mM DTT, 150 mM NaCl. The complex was concentrated using ultrafiltration (10,000 molecular weight cutoff; Vivaspin) followed by a buffer exchange into 30 mM HEPES pH 7.5, 5 mM $CaCl_2$, 1 mM DTT, 150 mM NaCl on a Superose 6 10/30 column (GE Healthcare). Here, SEC is an important step, because it separates the COMA-DNA complex from unbound COMA. COMA-FLAG was eluted from M2 affinity gel with 3xFLAG peptide (2 mg/ml) and not further purified by SEC.

6.2.5 AO and CM complex purification

AO, $AO^{15\text{-}324}$ as well as the CM complex also copurified *E. Coli* DNA. To remove the DNA identical steps were used as for the COMA purification. The protocol differed in the lysis- and washing buffers, these contained 30 mM HEPES pH 7.5, 30 mM imidazole, 1 to 2 M NaCl. Proteins were eluted using 30 mM HEPES pH 7.5, 300 mM imidazole, 150 mM NaCl followed by a concentration with a 50,000 molecular weight cutoff (Vivaspin).

6.2.6 COMA-CI purification

Chl4-FLAG and Iml3 (CI) were cloned into cassette 1 and 2 of pCOLADuet-1 and cotransfected with the pST39 vector carrying the COMA genes with a 6xhistidine tag. Purification was conducted as described for the COMA with the exception that Anti-FLAG affinity gel (Sigma) was used and the protein was eluted with 3xFALG peptide. As chromatography purification Superdex 3.2/30 was used.

6.2.7 Mif2 purification

For expression and purification of 6xHis-Mif2 cells were lysed in 50mM HEPES pH 7.5, 1 M NaCl, 30mM imidazole, 0.25% Tween 20 and after incubation with Ni-NTA beads 6xHis-Mif2 was eluted with 50 mM HEPES pH 8.5, 500 mM NaCl, 250mM imidazole. Protein eluate was concentrated using ultrafiltration (100,000 molecular weight cutoff; Vivaspin) and subsequently gelfiltered on a Superdex 200 16/60 column (GE Healthcare). After selecting the purest fractions the protein was loaded directly onto an anion exchange chromatography (IEX) MonoQ5/50 GL column (GE Healthcare). The IEX was performed with a step gradient - buffer 30 mM Tris HCl pH 8.5, 5% Glycerol from buffer A 80 mM to buffer B 1M NaCl using a flow rate of 0.8 ml/min. The first step includes three CV up to 20% of buffer B. The conductivity has to be kept under 26 mS/cm. After 15 CV the protein is eluted within 1 CV by increasing buffer B to 50%.

6.2.8 Ndc80 complex expression and purification

The Ndc80 complex subunits Ndc80-6xHis/Nuf2 (Nuf2-EGFP) and Spc25/Spc24-6xHis were separately expressed in *E. coli* BL21 (DE3). Before the full length Ndc80c was reconstituted both subcomplexes were purified alone. Lysis- and wash buffer contained 300 mM NaCl, 30 mM HEPES pH 7.5, 30 mM imidazole. Protein were eluted from Ni-NTA beads (Qiagen) with 150 mM NaCl, 30 mM HEPES pH 7.5, 250 mM imidazole and subsequently mixed in approximately a 1:1 stoichiometry. After incubation for 10 min on ice the reconstituted Ndc80 complex was concentrated (30,000 molecular weight cutoff, Vivaspin). The complex was further purified by SEC Superdex 200 HiLoad 16/60 (GE Healthcare) in the buffer 150 mM NaCl, 30 mM HEPES pH 7.5.

6.2.9 Dam1 complex purification

Dam1 complex expression and purification where performed as previously described (Westermann et al., 2005)

6.2.10 Coexpression and purification of MNc with Ame1

Ame1-FLAG was cloned into cassette 4 of the pST39 plasmid that already contained the subunits Mtw1, Nsl1, Nnf1-6xHis. Bacterial expression was performed at 37℃ for 4h. Lysis buffer was PBS (phosphate buffered saline) with 5% glycerol. After binding to the M2 affinity gel

(Sigma) beads were washed with PBS, 5% glycerol and either 150 mM or 600 mM NaCl. Elution was performed with 3xFLAG peptide (2 mg/ml). Complex formation was detectable even under conditions of 600 mM NaCl.

6.3 Interaction studies using size exclusion chromatography

Analytical SEC experiments were performed on Superose 10/30 (CMc + Mtw1c), Superdex 200 16/60 (Dam1c + Ndc80c) and the rest of the SEC interaction experiments on Superose 6 3.2/30 columns. All SEC interaction studies were conducted under isocratic elution conditions at 4℃. The protein elution was monitored by absorbance at a wavelength of 280 nm. For analytical SEC, proteins were mix in equimolar ratios between 5 and 15 µM and incubated for 10-30 min on ice. The eluates were fractioned, loaded onto SDS-PAGEs and stained with Coomassie.

6.4 Pull down experiments

Kinetochore proteins were immobilized to 20 µl affinity beads (anti FLAG M2- or Ni-NTA agarose beads) in a concentration of 0.1-1 µM in 0.5 ml binding buffer (TBS or PBS; for Ni-NTA 30 mM imidazole). The binding partner was added in a concentration of approximately 1 µM. After incubation for 1h at 4℃ the beads were washe d three times with binding buffer and 0.1% (vol/vol) NP-40. Finally the bound proteins were specifically eluted with either 3xFLAG peptide or 250 mM imidazole.

6.5 Electron microscopy

The Mtw1c was imaged with GraFix method (Kastner et al., 2008). Therefore 150 µg of the Mtw1c was fixed in a 5-40% glycerol gradient containing 0.002-0.15% glutaraldehyde gradient, 20 mM Hepes pH 7.6, 100 mM NaCl, 1 mM ethylenediaminetetraacetic acid and 1 mM DTT. After ultracentrifugation at 55000 rpm for 13 h in a TLS55 rotor at 4℃ the fraction containing the monomeric crosslinked complex was layered ont a glow-discharged C-flat grid (Protochip) that has a thin layer of carbon. Subsequently, the grid was stained with 2% uranyl formate. 5000 particels were selected with the BOXER program (Ludtke et al., 1999) and subjected to reference free classification.

6.6 Densitometry and protein concentration determination

Quantitative analysis of Coomassie gels following SDS-PAGE were performed with the Software IamgeJ (National Institutes of Health). Protein concentrations in solution were determined colorimetrically with the DC-assay (Biorad).

6.7 Determination of the Mtw1 complex molecular mass

SEC was performed on an Ettan LC or Äkta Chromatography System (Amersham Biosciences) using Superose 6 3.2/30. The following standard proteins were used (thyroglobulin - 670 kD, 85 Å; bovine gamma-globulin - 158 kDa, 53 Å; chicken ovalbumin - 44 kDa, 31 Å; equine myoglobulin - 17 kDa, 21 Å; vitamin B12 – 1.35 kDa, 2 Å). Since the elution volume of proteins correlates with the Stokes radius (Siegel and Monty, 1966), the Stokes radius from three independent experiments was calculated for the Mtw1c.

The Sedimentation coefficient was determined by glycerol gradient centrifugation. TLS55 (Beckmann Instruments) tubes with a volume of 2 ml were used, gradients were prepared by layering 0.4 ml steps of 25, 20, 15, 10, 5 % (v/v) glycerol in gel filtration buffer (20 mM phosphate buffer, 150 mM NaCl, 1mM EDTA). The gradients were incubated for 3 - 4 h at 4 ℃ to form a linear gradient. 50 µg of the Mtw1c was loaded onto the top 5 % glycerol layer. Standard proteins with known sedimentation coefficients were analyzed in parallel gradients (thyroglobulin (19.3 S), catalase (11.3 S), aldolase (7.35 S), ovalbumin (3.5 S) ribonuclease A (1.85 S). The Mtw1c and standard proteins were loaded on the basis of equal protein volumes and protein concentrations. The samples were run for 7.5 h at 50000 rpm, 4℃ in the TLS55 rotor (Beckmann). Finally, fractions were loaded onto an SDS-PAGE and visualized by Coomassie or silver staining. Protein band intensities were quantified by Image J Software and protein concentrations were determined by the DC-Assay (Biorad). The sedimentation coefficient was determined from two independent experiments.

The molecular weight of the Mtw1 complex was determined using equation $M=S*N(6*\pi*\eta*R_s)/(1-vp)$ and the frictional coefficient was given by $f/f_0=a/((3vM/4\pi N))^{1/3}$, with M = molecular weight, R_s = Stokes radius, N = Avogodro's number, v = partial specific volume, η = viscosity of the solvent H_2O, p = density of medium, s = sedimentation coefficient (Siegel and Monty, 1966). Because the partial specific volume of the Mtw1c has not been determined, I used the general average value of proteins of 0.725 cm^3/g. Stokes radii were calculated using $K_{av}= V_e-V_0/V_t-V_0$ (V_e= elution volume, V_o = void volume, V_t = volume total) and plotting (-

$\log(K_{av}))^{1/2}$ against R_s results in a linear correlation (Amersham Biosciences, 2002). The Svedberg coefficient of the standard proteins correlate linear to the taken fraction as shown previously (Russell et al., 1999).

6.8 Microtubule cosedimentation assay

Tubulin was isolated as previously described, except porcine brain was used instead of bovine brain (Ashford et al., 1998). Aliquots of porcine brain tubulin were thawed and pre-cleared for 5 minutes in a microfuge at 4℃. 2.5 mM of GTP and G- PEM (50% glycerol in PEM (80 mM Pipes-KOH, pH 6.8, 1 mM EGTA, 1 mM $MgCl_2$, 0.02% azide, store at 4℃) was added to give a final concentration of 55 µM microtubules. Tubulin was incubated at 35℃ for 30 minutes to assemble microtubules. A final concentration of 10 µM taxol in DMSO (about 1 µl volume) was added to the reaction. Microtubules were allowed to rest for at least 10 minutes at RT. Afterwards, microtubules were diluted in PEM (+1 mM GTP +10 µM taxol) to obtain the appropriate microtubule concentrations. For microtubule-binding reactions, gel filtration purified proteins were precleared by spinning for 5 minutes at 60.000 rpm in TLA-100 tubes (Beckmann Instruments) at 4 ℃. Dependent on the experiment, purified protein was diluted in PEM buffer and alternatively BSA (0.1 – 0.5 mg/ml) was added. Taxol stabilized microtubules and purified proteins were added in TLA-100 tubes by mixing 20 µl microtubules + 20 µl test protein with a cut off pipette tip. The mixture was incubated at room temperature for 10 - 15 minutes and subsequently centrifuged in the TLA100 rotor for 20 minutes at 60.000 rpm at 25° C in the Optima ultracentrifuge (Beckmann Instruments). 40 µl of supernatant was removed and the pellet sample was dissolved by adding 40µl PEM + 10 mM $CaCl_2$ and incubated 10 min on ice. Equal amounts of supernatant (S) and pellet (P) were visualized on a Coomassie-stained SDS-PAGE or in case of the Ndc80-EGFP complex transferred into a 96 well plate for fluorescence quantification with the microplate reader Synergy2.

6.9 Electrophoretic mobility shift assay

0.8 µM of AOc were mixed with 200 ng of CEN-DNA or salmon sperm DNA and incubated 10 min at room temperature (RT) before loading on a 1% agarose gel. The gel was run at low voltage of 40V at 4℃. For imaging the DNA was stai ned with ethidume bromide and also proteins were visualized with Coomassie.

6.10 Plasmid list

Number	Plasmid
PPH7	pST39-Mtw1/Nsl1/Nnf1-6xHis/Dsn1
PPH13	pST39-Mtw1/Nsl1/Nnf1-6xHis
PPH62	pET28-Dsn1$^{172-576}$
PPH173	pST39-Mtw1/Nnf1-6xHis
PPH20	pST39-Mtw1/Nsl1-6xHis/Dsn1
PPH35	pETDuett-Spc24-6xHis/Spc25
PPH18	pACYCDuet1-Ndc80-6xHis/Nuf2
PPH60	pST39-Ctf19/Mcm21/Okp1/Ame6xHis
PPH64	pST39-Ctf19/Mcm21/Okp1/Ame6xFLAG
PPH71	pST39-Ctf19-6xHis/Mcm21
PPH74	pST39-Okp1-Ame1-6xHis
PPH117	pCOLA-Iml3/Chl4-FLAG
PPH123	pET28-6xHis-Mif2
PPH108	pST39-Mtw1/Nsl1/Nnf1/6xHis-Dsn1
PPH96	pST39-Mtw1/Nnf1-6xHis/Ame1-FLAG
PH174	pST39-Okp1/Ame1$^{15-324}$-6xHis
PPH112	pRS316-Ame1^{WT}
PPH111	pRS316-Ame1$^{15-324}$
PPH145	pRS306- Ame1^{WT}-6x-FLAG
PPH146	pRS306- Ame1$^{15-324}$-6x-FLAG
PPH156	pRS306-Ame1^{WT}-EGFP
PPH157	pRS306-Ame1$^{15-324}$-EGFP
PPH160	pRS306-Ame1^{R3D}-EGFP
PPH170	pRS306-Ame1^{R10D}-EGFP
PPH168	pRS306-Ame1^{R12D}-EGFP
PPH169	pRS306-Ame1^{R10A}-EGFP
PPH167	pRS306-Ame1^{R12A}-EGFP
PPH172	pGEX6P1-Ame1$^{1-30}$
PPH171	pGEX6P1-Ame1$^{1-114}$

6.11 Yeast genetics

All yeast strains belong to S288C background. Yeast strain generation and methods were performed by standard procedures.

Strain	Genotype
SWY536	*MAT a, tor1-1, fpr1::loxP-Leu2-loxP, RPL13A-2xFKBP12::lox-TRP1-loxP, Ame1-FRB::KanMX*
YPH 18	*MAT a, tor1-1, fpr1::loxP-Leu2-loxP, RPL13A-2xFKBP12::lox-TRP1-loxP, Ame1-FRB::KanMX, pRS316-Ame1::URA*
YPH 19	*MAT a, tor1-1, fpr1::loxP-Leu2-loxP, RPL13A-2xFKBP12::lox-TRP1-loxP, Ame1-FRB::KanMX, pRS316-Ame1$^{15-324}$::URA*
YPH 24	*MAT a, tor1-1, fpr1::loxP-Leu2-loxP, RPL13A-2xFKBP12::lox-TRP1-loxP, Ame1-FRB::KanMX, Ame1-6xFLAG::URA*
YPH 25	*MAT a, tor1-1, fpr1::loxP-Leu2-loxP, RPL13A-2xFKBP12::lox-TRP1-loxP, Ame1-FRB::KanMX, Ame1$^{15-324}$6xFLAG::URA*
YPH 26	*MATa/alpha, leu2-3,112/leu2-3,112, ura3-52/ura3-52, ade2-1/ADE2, lys2/LYS, CNN1/cnn1Δ::HIS3, Ame1::URA3*
YPH 27	*MATa/alpha, leu2-3,112/leu2-3,112, ura3-52/ura3-52, ade2-1/ADE2, lys2/LYS, CNN1/cnn1Δ::HIS3, Ame1(15-324)::URA3*
YPH 29	*MAT a, tor1-1, fpr1::loxP-Leu2-loxP, RPL13A-2xFKBP12::lox-TRP1-loxP, Ame1-FRB::KanMX, Ame1-6xFLAG::URA, Pds1-HA::natNT2*
YPH 30	*MAT a, tor1-1, fpr1::loxP-Leu2-loxP, RPL13A-2xFKBP12::lox-TRP1-loxP, Ame1-FRB::KanMX, Ame1$^{15-324}$6xFLAG::URA, Pds1-HA::natNT2*
YPH 31	*MAT a, tor1-1, fpr1::loxP-Leu2-loxP, RPL13A-2xFKBP12::lox-TRP1-loxP, Ame1-FRB::KanMX, Ame1-EGFP::URA*
YPH 32	*MAT a, tor1-1, fpr1::loxP-Leu2-loxP, RPL13A-2xFKBP12::lox-TRP1-loxP, Ame1-FRB::KanMX, Ame1-EGFP$^{15-324}$::URA*
YPH 33	*MAT a, tor1-1, fpr1::loxP-Leu2-loxP, RPL13A-2xFKBP12::lox-TRP1-loxP, Ame1-FRB::KanMX, Ame1-EGFP::URA, Mif2-mCherry::His*
YPH 34	*MAT a, tor1-1, fpr1::loxP-Leu2-loxP, RPL13A-2xFKBP12::lox-TRP1-loxP, Ame1-FRB::KanMX, Ame1-EGFP$^{15-324}$::URA, Mif2-mCherry::His*
YPH 35	*MAT a, tor1-1, fpr1::loxP-Leu2-loxP, RPL13A-2xFKBP12::lox-TRP1-loxP, Ame1-FRB::KanMX, Ame1-EGFP::URA, Mtw1-mCherry::His*
YPH 37	*MAT a, tor1-1, fpr1::loxP-Leu2-loxP, RPL13A-2xFKBP12::lox-TRP1-loxP, Ame1-FRB::KanMX, Ame1-EGFP$^{15-324}$::URA, Mtw1-mCherry::His*
YPH 41	*MAT a, tor1-1, fpr1::loxP-Leu2-loxP, RPL13A-2xFKBP12::lox-TRP1-loxP, Ame1-FRB::KanMX, Ame1-R3D, R10D, R12D -6xFLAG::URA*
YPH 43	*MAT a, tor1-1, fpr1::loxP-Leu2-loxP, RPL13A-2xFKBP12::lox-TRP1-loxP, Ame1-FRB::KanMX, Ame1-EGFP-R3A::URA*

Strain	Genotype
YPH 44	*MAT a, tor1-1, fpr1::loxP-Leu2-loxP, RPL13A-2xFKBP12::lox-TRP1-loxP, Ame1-FRB::KanMX, Ame1-EGFP-R10D::URA*
YPH 45	*MAT a, tor1-1, fpr1::loxP-Leu2-loxP, RPL13A-2xFKBP12::lox-TRP1-loxP, Ame1-FRB::KanMX, Ame1-EGFP-R12A::URA*
YPH 46	*MAT a, tor1-1, fpr1::loxP-Leu2-loxP, RPL13A-2xFKBP12::lox-TRP1-loxP, Ame1-FRB::KanMX, Ame1-EGFP-R12D::URA*

7 References

Akey, C.W., and M. Radermacher. 1993. Architecture of the Xenopus nuclear pore complex revealed by three-dimensional cryo-electron microscopy. *J Cell Biol*. 122:1-19.

Akiyoshi, B., and S. Biggins. 2012. Reconstituting the kinetochore-microtubule interface: what, why, and how. *Chromosoma*.

Akiyoshi, B., C.R. Nelson, J.A. Ranish, and S. Biggins. 2009. Analysis of Ipl1-mediated phosphorylation of the Ndc80 kinetochore protein in Saccharomyces cerevisiae. *Genetics*. 183:1591-5.

Akiyoshi, B., K.K. Sarangapani, A.F. Powers, C.R. Nelson, S.L. Reichow, H. Arellano-Santoyo, T. Gonen, J.A. Ranish, C.L. Asbury, and S. Biggins. 2010. Tension directly stabilizes reconstituted kinetochore-microtubule attachments. *Nature*. 468:576-9.

Alushin, G.M., V.H. Ramey, S. Pasqualato, D.A. Ball, N. Grigorieff, A. Musacchio, and E. Nogales. 2010. The Ndc80 kinetochore complex forms oligomeric arrays along microtubules. *Nature*. 467:805-10.

Amano, M., A. Suzuki, T. Hori, C. Backer, K. Okawa, I.M. Cheeseman, and T. Fukagawa. 2009. The CENP-S complex is essential for the stable assembly of outer kinetochore structure. *J Cell Biol*. 186:173-82.

Amaro, A.C., C.P. Samora, R. Holtackers, E. Wang, I.J. Kingston, M. Alonso, M. Lampson, A.D. McAinsh, and P. Meraldi. 2010. Molecular control of kinetochore-microtubule dynamics and chromosome oscillations. *Nat Cell Biol*. 12:319-29.

Amersham Biosciences. 2002. Instruction of gel filtration calibration kits. *Instruction manual*:16-18.

Ando, S., H. Yang, N. Nozaki, T. Okazaki, and K. Yoda. 2002. CENP-A, -B, and -C chromatin complex that contains the I-type alpha-satellite array constitutes the prekinetochore in HeLa cells. *Mol Cell Biol*. 22:2229-41.

Asbury, C.L., D.R. Gestaut, A.F. Powers, A.D. Franck, and T.N. Davis. 2006. The Dam1 kinetochore complex harnesses microtubule dynamics to produce force and movement. *Proc Natl Acad Sci U S A*. 103:9873-8.

Ashford, A.J., S.S. Andersen, and A.A. Hyman. 1998. Preparation of tubulin from bovine brain. Cell Biology: A laboratory handbook. *Academic Press/UK, London*. 2 ed. J.E. Celis, editor:205-212.

Black, B.E., and E.A. Bassett. 2008. The histone variant CENP-A and centromere specification. *Curr Opin Cell Biol*. 20:91-100.

Buschhorn, B.A., and J.M. Peters. 2006. How APC/C orders destruction. *Nat Cell Biol*. 8:209-11.

Carroll, C.W., K.J. Milks, and A.F. Straight. 2010. Dual recognition of CENP-A nucleosomes is required for centromere assembly. *J Cell Biol*. 189:1143-55.

Carroll, C.W., M.C. Silva, K.M. Godek, L.E. Jansen, and A.F. Straight. 2009. Centromere assembly requires the direct recognition of CENP-A nucleosomes by CENP-N. *Nat Cell Biol*. 11:896-902.

Chan, Y.W., A.A. Jeyaprakash, E.A. Nigg, and A. Santamaria. 2012. Aurora B controls kinetochore-microtubule attachments by inhibiting Ska complex-KMN network interaction. *J Cell Biol*. 196:563-71.

Cheeseman, I.M., S. Anderson, M. Jwa, E.M. Green, J. Kang, J.R. Yates, 3rd, C.S. Chan, D.G. Drubin, and G. Barnes. 2002. Phospho-regulation of kinetochore-microtubule attachments by the Aurora kinase Ipl1p. *Cell*. 111:163-72.

Cheeseman, I.M., J.S. Chappie, E.M. Wilson-Kubalek, and A. Desai. 2006. The conserved KMN network constitutes the core microtubule-binding site of the kinetochore. *Cell*. 127:983-97.

Cheeseman, I.M., and A. Desai. 2008. Molecular architecture of the kinetochore-microtubule interface. *Nat Rev Mol Cell Biol*. 9:33-46.

Cheeseman, I.M., M. Enquist-Newman, T. Muller-Reichert, D.G. Drubin, and G. Barnes. 2001. Mitotic spindle integrity and kinetochore function linked by the Duo1p/Dam1p complex. *J Cell Biol*. 152:197-212.

Cheeseman, I.M., T. Hori, T. Fukagawa, and A. Desai. 2008. KNL1 and the CENP-H/I/K complex coordinately direct kinetochore assembly in vertebrates. *Mol Biol Cell*. 19:587-94.

Cheeseman, I.M., S. Niessen, S. Anderson, F. Hyndman, J.R. Yates, 3rd, K. Oegema, and A. Desai. 2004. A conserved protein network controls assembly of the outer kinetochore and its ability to sustain tension. *Genes Dev*. 18:2255-68.

Cho, U.S., and S.C. Harrison. 2012. Ndc10 is a platform for inner kinetochore assembly in budding yeast. *Nat Struct Mol Biol*. 19:48-55.

Ciferri, C., S. Pasqualato, E. Screpanti, G. Varetti, S. Santaguida, G. Dos Reis, A. Maiolica, J. Polka, J.G. De Luca, P. De Wulf, M. Salek, J. Rappsilber, C.A. Moores, E.D. Salmon, and A. Musacchio. 2008. Implications for kinetochore-microtubule attachment from the structure of an engineered Ndc80 complex. *Cell*. 133:427-39.

Ciosk, R., W. Zachariae, C. Michaelis, A. Shevchenko, M. Mann, and K. Nasmyth. 1998. An ESP1/PDS1 complex regulates loss of sister chromatid cohesion at the metaphase to anaphase transition in yeast. *Cell*. 93:1067-76.

Clarke, L. 1985. Structure and function of Saccharomyces cerevisiae centromeres. *Oxf Surv Eukaryot Genes*. 2:74-95.

Clarke, L., and J. Carbon. 1985. The structure and function of yeast centromeres. *Annu Rev Genet*. 19:29-55.

Cleveland, D.W., Y. Mao, and K.F. Sullivan. 2003. Centromeres and kinetochores: from epigenetics to mitotic checkpoint signaling. *Cell*. 112:407-21.

Cohen, R.L., C.W. Espelin, P. De Wulf, P.K. Sorger, S.C. Harrison, and K.T. Simons. 2008. Structural and functional dissection of Mif2p, a conserved DNA-binding kinetochore protein. *Mol Biol Cell*. 19:4480-91.

Coue, M., V.A. Lombillo, and J.R. McIntosh. 1991. Microtubule depolymerization promotes particle and chromosome movement in vitro. *J Cell Biol*. 112:1165-75.

De Wulf, P., A.D. McAinsh, and P.K. Sorger. 2003. Hierarchical assembly of the budding yeast kinetochore from multiple subcomplexes. *Genes Dev*. 17:2902-21.

DeLuca, J.G., Y. Dong, P. Hergert, J. Strauss, J.M. Hickey, E.D. Salmon, and B.F. McEwen. 2005. Hec1 and nuf2 are core components of the kinetochore outer plate essential for organizing microtubule attachment sites. *Mol Biol Cell*. 16:519-31.

DeLuca, J.G., W.E. Gall, C. Ciferri, D. Cimini, A. Musacchio, and E.D. Salmon. 2006. Kinetochore microtubule dynamics and attachment stability are regulated by Hec1. *Cell*. 127:969-82.

DeLuca, J.G., B.J. Howell, J.C. Canman, J.M. Hickey, G. Fang, and E.D. Salmon. 2003. Nuf2 and Hec1 are required for retention of the checkpoint proteins Mad1 and Mad2 to kinetochores. *Curr Biol*. 13:2103-9.

Desai, A., S. Rybina, T. Muller-Reichert, A. Shevchenko, A. Hyman, and K. Oegema. 2003. KNL-1 directs assembly of the microtubule-binding interface of the kinetochore in C. elegans. *Genes Dev*. 17:2421-35.

Euskirchen, G.M. 2002. Nnf1p, Dsn1p, Mtw1p, and Nsl1p: a new group of proteins important for chromosome segregation in Saccharomyces cerevisiae. *Eukaryot Cell*. 1:229-40.

Foltz, D.R., L.E. Jansen, B.E. Black, A.O. Bailey, J.R. Yates, 3rd, and D.W. Cleveland. 2006. The human CENP-A centromeric nucleosome-associated complex. *Nat Cell Biol*. 8:458-69.

Gaitanos, T.N., A. Santamaria, A.A. Jeyaprakash, B. Wang, E. Conti, and E.A. Nigg. 2009. Stable kinetochore-microtubule interactions depend on the Ska complex and its new component Ska3/C13Orf3. *EMBO J*. 28:1442-52.

Gascoigne, K.E., and I.M. Cheeseman. 2012. T time for point centromeres. *Nat Cell Biol*. 14:559-61.

Gascoigne, K.E., K. Takeuchi, A. Suzuki, T. Hori, T. Fukagawa, and I.M. Cheeseman. 2011. Induced ectopic kinetochore assembly bypasses the requirement for CENP-A nucleosomes. *Cell*. 145:410-22.

Ghosh, S.K., A. Poddar, S. Hajra, K. Sanyal, and P. Sinha. 2001. The IML3/MCM19 gene of Saccharomyces cerevisiae is required for a kinetochore-related process during chromosome segregation. *Mol Genet Genomics*. 265:249-57.

Guimaraes, G.J., Y. Dong, B.F. McEwen, and J.G. Deluca. 2008. Kinetochore-microtubule attachment relies on the disordered N-terminal tail domain of Hec1. *Curr Biol*. 18:1778-84.

Guse, A., C.W. Carroll, B. Moree, C.J. Fuller, and A.F. Straight. 2011. In vitro centromere and kinetochore assembly on defined chromatin templates. *Nature*. 477:354-8.

Haruki, H., J. Nishikawa, and U.K. Laemmli. 2008. The anchor-away technique: rapid, conditional establishment of yeast mutant phenotypes. *Mol Cell*. 31:925-32.

Hemmerich, P. 2008. Dynamics of inner kientochore assembly and maintenance in living cells. *J. Cell Biol.* 180:1101-1114.

Hori, T., M. Amano, A. Suzuki, C.B. Backer, J.P. Welburn, Y. Dong, B.F. McEwen, W.H. Shang, E. Suzuki, K. Okawa, I.M. Cheeseman, and T. Fukagawa. 2008a. CCAN makes multiple contacts with centromeric DNA to provide distinct pathways to the outer kinetochore. *Cell*. 135:1039-52.

Hori, T., M. Okada, K. Maenaka, and T. Fukagawa. 2008b. CENP-O class proteins form a stable complex and are required for proper kinetochore function. *Mol Biol Cell*. 19:843-54.

Hornung, P., M. Maier, G.M. Alushin, G.C. Lander, E. Nogales, and S. Westermann. 2011. Molecular architecture and connectivity of the budding yeast Mtw1 kinetochore complex. *J Mol Biol*. 405:548-59.

Howell, B.J., B.F. McEwen, J.C. Canman, D.B. Hoffman, E.M. Farrar, C.L. Rieder, and E.D. Salmon. 2001. Cytoplasmic dynein/dynactin drives kinetochore protein transport to the spindle poles and has a role in mitotic spindle checkpoint inactivation. *J Cell Biol*. 155:1159-72.

Hyland, K.M., J. Kingsbury, D. Koshland, and P. Hieter. 1999. Ctf19p: A novel kinetochore protein in Saccharomyces cerevisiae and a potential link between the kinetochore and mitotic spindle. *J Cell Biol*. 145:15-28.

Janke, C., J. Ortiz, J. Lechner, A. Shevchenko, M.M. Magiera, C. Schramm, and E. Schiebel. 2001. The budding yeast proteins Spc24p and Spc25p interact with Ndc80p and Nuf2p at the kinetochore and are important for kinetochore clustering and checkpoint control. *EMBO J*. 20:777-91.

Janke, C., J. Ortiz, T.U. Tanaka, J. Lechner, and E. Schiebel. 2002. Four new subunits of the Dam1-Duo1 complex reveal novel functions in sister kinetochore biorientation. *EMBO J*. 21:181-93.

Joglekar, A.P., K. Bloom, and E.D. Salmon. 2009. In vivo protein architecture of the eukaryotic kinetochore with nanometer scale accuracy. *Curr Biol*. 19:694-9.

Joglekar, A.P., D. Bouck, K. Finley, X. Liu, Y. Wan, J. Berman, X. He, E.D. Salmon, and K.S. Bloom. 2008. Molecular architecture of the kinetochore-microtubule attachment site is conserved between point and regional centromeres. *J Cell Biol*. 181:587-94.

Joglekar, A.P., D.C. Bouck, J.N. Molk, K.S. Bloom, and E.D. Salmon. 2006. Molecular architecture of a kinetochore-microtubule attachment site. *Nat Cell Biol*. 8:581-5.

Johnston, K., A. Joglekar, T. Hori, A. Suzuki, T. Fukagawa, and E.D. Salmon. 2010. Vertebrate kinetochore protein architecture: protein copy number. *J Cell Biol*. 189:937-43.

Kastner, B., N. Fischer, M.M. Golas, B. Sander, P. Dube, D. Boehringer, K. Hartmuth, J. Deckert, F. Hauer, E. Wolf, H. Uchtenhagen, H. Urlaub, F. Herzog, J.M. Peters, D. Poerschke, R. Luhrmann, and H.

Stark. 2008. GraFix: sample preparation for single-particle electron cryomicroscopy. *Nat Methods*. 5:53-5.

Keating, P., N. Rachidi, T.U. Tanaka, and M.J. Stark. 2009. Ipl1-dependent phosphorylation of Dam1 is reduced by tension applied on kinetochores. *J Cell Sci*. 122:4375-82.

Kemmler, S., M. Stach, M. Knapp, J. Ortiz, J. Pfannstiel, T. Ruppert, and J. Lechner. 2009. Mimicking Ndc80 phosphorylation triggers spindle assembly checkpoint signalling. *EMBO J*. 28:1099-110.

Kiyomitsu, T., H. Murakami, and M. Yanagida. 2011. Protein interaction domain mapping of human kinetochore protein Blinkin reveals a consensus motif for binding of spindle assembly checkpoint proteins Bub1 and BubR1. *Mol Cell Biol*. 31:998-1011.

Kiyomitsu, T., C. Obuse, and M. Yanagida. 2007. Human Blinkin/AF15q14 is required for chromosome alignment and the mitotic checkpoint through direct interaction with Bub1 and BubR1. *Dev Cell*. 13:663-76.

Kline, S.L., I.M. Cheeseman, T. Hori, T. Fukagawa, and A. Desai. 2006. The human Mis12 complex is required for kinetochore assembly and proper chromosome segregation. *J Cell Biol*. 173:9-17.

Knockleby, J., and J. Vogel. 2009. The COMA complex is required for Sli15/INCENP-mediated correction of defective kinetochore attachments. *Cell Cycle*. 8:2570-7.

Koshland, D.E., T.J. Mitchison, and M.W. Kirschner. 1988. Polewards chromosome movement driven by microtubule depolymerization in vitro. *Nature*. 331:499-504.

Lampert, F., P. Hornung, and S. Westermann. The Dam1 complex confers microtubule plus end-tracking activity to the Ndc80 kinetochore complex. *J Cell Biol*. 189:641-9.

Lampert, F., P. Hornung, and S. Westermann. 2010. The Dam1 complex confers microtubule plus end-tracking activity to the Ndc80 kinetochore complex. *J Cell Biol*. 189:641-9.

Lampert, F., and S. Westermann. 2011. A blueprint for kinetochores - new insights into the molecular mechanics of cell division. *Nat Rev Mol Cell Biol*. 12:407-12.

Lawrimore, J., K.S. Bloom, and E.D. Salmon. 2011. Point centromeres contain more than a single centromere-specific Cse4 (CENP-A) nucleosome. *J Cell Biol*. 195:573-82.

Lechner, J., and J. Carbon. 1991. A 240 kd multisubunit protein complex, CBF3, is a major component of the budding yeast centromere. *Cell*. 64:717-25.

Li, Y., J. Bachant, A.A. Alcasabas, Y. Wang, J. Qin, and S.J. Elledge. 2002. The mitotic spindle is required for loading of the DASH complex onto the kinetochore. *Genes Dev*. 16:183-97.

Liu, D., G. Vader, M.J. Vromans, M.A. Lampson, and S.M. Lens. 2009. Sensing chromosome bi-orientation by spatial separation of aurora B kinase from kinetochore substrates. *Science*. 323:1350-3.

Liu, S.T., J.C. Hittle, S.A. Jablonski, M.S. Campbell, K. Yoda, and T.J. Yen. 2003. Human CENP-I specifies localization of CENP-F, MAD1 and MAD2 to kinetochores and is essential for mitosis. *Nat Cell Biol*. 5:341-5.

Liu, S.T., J.B. Rattner, S.A. Jablonski, and T.J. Yen. 2006. Mapping the assembly pathways that specify formation of the trilaminar kinetochore plates in human cells. *J Cell Biol*. 175:41-53.

London, N., S. Ceto, J.A. Ranish, and S. Biggins. 2012. Phosphoregulation of Spc105 by Mps1 and PP1 Regulates Bub1 Localization to Kinetochores. *Curr Biol*.

Ludtke, S.J., P.R. Baldwin, and W. Chiu. 1999. EMAN: semiautomated software for high-resolution single-particle reconstructions. *J Struct Biol*. 128:82-97.

Maresca, T.J., and E.D. Salmon. 2009. Intrakinetochore stretch is associated with changes in kinetochore phosphorylation and spindle assembly checkpoint activity. *J Cell Biol*. 184:373-81.

Maskell, D.P., X.W. Hu, and M.R. Singleton. 2010. Molecular architecture and assembly of the yeast kinetochore MIND complex. *J Cell Biol*. 190:823-34.

Matson, D.R., P.B. Demirel, P.T. Stukenberg, and D.J. Burke. A conserved role for COMA/CENP-H/I/N kinetochore proteins in the spindle checkpoint. *Genes Dev*. 26:542-7.

Maure, J.F., S. Komoto, Y. Oku, A. Mino, S. Pasqualato, K. Natsume, L. Clayton, A. Musacchio, and T.U. Tanaka. 2011. The Ndc80 loop region facilitates formation of kinetochore attachment to the dynamic microtubule plus end. *Curr Biol*. 21:207-13.

McAinsh, A.D., P. Meraldi, V.M. Draviam, A. Toso, and P.K. Sorger. 2006. The human kinetochore proteins Nnf1R and Mcm21R are required for accurate chromosome segregation. *EMBO J*. 25:4033-49.

McCleland, M.L., R.D. Gardner, M.J. Kallio, J.R. Daum, G.J. Gorbsky, D.J. Burke, and P.T. Stukenberg. 2003. The highly conserved Ndc80 complex is required for kinetochore assembly, chromosome congression, and spindle checkpoint activity. *Genes Dev*. 17:101-14.

McEwen, B.F., G.K. Chan, B. Zubrowski, M.S. Savoian, M.T. Sauer, and T.J. Yen. 2001. CENP-E is essential for reliable bioriented spindle attachment, but chromosome alignment can be achieved via redundant mechanisms in mammalian cells. *Mol Biol Cell*. 12:2776-89.

Meluh, P.B., and D. Koshland. 1997. Budding yeast centromere composition and assembly as revealed by in vivo cross-linking. *Genes Dev*. 11:3401-12.

Miranda, J.J., P. De Wulf, P.K. Sorger, and S.C. Harrison. 2005. The yeast DASH complex forms closed rings on microtubules. *Nat Struct Mol Biol*. 12:138-43.

Morgan, D.O. 2007. The Cell Cycle.

Musacchio, A., and E.D. Salmon. 2007. The spindle-assembly checkpoint in space and time. *Nat Rev Mol Cell Biol*. 8:379-93.

Nekrasov, V.S., M.A. Smith, S. Peak-Chew, and J.V. Kilmartin. 2003. Interactions between centromere complexes in Saccharomyces cerevisiae. *Mol Biol Cell*. 14:4931-46.

Nishino, T., K. Takeuchi, K.E. Gascoigne, A. Suzuki, T. Hori, T. Oyama, K. Morikawa, I.M. Cheeseman, and T. Fukagawa. 2012. CENP-T-W-S-X forms a unique centromeric chromatin structure with a histone-like fold. *Cell*. 148:487-501.

Nogales, E., and V.H. Ramey. 2009. Structure-function insights into the yeast Dam1 kinetochore complex. *J Cell Sci*. 122:3831-6.

Obuse, C., O. Iwasaki, T. Kiyomitsu, G. Goshima, Y. Toyoda, and M. Yanagida. 2004. A conserved Mis12 centromere complex is linked to heterochromatic HP1 and outer kinetochore protein Zwint-1. *Nat Cell Biol*. 6:1135-41.

Okada, M., I.M. Cheeseman, T. Hori, K. Okawa, I.X. McLeod, J.R. Yates, 3rd, A. Desai, and T. Fukagawa. 2006. The CENP-H-I complex is required for the efficient incorporation of newly synthesized CENP-A into centromeres. *Nat Cell Biol*. 8:446-57.

Ortiz, J., O. Stemmann, S. Rank, and J. Lechner. 1999. A putative protein complex consisting of Ctf19, Mcm21, and Okp1 represents a missing link in the budding yeast kinetochore. *Genes Dev*. 13:1140-55.

Pagliuca, C., V.M. Draviam, E. Marco, P.K. Sorger, and P. De Wulf. 2009. Roles for the conserved spc105p/kre28p complex in kinetochore-microtubule binding and the spindle assembly checkpoint. *PLoS One*. 4:e7640.

Perriches, T., and M.R. Singleton. 2012. Structure of yeast kinetochore Ndc10 DNA-binding domain reveals unexpected evolutionary relationship to tyrosine recombinases. *J Biol Chem*. 287:5173-9.

Petrovic, A., S. Pasqualato, P. Dube, V. Krenn, S. Santaguida, D. Cittaro, S. Monzani, L. Massimiliano, J. Keller, A. Tarricone, A. Maiolica, H. Stark, and A. Musacchio. 2010. The MIS12 complex is a protein interaction hub for outer kinetochore assembly. *J Cell Biol*. 190:835-52.

Pinsky, B.A., S.Y. Tatsutani, K.A. Collins, and S. Biggins. 2003. An Mtw1 complex promotes kinetochore biorientation that is monitored by the Ipl1/Aurora protein kinase. *Dev Cell*. 5:735-45.

Poddar, A., N. Roy, and P. Sinha. 1999. MCM21 and MCM22, two novel genes of the yeast Saccharomyces cerevisiae are required for chromosome transmission. *Mol Microbiol*. 31:349-60.

Pot, I., J. Knockleby, V. Aneliunas, T. Nguyen, S. Ah-Kye, G. Liszt, M. Snyder, P. Hieter, and J. Vogel. 2005. Spindle checkpoint maintenance requires Ame1 and Okp1. *Cell Cycle*. 4:1448-56.

Pot, I., V. Measday, B. Snydsman, G. Cagney, S. Fields, T.N. Davis, E.G. Muller, and P. Hieter. 2003. Chl4p and iml3p are two new members of the budding yeast outer kinetochore. *Mol Biol Cell*. 14:460-76.

Przewloka, M.R., Z. Venkei, V.M. Bolanos-Garcia, J. Debski, M. Dadlez, and D.M. Glover. 2011. CENP-C is a structural platform for kinetochore assembly. *Curr Biol*. 21:399-405.

Przewloka, M.R., W. Zhang, P. Costa, V. Archambault, P.P. D'Avino, K.S. Lilley, E.D. Laue, A.D. McAinsh, and D.M. Glover. 2007. Molecular analysis of core kinetochore composition and assembly in Drosophila melanogaster. *PLoS One*. 2:e478.

Putkey, F.R., T. Cramer, M.K. Morphew, A.D. Silk, R.S. Johnson, J.R. McIntosh, and D.W. Cleveland. 2002. Unstable kinetochore-microtubule capture and chromosomal instability following deletion of CENP-E. *Dev Cell*. 3:351-65.

Ramey, V.H., H.W. Wang, Y. Nakajima, A. Wong, J. Liu, D. Drubin, G. Barnes, and E. Nogales. 2011. The Dam1 ring binds to the E-hook of tubulin and diffuses along the microtubule. *Mol Biol Cell*. 22:457-66.

Regnier, V., P. Vagnarelli, T. Fukagawa, T. Zerjal, E. Burns, D. Trouche, W. Earnshaw, and W. Brown. 2005. CENP-A is required for accurate chromosome segregation and sustained kinetochore association of BubR1. *Mol Cell Biol*. 25:3967-81.

Rieder, C.L., and E.D. Salmon. 1998. The vertebrate cell kinetochore and its roles during mitosis. *Trends Cell Biol*. 8:310-8.

Russell, I.D., A.S. Grancell, and P.K. Sorger. 1999. The unstable F-box protein p58-Ctf13 forms the structural core of the CBF3 kinetochore complex. *J Cell Biol*. 145:933-50.

Scharfenberger, M., J. Ortiz, N. Grau, C. Janke, E. Schiebel, and J. Lechner. 2003. Nsl1p is essential for the establishment of bipolarity and the localization of the Dam-Duo complex. *EMBO J*. 22:6584-97.

Schleiffer, A., M. Maier, G. Litos, F. Lampert, P. Hornung, K. Mechtler, and S. Westermann. 2012. CENP-T proteins are conserved centromere receptors of the Ndc80 complex. *Nat Cell Biol*.

Screpanti, E., A. De Antoni, G.M. Alushin, A. Petrovic, T. Melis, E. Nogales, and A. Musacchio. 2011. Direct binding of Cenp-C to the Mis12 complex joins the inner and outer kinetochore. *Curr Biol*. 21:391-8.

Siegel, L.M., and K.J. Monty. 1966. Determination of molecular weights and frictional ratios of proteins in impure systems by use of gel filtration and density gradient centrifugation. Application to crude preparations of sulfite and hydroxylamine reductases. *Biochim Biophys Acta*. 112:346-62.

Stoffler, D., B. Feja, B. Fahrenkrog, J. Walz, D. Typke, and U. Aebi. 2003. Cryo-electron tomography provides novel insights into nuclear pore architecture: implications for nucleocytoplasmic transport. *J Mol Biol*. 328:119-30.

Sugimoto, K., K. Kuriyama, A. Shibata, and M. Himeno. 1997. Characterization of internal DNA-binding and C-terminal dimerization domains of human centromere/kinetochore autoantigen CENP-C in vitro: role of DNA-binding and self-associating activities in kinetochore organization. *Chromosome Res*. 5:132-41.

Sugimoto, K., H. Yata, Y. Muro, and M. Himeno. 1994. Human centromere protein C (CENP-C) is a DNA-binding protein which possesses a novel DNA-binding motif. *J Biochem*. 116:877-81.

Takeuchi, K., and T. Fukagawa. 2012. Molecular architecture of vertebrate kinetochores. *Exp Cell Res*.

Tanaka, K., E. Kitamura, Y. Kitamura, and T.U. Tanaka. 2007. Molecular mechanisms of microtubule-dependent kinetochore transport toward spindle poles. *J Cell Biol*. 178:269-81.

Tanaka, K., N. Mukae, H. Dewar, M. van Breugel, E.K. James, A.R. Prescott, C. Antony, and T.U. Tanaka. 2005. Molecular mechanisms of kinetochore capture by spindle microtubules. *Nature*. 434:987-94.

Tanaka, T.U., and A. Desai. 2008. Kinetochore-microtubule interactions: the means to the end. *Curr Opin Cell Biol*. 20:53-63.

Tanaka, T.U., N. Rachidi, C. Janke, G. Pereira, M. Galova, E. Schiebel, M.J. Stark, and K. Nasmyth. 2002. Evidence that the Ipl1-Sli15 (Aurora kinase-INCENP) complex promotes chromosome bi-orientation by altering kinetochore-spindle pole connections. *Cell*. 108:317-29.

Uchida, K.S., K. Takagaki, K. Kumada, Y. Hirayama, T. Noda, and T. Hirota. 2009. Kinetochore stretching inactivates the spindle assembly checkpoint. *J Cell Biol*. 184:383-90.

Wan, X., R.P. O'Quinn, H.L. Pierce, A.P. Joglekar, W.E. Gall, J.G. DeLuca, C.W. Carroll, S.T. Liu, T.J. Yen, B.F. McEwen, P.T. Stukenberg, A. Desai, and E.D. Salmon. 2009. Protein architecture of the human kinetochore microtubule attachment site. *Cell*. 137:672-84.

Wang, H.W., S. Long, C. Ciferri, S. Westermann, D. Drubin, G. Barnes, and E. Nogales. 2008. Architecture and flexibility of the yeast Ndc80 kinetochore complex. *J Mol Biol*. 383:894-903.

Wei, R.R., J. Al-Bassam, and S.C. Harrison. 2007. The Ndc80/HEC1 complex is a contact point for kinetochore-microtubule attachment. *Nat Struct Mol Biol*. 14:54-9.

Wei, R.R., J.R. Schnell, N.A. Larsen, P.K. Sorger, J.J. Chou, and S.C. Harrison. 2006. Structure of a central component of the yeast kinetochore: the Spc24p/Spc25p globular domain. *Structure*. 14:1003-9.

Wei, R.R., P.K. Sorger, and S.C. Harrison. 2005. Molecular organization of the Ndc80 complex, an essential kinetochore component. *Proc Natl Acad Sci U S A*. 102:5363-7.

Welburn, J.P., E.L. Grishchuk, C.B. Backer, E.M. Wilson-Kubalek, J.R. Yates, 3rd, and I.M. Cheeseman. 2009. The human kinetochore Ska1 complex facilitates microtubule depolymerization-coupled motility. *Dev Cell*. 16:374-85.

Westermann, S., A. Avila-Sakar, H.W. Wang, H. Niederstrasser, J. Wong, D.G. Drubin, E. Nogales, and G. Barnes. 2005. Formation of a dynamic kinetochore- microtubule interface through assembly of the Dam1 ring complex. *Mol Cell*. 17:277-90.

Westermann, S., I.M. Cheeseman, S. Anderson, J.R. Yates, 3rd, D.G. Drubin, and G. Barnes. 2003. Architecture of the budding yeast kinetochore reveals a conserved molecular core. *J Cell Biol*. 163:215-22.

Westermann, S., D.G. Drubin, and G. Barnes. 2007. Structures and functions of yeast kinetochore complexes. *Annu Rev Biochem*. 76:563-91.

Westermann, S., H.W. Wang, A. Avila-Sakar, D.G. Drubin, E. Nogales, and G. Barnes. 2006. The Dam1 kinetochore ring complex moves processively on depolymerizing microtubule ends. *Nature*. 440:565-9.

Wigge, P.A., and J.V. Kilmartin. 2001. The Ndc80p complex from Saccharomyces cerevisiae contains conserved centromere components and has a function in chromosome segregation. *J Cell Biol*. 152:349-60.

Wong, J., Y. Nakajima, S. Westermann, C. Shang, J.S. Kang, C. Goodner, P. Houshmand, S. Fields, C.S. Chan, D. Drubin, G. Barnes, and T. Hazbun. 2007. A protein interaction map of the mitotic spindle. *Mol Biol Cell*. 18:3800-9.

Zhang, G., C.D. Kelstrup, X.W. Hu, M.J. Hansen, M.R. Singleton, J.V. Olsen, and J. Nilsson. 2012. The Ndc80 internal loop is required for recruitment of the Ska complex to establish end-on microtubule attachment to kinetochores. *J Cell Sci*.

8 Appendix

8.1 Abbreviation

6xHis	Six times histidine tag
c	Complex
C-	C-terminal
CCAN	Constitutive Centromere Associated Network
CDE	Centromeric DNA elements
CEN	Centromere/centromeric
CHIP	*chromatin immunoprecipitation*
EM	Electron microscopy
IEX	Anion-exchange chromatography
IPTG	isopropyl β-D-1-thiogalactopyranoside
Kd	Apperant dissociation constant
N-	N-terminal
Ni-NTA	nickel-nitrilotriacetic acid
ON	Overnight
PBS	*Phosphate buffered saline*
PMSF	phenylmethanesulfonylfluoride
RT	Room temerpature
SDS-PAGE	Sodium dodecylsulfate polyacrylamide gel electrophoresis
SEC	Size exclusion chromatography
SS	Salmon sperm
ts	Temperature sensitive
URA3	Orotidine-5'-phosphate decarboxylase
WT	Wild type

8.2 Curriculum Vitae

PERSONAL DATA

Name: Peter Hornung
Date of birth: March 3rd, 1979
Place of birth: Memmingen
Gender: Male

EDUCATION

08/2008 – present	Research Institute of Molecular Pathology (IMP), Vienna, Austria PhD thesis
10/2006 – 06/2008	Westfälische Wilhelms University, Münster, Germany Master of Science - Biology (grade 1.0)
03/2002 – 09/2006	University of Applied Science, Mannheim, Germany Diploma in engineering - Biological Chemistry (grade 2.3)
10/2001 – 03/2002	University of Applied Science Weihenstephan, Freising, Germany Study of Biotechnology
09/2000 – 07/2001	Berufskolleg, Weil am Rhein, Germany Fachhochschulreife (grade 1.5)
09/1999 – 07/2000	Handicapped Kindergarten Emma Fackler, Weil am Rhein Civil service
08/1996 – 08/1999	Company Stern Optik, Weil am Rhein Apprenticeship to an optician (certificate of apprenticeship)
1986 – 1999	Primary school and secondary school, Weil am Rhein

8.3 Acknowledgments

I would like to thank Dr. Stefan Westermann for giving me the chance to work on such an interesting project and for his excellent and constant supervision during my PhD. Thank you very much.

I am greatful towards all group members of the Westermann lab for the time inside and also outside of the lab. I really liked spending time with all of you.

During my PhD thesis I work successfully with several cooperators to those I express my gratitude. In particular I thank Michael Maier, Fabienne Lampert and Gregory Alushin.

8.4 Publications

Hornung, P., M. Maier, G.M. Alushin, G.C. Lander, E. Nogales, and S. Westermann. 2011. Molecular architecture and connectivity of the budding yeast Mtw1 kinetochore complex. *J Mol Biol*. 405:548-59.

Lampert, F., **P. Hornung**, and S. Westermann. The Dam1 complex confers microtubule plus end-tracking activity to the Ndc80 kinetochore complex. *J Cell Biol*. 189:641-9.

Schleiffer, A., M. Maier, G. Litos, F. Lampert, **P. Hornung**, K. Mechtler, and S. Westermann. 2012. CENP-T proteins are conserved centromere receptors of the Ndc80 complex. *Nat Cell Biol*.

doi:10.1016/j.jmb.2010.11.012 J. Mol. Biol. (2011) 405, 548–559

Contents lists available at www.sciencedirect.com

Journal of Molecular Biology

journal homepage: http://ees.elsevier.com.jmb

Molecular Architecture and Connectivity of the Budding Yeast Mtw1 Kinetochore Complex

Peter Hornung[1], Michael Maier[1], Gregory M. Alushin[2], Gabriel C. Lander[3], Eva Nogales[3,4,5] and Stefan Westermann[1]*

[1]*Research Institute of Molecular Pathology, Dr. Bohr Gasse 7, 1030 Vienna, Austria*
[2]*Biophysics Graduate Group, University of California, Berkeley, Berkeley, CA 94720, USA*
[3]*Life Science Division, Lawrence Berkeley National Laboratory, 1 Cyclotron Road, Berkeley, CA 94720, USA*
[4]*Department of Molecular and Cell Biology, University of California, Berkeley, Berkeley, CA 94720, USA*
[5]*Howard Hughes Medical Institute, Chevy Chase, MD, USA*

Received 27 August 2010; received in revised form 24 October 2010; accepted 4 November 2010
Available online 12 November 2010

Edited by W. Baumeister

Keywords:
kinetochore;
KMN network;
chromosome segregation;
force generation;
microtubule

Kinetochores are large multiprotein complexes that connect centromeres to spindle microtubules in all eukaryotes. Among the biochemically distinct kinetochore complexes, the conserved four-protein Mtw1 complex is a central part of the kinetochore in all organisms. Here we present the biochemical reconstitution and characterization of the budding yeast Mtw1 complex. Direct visualization by electron microscopy revealed an elongated bilobed structure with a 25-nm-long axis. The complex can be assembled from two stable heterodimers consisting of Mtw1p–Nnf1p and Dsn1p–Nsl1p, and it interacts directly with the microtubule-binding Ndc80 kinetochore complex via the centromere-proximal Spc24/Spc25 head domain. In addition, we have reconstituted a partial Ctf19 complex and show that it directly associates with the Mtw1 complex *in vitro*. Ndc80 and Ctf19 complexes do not compete for binding to the Mtw1 complex, suggesting that Mtw1 can bridge the microtubule-binding components of the kinetochore to the inner centromere.

Introduction

Interaction between chromosomes and spindle microtubules requires the action of a complex multiprotein machine termed the kinetochore.[1,2] Kinetochores are responsible for microtubule-based force generation that drives sister chromatid separation in anaphase. They additionally contain an error-correction mechanism that ensures the bipolar attachment of sister chromatids to opposite spindle poles,[3] and they relay signals to the mitotic checkpoint that prevents the cell from entering anaphase in the presence of unattached kinetochores.[4] In budding yeast, the structural core of the kinetochore consists of at least seven biochemically distinct subcomplexes that are present in fixed copy numbers in mature budding yeast kinetochores[5] and assemble on centromeric DNA in a hierarchical manner.[6] A current challenge in the field is to elucidate the architecture of the kinetochore by defining the binding interfaces between kinetochore complexes. Previous biochemical studies have focused on the reconstitution and functional analysis of two important parts of the budding yeast outer kinetochore: the Dam1 complex and the Ndc80 complex. Both of these complexes directly interact with microtubules and are required for force generation in yeast kinetochores.[7,8] The Dam1 complex has the ability to oligomerize into rings *in vitro*,[9,10] opening up the possibility that a Dam1 ring is a physiologically relevant coupling

*Corresponding author. E-mail address: westermann@imp.ac.at.

Abbreviations used: SEC, size-exclusion chromatography; EM, electron microscopy; CCAN, constitutive centromere-associated network; TBS, Tris-buffered saline.

device for kinetochores on microtubule plus ends in yeast. Recent experiments have demonstrated that Dam1 is a specialized plus-end tracking complex required for a persistent attachment of the Ndc80 complex to dynamic microtubule ends *in vitro*.[11,12]

The four-protein 180-kDa Ndc80 complex is a conserved component of all kinetochores. Biochemical isolations from extracts and *in vitro* reconstitution experiments using *Caenorhabditis elegans* Ndc80 subunits have demonstrated that the complex functions together with the conserved four-protein complex Mtw1 (also called Mis12 or MIND) and with the protein KNL-1/Blinkin (Spc105p in budding yeast) as part of a larger network termed KMN (*K*NL-1 *M*is12 *N*dc80).[13] Analysis of temperature-sensitive mutants of MTW1 complex subunits in fission yeast and budding yeast, as well as depletion experiments in worms and human cells, has demonstrated that the complex is essential for kinetochore biorientation and chromosome segregation.[14–16] Since biochemical reconstitution experiments have so far only been performed with *C. elegans* kinetochore proteins, it is an open question whether the architecture, topology, and biochemical activities of the KMN network are conserved among evolutionarily distinct eukaryotes. Furthermore, it is unknown how the KMN network is anchored to the inner kinetochore, a critical step in creating a microtubule attachment site specifically at the centromere. Here, we report the reconstitution and biochemical characterization of the budding yeast Mtw1 complex. Our analysis defines the architecture of this central kinetochore complex and is an important step towards a reconstitution of the full yeast kinetochore.

Results and Discussion

Reconstitution of the four-protein Mtw1 complex

To reconstitute the budding yeast Mtw1 complex, we employed a polycistronic expression strategy. Genes encoding all four subunits (DSN1, MTW1, NNF1, and NSL1) of the complex were placed under the control of a T7 promoter and expressed in BL21 (DE3) cells. The purification strategy used a 6×His tag on the Nnf1p subunit, allowing initial purification with a Ni-NTA resin. After elution, the complex was further purified by size-exclusion chromatography (SEC) (Fig. 1a). Analysis of the complex on Coomassie-stained gels revealed that all four subunits of the complex were present at a stoichiometry of 1:1:1:1. The complex eluted earlier than expected from SEC with a Stokes radius of 74.3 Å. The sedimentation coefficient of the Mtw1 complex was determined by glycerol gradient centrifugation and estimated to be 6S (data not shown). Thus, the native molecular mass of the recombinant complex is 183 kDa, compared to the calculated molecular mass of 148 kDa, and the frictional coefficient f/f_0 is 2.0, predicting a complex that is moderately to highly elongated. These values are in close agreement to those obtained for the Mtw1 complex in yeast extracts,[17] suggesting that the recombinant complex closely resembles its native counterpart. We noticed that the Dsn1p subunit of the complex was particularly prone to proteolytic degradation during purification (Fig. 1a). Sequencing of the major proteolysis products revealed that the N-terminus of Dsn1p is easily cleaved. We subsequently cloned an N-terminally shortened version of the Dsn1 subunit corresponding to the major proteolysis product, which lacks amino acids 1–171. Expression of Dsn1$^{172–567}$, in combination with full-length MTW1, NNF1-6×His, and NSL1, allowed the purification of the entire four-protein Mtw1 complex (Fig. 1b). We conclude that the N-terminal extension of Dsn1, which is unusually long in budding yeast compared to other eukaryotes and is predicted to be unstructured, is dispensable for complex formation *in vitro*. To determine whether this N-terminal extension has an essential function *in vivo*, we expressed wild-type or N-terminally truncated DSN1$^{172–576}$ on centromeric plasmids in a haploid DSN1 deletion strain that was kept viable by containing a wild-type copy of DSN1 on a CEN-based URA plasmid. Selection against the URA plasmid on 5-fluoroorotic acid plates demonstrated that Dsn1$^{172–576}$ supported wild-type growth (Supplementary Fig. 1). Thus, the N-terminal 172 amino acids of Dsn1 are not required for complex formation *in vitro* and do not have an essential function *in vivo*.

The Mtw1 complex can be assembled from two stable heterodimers

SEC analysis of epitope-tagged kinetochore proteins in yeast extracts suggests that Dam1 and Ndc80 complexes are present only in their fully assembled

Fig. 1. Reconstitution of the Mtw1 complex. (a) Expression and purification of the Mtw1 complex. The Coomassie-stained gel shows different steps of the purification scheme: control extract and extract after induction with IPTG, eluate from Ni-NTA beads, and purified fraction after SEC. Note the presence of the degradation products of the Dsn1p subunit. (b) Expression and purification of a complex with an N-terminally truncated Dsn1p subunit. (c) Expression and purification of a stable Dsn1–Nsl1 heterodimer. IEX denotes anion-exchange chromatography. Asterisks in (a), (b), and (c) indicate contamination with the *E. coli* Hsp70 chaperone. (d) Expression and purification of the Mtw1–Nnf1 heterodimer. (e) SEC runs of Dsn1p–Nsl1p and Mtw1p–Nnf1p subcomplexes (8 μM each) and of the full complex after reconstitution. (f) Coomassie-stained SDS-PAGE of fractions from (e). Asterisks indicate an Nnf1 truncation product.

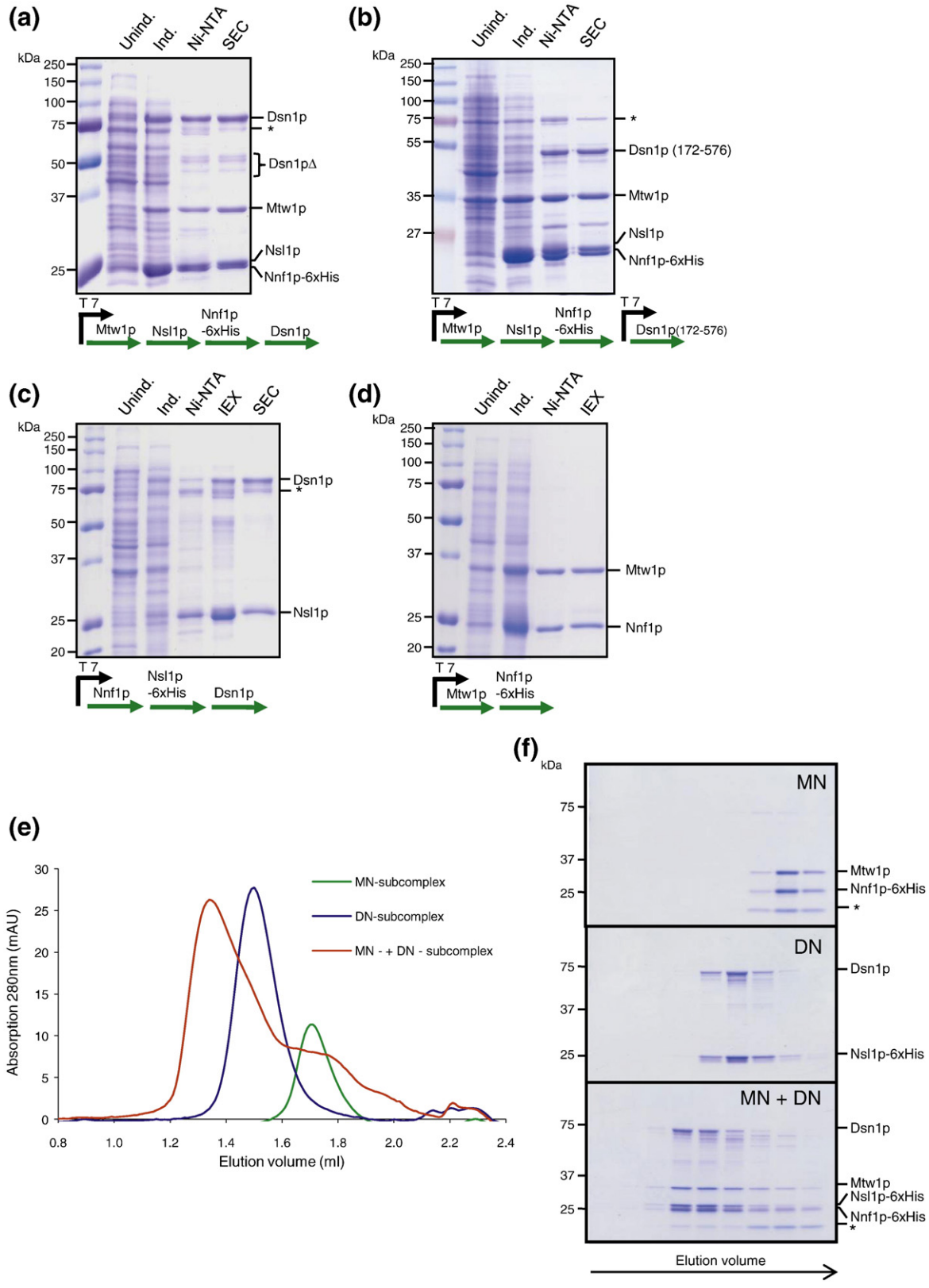

Fig. 1 (*legend on previous page*)

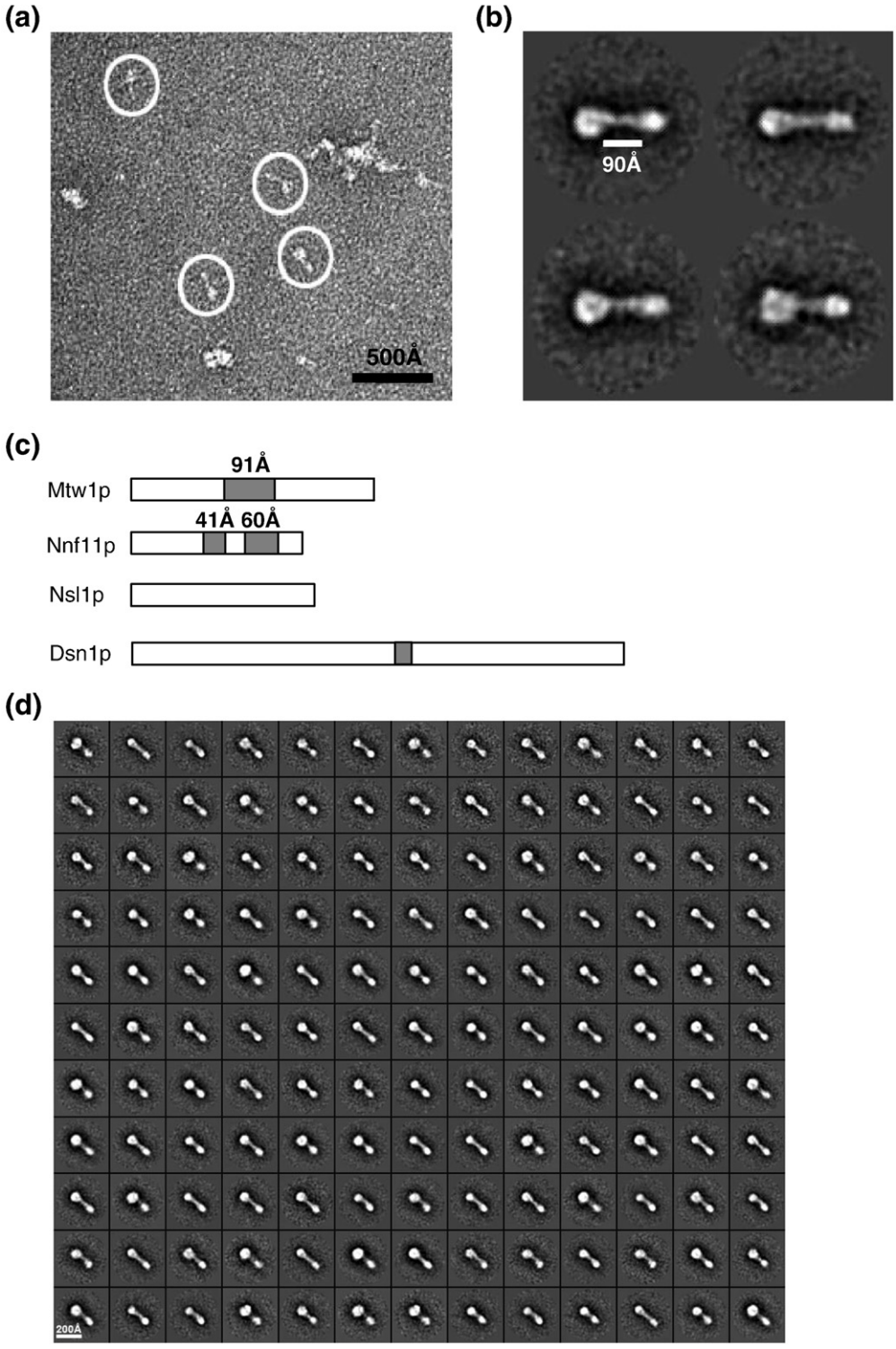

Fig. 2. EM analysis of the Mtw1 complex. (a) Negative-stain EM image of the Mtw1 complex. Note the heterogeneous composition of the sample. White circles correspond to particles chosen for further analysis. (b) Selected class averages showing the architecture and dimensions of the complex. The complex is a bilobed rod, with one large globular domain and one small globular domain. (c) Coiled-coil predictions for the protein subunits of the complex. Gray regions correspond to greater than 50% coiled-coil probability. (d) Entire complement of class averages obtained for the complex. They all display the bilobed architecture, with much heterogeneity occurring in the size of the larger globular domain.

state, although Mtw1 complexes of different compositions can be detected.[17] To identify such stable subcomplexes, we expressed various combinations of Mtw1 complex subunits. We were able to express and purify two stable complexes: a heterodimer consisting of Mtw1p and Nnf1p (MN complex) (Fig. 1d), and a heterodimer consisting of Dsn1p and Nsl1p (DN complex) (Fig. 1c). We next asked whether the Mtw1 heterotetramer can be reconstituted by combining the two stable dimers. After the mixing of MN and DN subcomplexes, followed by SEC, we observed a reconstitution of the full Mtw1 complex, which eluted at a position identical with that of the native complex (Fig. 1e). Thus, the four-protein Mtw1 complex is composed of two stable heterodimers consisting of Mtw1p–Nnf1p and Dsn1p–Nsl1p, a result that is in agreement with binary two-hybrid interactions between these subunits.[18]

Electron microscopy analysis of the reconstituted Mtw1 complex

Negative-stain single-particle electron microscopy (EM) was used to characterize the structural architecture of the Mtw1 complex. Despite our efforts to cross-link and purify the complex, the imaged fields of particles contained a heterogeneous mixture of aggregates and small fragments, as well as the monomeric full-size complex (Fig. 2a). We manually picked the particle images that appeared to correspond to the monomeric full-length complex based on their consistent size (Fig. 2a, white circles). After reference-free classification, we observed a distinct bilobed rod-like structure that is approximately 250 Å in length, with one of the lobes consistently appearing slightly larger than the other (Fig. 2b and d). The larger lobe varied in size, likely reflecting the presence of degrons in the Dsn1p subunit and/or different views around the long axis of the complex.

The larger globular lobe has an approximate diameter of 71 Å, and the smaller lobe has an approximate diameter of 47 Å. Assuming a spherical shape for each, this would correspond to an approximate mass of 150 kDa and 45 kDa, respectively, the sum of which (195 kDa) very closely matches the experimentally determined mass. The calculated mass of the smaller lobe matches well with the combined predicted masses of Mtw1p and Nnf1p (57 kDa), assuming that their coiled-coil domains project outwards from the lobe. The calculated mass of the larger lobe exceeds the combined masses of Dsn1p and Nsl1p (91 kDa), suggesting that this lobe deviates from spherical geometry (the smaller lobe is too small to accommodate the mass of this subcomplex). The thin density connecting the two globular lobes is approximately 90 Å long (Fig. 2b), which matches the length of a predicted dimeric coiled coil between the Mtw1p subunits and the Nnf1p subunits (Fig. 2c). We also experimentally demonstrated that these two proteins form a stable subcomplex, supporting the proposal that the coiled-coil regions of these two proteins probably dimerize in the context of the full complex. While this is the most parsimonious explanation for a complex topology, we cannot exclude the possibility that each globular head is occupied by more than two subunits.

In vivo, the Mtw1 complex acts as a bridge between the microtubule-binding Ndc80 complex and the inner kinetochore.[6] The Ndc80 complex is 57 nm in length,[19] and the Mtw1 complex is 25 nm in length. Taken together, these dimensions suggest that the KMN network is long enough to span the full length of the outer kinetochore, consistent with high-resolution fluorescence microscopy studies.[20]

Reconstitution of the interaction between Ndc80 complexes and Mtw1 complexes

We next asked whether the recombinant Mtw1 complex can directly interact with the Ndc80 complex. To this end, we purified the four-protein Ndc80 complex by expressing the Nuf2–Ndc80 and Spc24–Spc25 heterodimers individually and then reconstituted the entire complex using SEC (Fig. 3a). When the Mtw1 and Ndc80 complexes were mixed and subjected to gel filtration, the elution profile of the assembly was shifted with respect to the individual complexes. Coomassie-stained gels revealed that the complexes coeluted, and the densitometry of the Coomassie-stained bands indicated a 1:1 stoichiometry of the Mtw1–Ndc80 binary complex (Fig. 3b and c). The elution position indicated that the Ndc80–Mtw1 assembly is a dimer containing one copy of each complex. The Ndc80–Mtw1 stoichiometry obtained from this biochemical experiment is in agreement with quantitative fluorescence microscopy data indicating the presence of nearly identical numbers of Ndc80 (eight copies) and Mtw1 (six to seven copies) complexes for each budding yeast kinetochore.[5] Another important implication is that budding yeast Ndc80 and Mtw1 complexes form a stable association that does not depend on the presence of the KNL-1 protein Spc105p. This is in contrast to the *in-vitro*-reconstituted *C. elegans* KMN network, where only a Mis12–KNL-1 association is competent to interact with the Ndc80 complex.[13] Thus, while the overall association of Ndc80 and Mtw1 complexes is critical for the function of all kinetochores, the molecular details of this association can vary significantly in different organisms. Despite extensive efforts, we were unable to express sufficient amounts of full-length or partial KNL-1/Spc105p fragments, leaving open the possibility that the affinity of the Mtw1 complex for the Ndc80 complex may be increased by the presence of Spc105p.

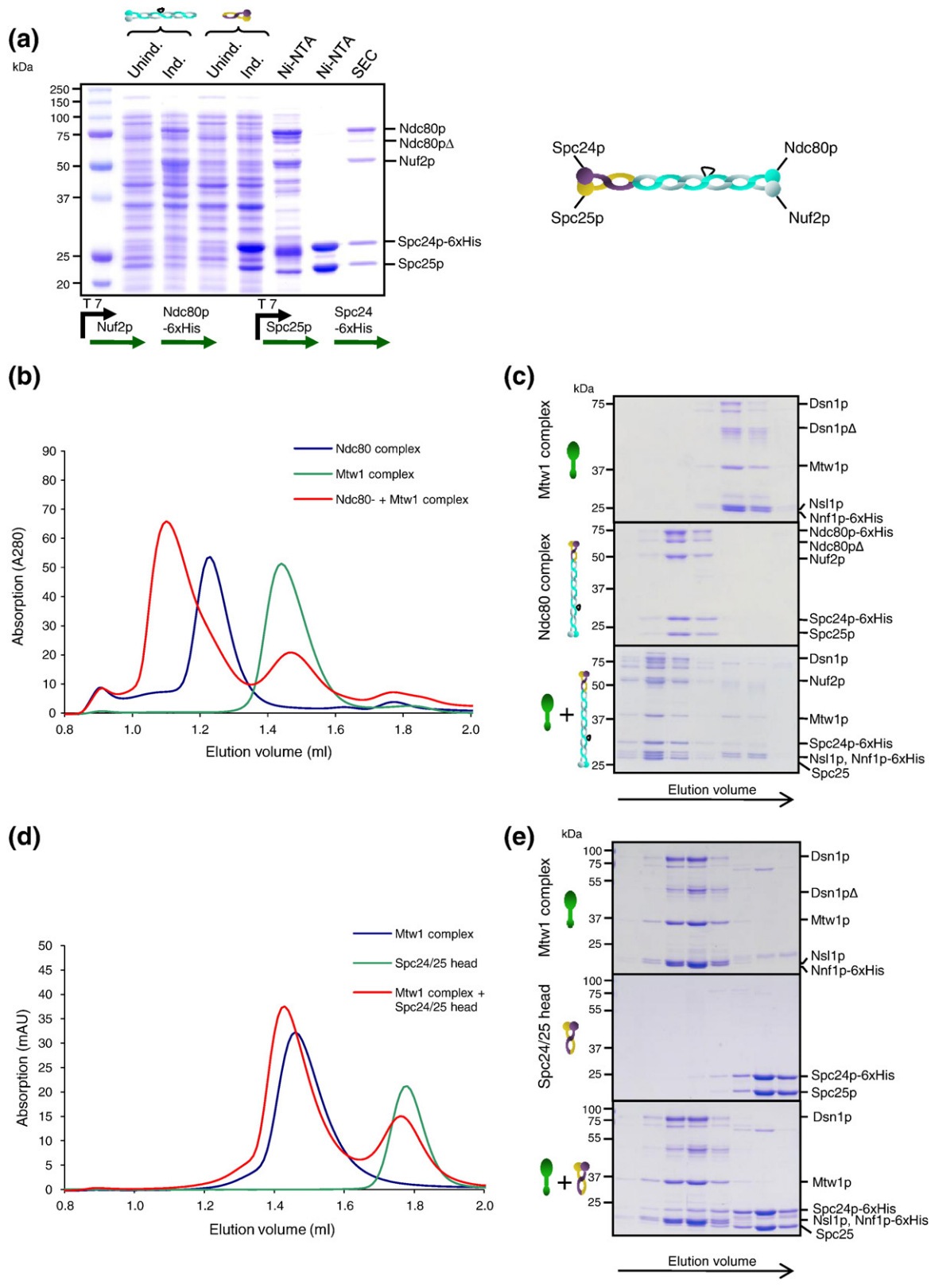

Fig. 3 (*legend on next page*)

The two globular domains of the Ndc80 complex have different functions: the Ndc80–Nuf2 head displays microtubule binding activity through the presence of two calponin homology domains and a basic N-terminal tail.[8,21] The Spc24/Spc25 head, on the other hand, is thought to reside proximal to the centromere and to connect the Ndc80 complex to the rest of the kinetochore. We tested which of the Ndc80 subcomplexes provides the binding site for the Mtw1 complex. Therefore, we subjected the purified Spc24/Spc25 head of the Ndc80 complex and the Mtw1 complex to SEC individually and then in combination. Upon preincubation with the Mtw1 complex, part of the isolated Spc24/Spc25 head was found coeluting with the Mtw1 complex (Fig. 3d and e). The interaction with the head domain seemed to be less efficient when compared to the full Ndc80 complex, suggesting that high affinity may require the full Ndc80 complex. We conclude that the Ndc80 complex directly binds to the Mtw1 complex via its centromere-proximal Spc24/Spc25 head domain, a result that is in agreement with high-resolution microscopy data placing Spc24/Spc25 in the immediate vicinity of Mtw1 complex subunits.[20]

Consistent with the results obtained for the *C. elegans* KMN network, the reconstituted Mtw1 complex did not bind directly to Taxol-stabilized microtubules in cosedimentation experiments (Supplementary Fig. 2). Only upon inclusion of the purified Ndc80 complex was the Ndc80–Mtw1 assembly found copelleting with microtubules. Furthermore, binding of the Mtw1 complex did not significantly alter the microtubule-binding properties of the Ndc80 complex (Supplementary Fig. 2).

A Ctf19 core complex directly associates with the Mtw1 complex

High-resolution colocalization data place the Mtw1 complex close to the centromere–kinetochore interface,[20] but the inner centromere receptor for the complex has not been identified. The human Mis12 complex has been reported to copurify and directly interact with the inner centromere protein HP1 via the human NSL1 subunit.[22,23] The importance of this interaction for mitotic kinetochore function, however, is unclear, and an HP1 homolog is absent from the *Saccharomyces cerevisiae* genome. Biochemical purifications of epitope-tagged Mtw1 subunits from yeast extracts[17,24] have suggested two candidate interaction partners at the inner centromere interface: the budding yeast CENP-C homolog Mif2p and the Ctf19 complex. Initial experiments failed to detect a direct interaction between recombinant Mif2p fragments and the Mtw1 complex (data not shown), prompting us to focus on the Ctf19 complex as a potential binding partner. The yeast Ctf19 complex is the functional homolog of the constitutive centromere-associated network (CCAN) of higher eukaryotes. The CCAN was originally identified as a set of polypeptides that copurify with CENP-A-containing nucleosomes.[25,26] The budding yeast Ctf19 complex consists of at least 11 subunits, some of which are organized into more stable subcomplexes. We reconstituted a core Ctf19 complex consisting of the proteins Ctf19p, Okp1p, Mcm21p, and Ame1p (also termed COMA[17]) by coexpression in *Escherichia coli*. A purification procedure utilizing the 6×His-tagged Ame1p subunit allowed isolation of the four-protein complex to near homogeneity (Fig. 4a). Mcm21, Ame1-6×His, and Ctf19 polypeptides could be resolved on a 20-cm-long SDS-PAGE gel (Fig. 4a, right), and individual bands were excised and analyzed by mass spectrometry. This allowed assignment of the subunits to the corresponding bands on SDS-PAGE. The intensity of the Coomassie-stained bands suggests the presence of all four subunits of the COMA complex at a stoichiometry of 1:1:1:1.

To analyze potential associations with other kinetochore complexes, we immobilized different concentrations of FLAG-tagged COMA complex on beads; incubated them with recombinant Mtw1, Ndc80, and Dam1 kinetochore complexes; washed them; and subsequently eluted them with FLAG peptide (Fig. 4b). While we failed to detect a direct association of the purified COMA complex with recombinant Ndc80 and Dam1 complexes, the Mtw1 complex consistently coeluted with COMA in a concentration-dependent manner (Fig. 4c).

To verify a direct interaction between Mtw1 complexes and COMA complexes, we performed a reciprocal experiment in which 6×His-tagged Mtw1, Ndc80, and Dam1 complexes were each immobilized on Ni-NTA agarose, incubated with recombinant Ctf19–FLAG core complex, washed, and eluted with imidazole. Only in the presence of the Mtw1 complex is coelution of the COMA complex observed (Fig. 4c). To more stringently test the physical interaction, we analyzed the Mtw1 and COMA complexes by SEC and found that the complexes coeluted (Fig. 5). This result raises the possibility that

Fig. 3. The Mtw1 complex interacts with Ndc80 via the Spc24/Spc25 head. (a) Expression and purification of the Ndc80 kinetochore complex. The Ndc80–Nuf2 and Spc24–Spc25 heterodimers are expressed individually; in combination, the reconstituted full complex is purified by SEC. (b) Coomassie-stained gels of gel-filtration runs of the Mtw1 complex and the Ndc80 complex alone or in combination (9 μM each). (c) Gel-filtration profile corresponding to (b). (d) Coomassie-stained gels of the Mtw1 complex and the purified Spc24/Spc25 head domain alone or in combination (6 μM each). (e) Gel-filtration profile corresponding to (d).

COMA is involved in recruiting the Mtw1 complex to the inner centromere in budding yeast. A strong prediction from this hypothesis is that Ndc80 and COMA complexes should not compete for binding to the Mtw1 complex. We tested this by preincubating the Mtw1 and Ndc80 complexes, allowing formation of the binary Mtw1–Ndc80 assembly, followed by incubation with COMA–FLAG beads. Incubation

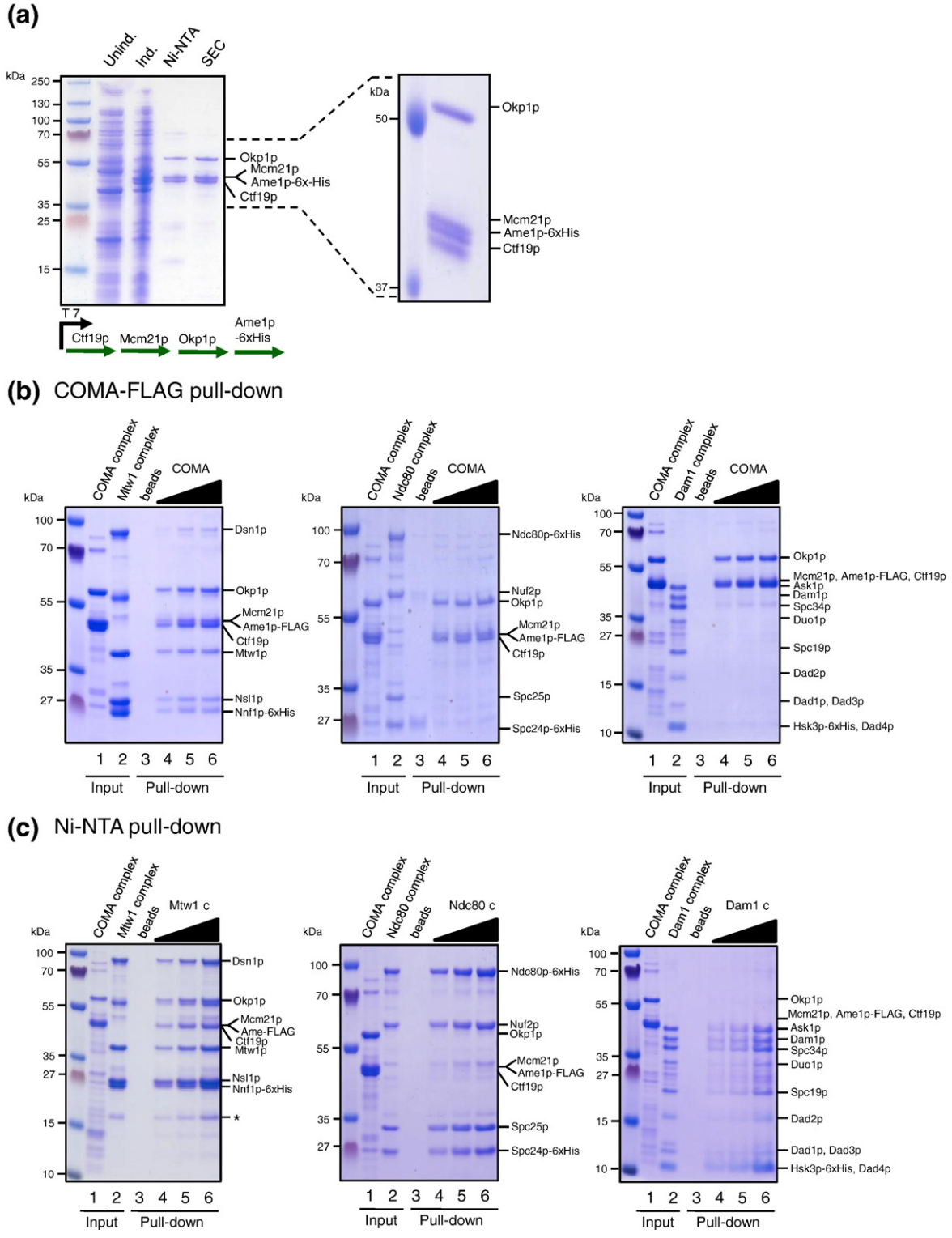

Fig. 4 (*legend on next page*)

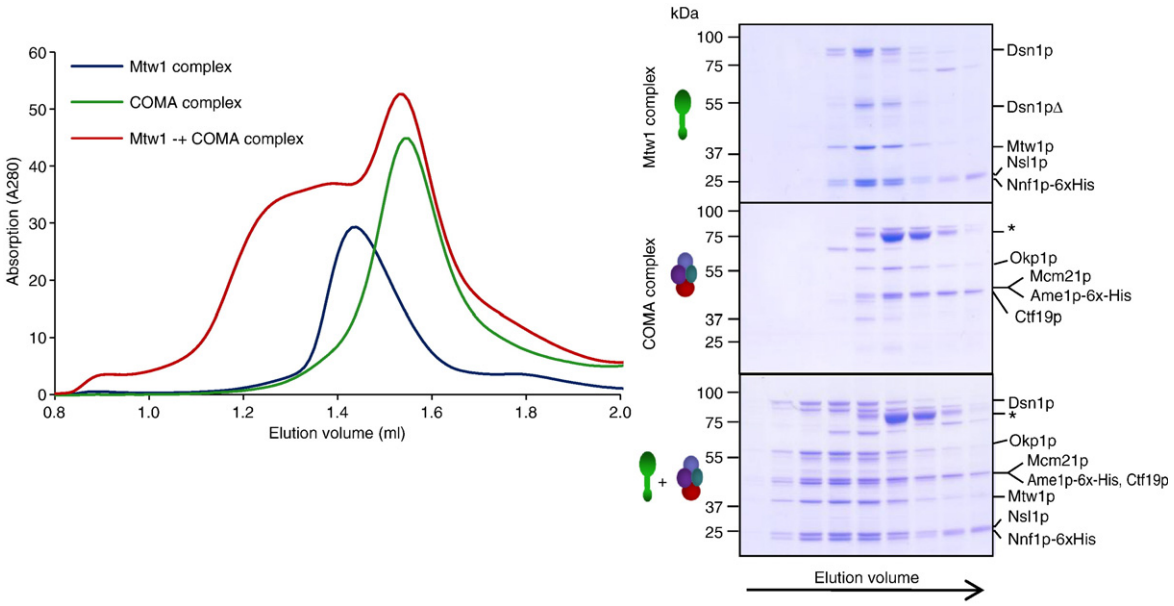

Fig. 5. SEC of Mtw1 and COMA complexes. Coomassie-stained gels and gel-filtration profiles of the Mtw1 complex and the Ndc80 complex individually or in combination (5 μM each). Asterisk indicates Hsp70 contamination in the COMA complex sample.

with Ndc80 did not prevent the interaction between COMA complexes and Mtw1 complexes, and both complexes coeluted from the beads (Fig. 6a). This result indicates that the Ndc80 and COMA complexes occupy different binding sites on the Mtw1 complex. When testing the Mtw1–Nnf1 (MN) and Dsn1–Nsl1 (DN) subcomplexes separately in pull-down experiments, we found that the MN subcomplex interacted more efficiently with COMA (Fig. 6b and c). Interestingly, among all Mtw1 subunits, high-resolution colocalization data place Nnf1p closest to the inner centromere in both humans and *S. cerevisiae*.[27] Since the size of the smaller lobe of the Mtw1 complex roughly fits the combined masses of Mtw1–Nnf1, we tentatively speculate that the larger lobe, predominantly consisting of Dsn1p and Nsl1p, interacts with Spc24/Spc25, while the smaller lobe makes contact to the inner centromere COMA complex. Further antibody decoration experiments and direct visualization by EM will have to test this hypothesis.

In summary, we have characterized the basic architecture of the budding yeast Mtw1 complex. Very recently, two manuscripts have described the reconstitution of the yeast complex[28] and the human Mis12 complex.[29] Our independent results on the overall shape of the yeast Mtw1 complex as judged by EM, its assembly from two stable heterodimers, and the high-affinity interaction with the Ndc80 complex are in close agreement with the experiments performed by Maskell *et al.* A comparison to the human Mis12 complex reveals interesting similarities and differences: the overall architecture of the complex, with its topology based on stable Mtw1–Nnf1 and Dsn1–Nsl1 heterodimers, is conserved between yeast and human. However, the molecular mechanism by which a high-affinity interaction with the Ndc80 complex is achieved differs considerably between the two organisms. In particular, a yeast Dsn1–Nsl1 heterodimer alone is not competent to bind the Ndc80 complex (our unpublished observations). Yeast Nsl1 lacks a

Fig. 4. Reconstitution of a Ctf19 core complex (COMA) and interaction with Mtw1. (a) Reconstitution of the COMA complex. Coomassie-stained gel at different stages of purification. Right: The four polypeptides of the complex are resolved on large SDS-PAGE gels. (b) Pull-down experiment with immobilized COMA complex. Different amounts of recombinant COMA complex (lane 1) were immobilized on Anti-FLAG M2 Affinity Gel and incubated with the Mtw1, Ndc80, or Dam1 complex (lane 2). Control pull-downs contained only M2 beads (lane 3). After the bound complexes had been washed, they were eluted with FLAG peptide (lanes 4–6). Note that the Mtw1 complex coelutes with COMA from the beads. (c) The COMA–FLAG complex (lane 1) was incubated with His-tagged Mtw1, Ndc80, or Dam1 complexes, which were immobilized on Ni-NTA beads (lane 2; lane 3 denotes Ni-NTA beads as negative control). After the bound complexes had been washed, they were eluted with imidazole (lanes 4–6). Note that the COMA complex is coeluted with the Mtw1 complex from Ni-NTA beads.

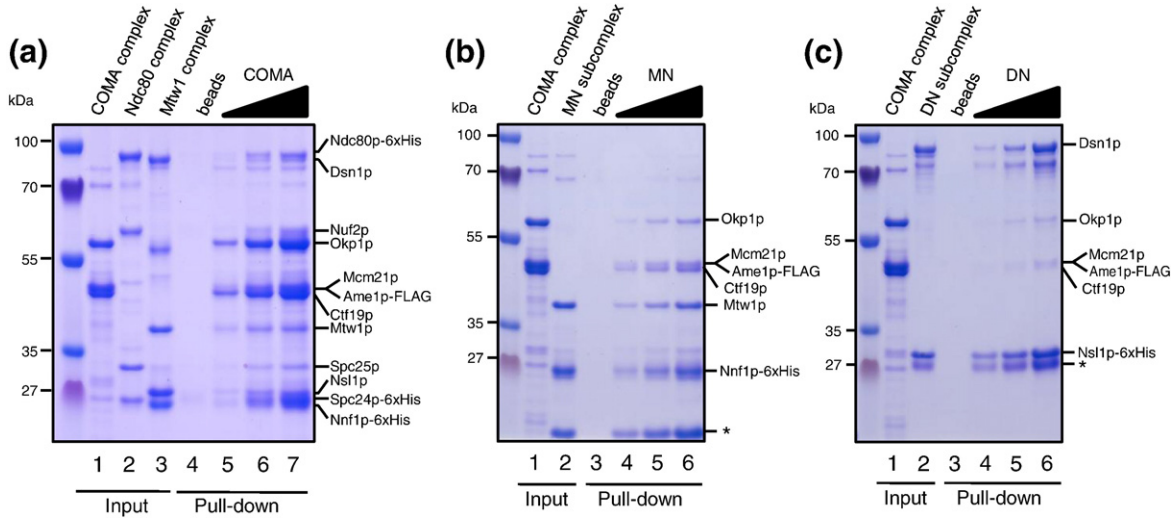

Fig. 6. Ndc80 and the COMA complex bind noncompetitively to the Mtw1 complex. (a) The COMA–FLAG complex (lane 1) was immobilized on M2 beads. Mtw1 complexes (lane 2) and Ndc80 complexes (lane 3) were premixed and incubated with control beads (lane 4) or COMA–FLAG beads. After the bound complexes had been washed, they were eluted with FLAG peptide (lanes 5–7). (b) Pull-down experiment using the 6×His-tagged MN subcomplex on Ni-NTA agarose and the FLAG-tagged COMA complex. Note the coelution of the complexes from the Ni-NTA beads. Asterisk indicates the Nnf1 truncation product. (c) Pull-down experiment using the 6×His-tagged DN subcomplex on Ni-NTA agarose and the FLAG-tagged COMA complex. The COMA complex fails to interact with the DN subcomplex. Asterisk denotes the Nsl1 truncation product.

critical binding motif (PVIHL) and a C-terminal tail, which is necessary for the interaction between human Nsl1 and the Ndc80 complex.[29] Instead, the binding interface between Mtw1 complexes and Ndc80 complexes seems to receive significant contributions from Mtw1 and/or Nnf1. These findings highlight the necessity to analyze kinetochores biochemically in evolutionarily distinct organisms in order to reveal common architectural principles and local binding interfaces.

Our results extend the studies of Maskell *et al.* and Petrovic *et al.* to provide a potential inner centromere receptor for the Mtw1 complex. The precise molecular basis for the interaction with the yeast Ctf19/COMA complex remains to be investigated. A puzzling aspect is that there is a considerably lower copy number of Ctf19 complex subunits (one to two) *versus* Mtw1 complexes (six to seven) for each budding yeast kinetochore, as judged by fluorescence microscopy.[5] Furthermore, only OKP1 and AME1 are essential genes in budding yeast.[30] It will be important to dissect in detail the molecular binding interface between Ctf19/COMA complexes and Mtw1 complexes and to evaluate the disruption of this binding interface *in vivo*. There may be considerable flexibility in the way the KMN network is anchored to the inner centromere. Some organisms such as *C. elegans* or *Drosophila melanogaster* seem to lack proteins entirely related to the CCAN.[2] In these kinetochores, the Mtw1 complex may rely on direct interactions with CENP-C for recruitment to the inner centromere.

Materials and Methods

Cloning of polycistronic expression vectors for Mtw1 and CTF19

Open reading frames corresponding to Mtw1 complex subunits were amplified from yeast genomic DNA, cloned, and expressed using the polycistronic expression system pET3aTr/pST39, which had been described previously.[31] Genes were subcloned from the monocistronic pET3aTr vector into the polycistronic cassettes (1–4) of pST39 in the following order for the Mtw1 complex: (1) MTW1, (2) NSL1, (3) NNF1-6×His, and (4) DSN1. The truncated version $DSN^{172–576}$ was cloned into pET28a(+) and expressed in combination with pST39 (MTW1-NSL1-NNF1-6×His).

The Ctf19/COMA subcomplex was cloned in the following order into the pST39 plasmid: (1) CTF19, (2) MCM21, (3) OKP1, and (4) AME1-6×His/FLAG. Because of the presence of an intron, MCM21 was amplified from yeast cDNA.

Protein expression and purification

The Mtw1 complex was expressed in BL21(DE3) (Novagen) for 4 h at 37 °C after induction at an OD_{600} of 0.6 with 0.4 mM isopropyl-β-D-thiogalactopyranoside (IPTG). Coexpression with $DSN^{172–576}$ was performed overnight in the presence of 0.2 mM IPTG. The Mtw1 subcomplexes MN and DN were cloned into cassettes 1 and 2 of the pST39 vector, and the expression conditions were 37 °C for 4 h (MN) and 18 °C overnight (DN). The COMA subcomplex was expressed at 18 °C overnight after induction with 0.2 mM IPTG.

Bacteria were lysed by sonication in the presence of protease inhibitors (Roche), and the fusion proteins were isolated using Ni-NTA agarose beads (Qiagen). Binding and subsequent washing were performed in 20 mM Hepes (pH 7.0), 300 mM NaCl, and 30 mM imidazole. The Mtw1 complex or its two subcomplexes were eluted from Ni-NTA beads with 20 mM Tris (pH 8.5), 80 mM NaCl, and 250 mM imidazole; subsequently, they were subjected to anion-exchange chromatography using a MonoQ 5/50 GL column (GE Healthcare) The column was developed with 10 bed volumes of a linear gradient from 80 mM to 1 M NaCl in 20 mM Tris (pH 8.5) containing 5% glycerol. The DN subcomplex was further purified using SEC on a Superose 6 10/30 column.

The COMA–6×His subcomplex was purified with Ni-NTA agarose beads or Anti-FLAG M2 Affinity Gel (Sigma Aldrich). COMA–6×His was eluted with 20 mM Hepes (pH 7), 150 mM NaCl, 5% glycerol, and 250 mM imidazole, and loaded onto a SEC Superdex 200 HiLoad 16/60 column equilibrated in 20 mM Hepes (pH 7), 150 mM NaCl, and 5% glycerol. COMA–FLAG was eluted from M2 Affinity Gel with 3× FLAG peptide in Tris-buffered saline (TBS), and the complex was concentrated using ultrafiltration (10,000 molecular weight cutoff; Vivaspins), followed by buffer exchange into 20 mM Hepes (pH 7.0), 150 mM NaCl, and 5% glycerol using PD-10 columns (GE Healthcare). Protein concentration was determined with DC Protein Assay kit (Bio-Rad Laboratories).

The Ndc80 and Dam1 kinetochore complexes were expressed and purified as described previously.[9,11,24]

Interaction studies

The kinetochore protein complex (0.1–1 μM) in 500 μl of binding buffer was immobilized on 20 μl of Anti-FLAG M2 Affinity Gel or 20 μl of Ni-NTA agarose beads. The interaction partner to be tested was used at 1 μM in binding buffer (TBS or phosphate-buffered saline containing 30 mM imidazole). After incubation for 1 h at 4 °C, the beads were washed three times in either TBS with 0.1% (vol/vol) NP-40 or phosphate-buffered saline with 30 mM imidazole, and the complexes were specifically eluted with 3× FLAG peptide or 250 mM imidazole.

Electron microscopy

The Mtw1 complex was thawed and prepared for EM analysis by the GraFix method.[32] One hundred fifty micrograms of the complex was layered onto a 5–40% glycerol gradient in 20 mM Hepes (pH 7.6), 100 mM NaCl, 1 mM ethylenediaminetetraacetic acid, and 1 mM DTT (which also contained a 0.02–0.15% glutaraldehyde gradient), and ultracentrifuged at 55,000 rpm for 13 h in a TLS55 rotor at 4 °C. Fractions were analyzed by SDS-PAGE, and the fraction containing the monomeric cross-linked complex was applied to a glow-discharged C-flat grid (Protochips) augmented with a layer of thin carbon and stained with 2% uranyl formate.

Images were collected on a Gatan 4000 × 4000 charge-coupled device camera using a Tecnai F20 electron microscope operating at 120 kV and at a magnification of 30,000×. Despite purification by glycerol gradient, the images contained a mixture of aggregates and fragments, as well as the monodispersed full complex. Approximately 5000 particles that appeared to correspond to the full monomeric complex were picked manually with the BOXER program[33] and subjected to reference-free classification, as described previously.[34]

Coiled-coil predictions were performed with the MARCOIL program.[35] The regions indicated with gray boxes in Fig. 2c correspond to areas of greater than 50% coiled-coil probability, all of which contain regions of greater than 80% coiled-coil probability.

Acknowledgements

The authors wish to thank all members of the Westermann laboratory for discussions and Fabienne Lampert for the gift of the purified Dam1 complex.

Research leading to these results received funding from the European Research Council under the European Community's Seventh Framework Program (S.W.; FP7/2007-2013)/European Research Council grant (agreement no. 203499), the Austrian Science Fund FWF (S.W.; SFB F34-B03), the National Institutes of Health (E.N.; PO1GM51487), and the Damon Ranyon Foundation (G.C.L.).

Supplementary Data

Supplementary data associated with this article can be found, in the online version, at doi:10.1016/j.jmb.2010.11.012

References

1. Cheeseman, I. M. & Desai, A. (2008). Molecular architecture of the kinetochore–microtubule interface. *Nat. Rev. Mol. Cell Biol.* **9**, 33–46.
2. Santaguida, S. & Musacchio, A. (2009). The life and miracles of kinetochores. *EMBO J.* **28**, 2511–2531.
3. Tanaka, T. U., Rachidi, N., Janke, C., Pereira, G., Galova, M., Schiebel, E. *et al.* (2002). Evidence that the Ipl1–Sli15 (Aurora kinase–INCENP) complex promotes chromosome bi-orientation by altering kinetochore–spindle pole connections. *Cell*, **108**, 317–329.
4. Musacchio, A. & Salmon, E. D. (2007). The spindle-assembly checkpoint in space and time. *Nat. Rev. Mol. Cell Biol.* **8**, 379–393.
5. Joglekar, A. P., Bouck, D. C., Molk, J. N., Bloom, K. S. & Salmon, E. D. (2006). Molecular architecture of a kinetochore–microtubule attachment site. *Nat. Cell Biol.* **8**, 581–585.
6. Westermann, S., Drubin, D. G. & Barnes, G. (2007). Structures and functions of yeast kinetochore complexes. *Annu. Rev. Biochem.* **76**, 563–591.
7. Westermann, S., Wang, H. W., Avila-Sakar, A., Drubin, D. G., Nogales, E. & Barnes, G. (2006). The Dam1 kinetochore ring complex moves processively

on depolymerizing microtubule ends. *Nature*, **440**, 565–569.
8. Ciferri, C., Pasqualato, S., Screpanti, E., Varetti, G., Santaguida, S., Dos Reis, G. *et al.* (2008). Implications for kinetochore–microtubule attachment from the structure of an engineered Ndc80 complex. *Cell*, **133**, 427–439.
9. Westermann, S., Avila-Sakar, A., Wang, H. W., Niederstrasser, H., Wong, J., Drubin, D. G. *et al.* (2005). Formation of a dynamic kinetochore–microtubule interface through assembly of the Dam1 ring complex. *Mol. Cell*, **17**, 277–290.
10. Miranda, J. J., De Wulf, P., Sorger, P. K. & Harrison, S. C. (2005). The yeast DASH complex forms closed rings on microtubules. *Nat. Struct. Mol. Biol.* **12**, 138–143.
11. Lampert, F., Hornung, P. & Westermann, S. (2010). The Dam1 complex confers microtubule plus end-tracking activity to the Ndc80 kinetochore complex. *J. Cell Biol.* **189**, 641–649.
12. Tien, J. F., Umbreit, N. T., Gestaut, D. R., Franck, A. D., Cooper, J., Wordeman, L. *et al.* (2010). Cooperation of the Dam1 and Ndc80 kinetochore complexes enhances microtubule coupling and is regulated by aurora B. *J. Cell Biol.* **189**, 713–723.
13. Cheeseman, I. M., Chappie, J. S., Wilson-Kubalek, E. M. & Desai, A. (2006). The conserved KMN network constitutes the core microtubule-binding site of the kinetochore. *Cell*, **127**, 983–997.
14. Goshima, G., Kiyomitsu, T., Yoda, K. & Yanagida, M. (2003). Human centromere chromatin protein hMis12, essential for equal segregation, is independent of CENP-A loading pathway. *J. Cell Biol.* **160**, 25–39.
15. Cheeseman, I. M., Niessen, S., Anderson, S., Hyndman, F., Yates, J. R., III, Oegema, K. & Desai, A. (2004). A conserved protein network controls assembly of the outer kinetochore and its ability to sustain tension. *Genes Dev.* **18**, 2255–2268.
16. Kline, S. L., Cheeseman, I. M., Hori, T., Fukagawa, T. & Desai, A. (2006). The human Mis12 complex is required for kinetochore assembly and proper chromosome segregation. *J. Cell Biol.* **173**, 9–17.
17. De Wulf, P., McAinsh, A. D. & Sorger, P. K. (2003). Hierarchical assembly of the budding yeast kinetochore from multiple subcomplexes. *Genes Dev.* **17**, 2902–2921.
18. Kiyomitsu, T., Obuse, C. & Yanagida, M. (2007). Human Blinkin/AF15q14 is required for chromosome alignment and the mitotic checkpoint through direct interaction with Bub1 and BubR1. *Dev. Cell*, **13**, 663–676.
19. Wang, H. W., Long, S., Ciferri, C., Westermann, S., Drubin, D., Barnes, G. & Nogales, E. (2008). Architecture and flexibility of the yeast Ndc80 kinetochore complex. *J. Mol. Biol.* **383**, 894–903.
20. Joglekar, A. P., Bloom, K. & Salmon, E. D. (2009). *In vivo* protein architecture of the eukaryotic kinetochore with nanometer scale accuracy. *Curr. Biol.* **19**, 694–699.
21. Wei, R. R., Al-Bassam, J. & Harrison, S. C. (2007). The Ndc80/HEC1 complex is a contact point for kinetochore–microtubule attachment. *Nat. Struct. Mol. Biol.* **14**, 54–59.
22. Obuse, C., Iwasaki, O., Kiyomitsu, T., Goshima, G., Toyoda, Y. & Yanagida, M. (2004). A conserved Mis12 centromere complex is linked to heterochromatic HP1 and outer kinetochore protein Zwint-1. *Nat. Cell Biol.* **6**, 1135–1141.
23. Kiyomitsu, T., Iwasaki, O., Obuse, C. & Yanagida, M. (2010). Inner centromere formation requires hMis14, a trident kinetochore protein that specifically recruits HP1 to human chromosomes. *J. Cell Biol.* **188**, 791–807.
24. Westermann, S., Cheeseman, I. M., Anderson, S., Yates, J. R., III, Drubin, D. G. & Barnes, G. (2003). Architecture of the budding yeast kinetochore reveals a conserved molecular core. *J. Cell Biol.* **163**, 215–222.
25. Foltz, D. R., Jansen, L. E., Black, B. E., Bailey, A. O., Yates, J. R., III & Cleveland, D. W. (2006). The human CENP-A centromeric nucleosome-associated complex. *Nat. Cell Biol.* **8**, 458–469.
26. Okada, M., Cheeseman, I. M., Hori, T., Okawa, K., McLeod, I. X., Yates, J. R., III *et al.* (2006). The CENP-H-I complex is required for the efficient incorporation of newly synthesized CENP-A into centromeres. *Nat. Cell Biol.* **8**, 446–457.
27. Wan, X., O'Quinn, R. P., Pierce, H. L., Joglekar, A. P., Gall, W. E., DeLuca, J. G. *et al.* (2009). Protein architecture of the human kinetochore microtubule attachment site. *Cell*, **137**, 672–684.
28. Maskell, D. P., Hu, X. W. & Singleton, M. R. (2010). Molecular architecture and assembly of the yeast kinetochore MIND complex. *J. Cell Biol.* **190**, 823–834.
29. Petrovic, A., Pasqualato, S., Dube, P., Krenn, V., Santaguida, S., Cittaro, D. *et al.* (2010). The MIS12 complex is a protein interaction hub for outer kinetochore assembly. *J. Cell Biol.* **190**, 835–852.
30. Ortiz, J., Stemmann, O., Rank, S. & Lechner, J. (1999). A putative protein complex consisting of Ctf19, Mcm21, and Okp1 represents a missing link in the budding yeast kinetochore. *Genes Dev.* **13**, 1140–1155.
31. Tan, S. (2001). A modular polycistronic expression system for overexpressing protein complexes in *Escherichia coli*. *Protein Expression Purif.* **21**, 224–234.
32. Kastner, B., Fischer, N., Golas, M. M., Sander, B., Dube, P., Boehringer, D. *et al.* (2008). GraFix: sample preparation for single-particle electron cryomicroscopy. *Nat. Methods*, **5**, 53–55.
33. Ludtke, S. J., Baldwin, P. R. & Chiu, W. (1999). EMAN: semiautomated software for high-resolution single-particle reconstructions. *J. Struct. Biol.* **128**, 82–97.
34. Ramey, V. H., Wang, H. W. & Nogales, E. (2009). Ab initio reconstruction of helical samples with heterogeneity, disorder and coexisting symmetries. *J. Struct. Biol.* **167**, 97–105.
35. Delorenzi, M. & Speed, T. (2002). An HMM model for coiled-coil domains and a comparison with PSSM-based predictions. *Bioinformatics*, **18**, 617–625.

The Dam1 complex confers microtubule plus end–tracking activity to the Ndc80 kinetochore complex

Fabienne Lampert, Peter Hornung, and Stefan Westermann

Research Institute of Molecular Pathology, 1030 Vienna, Austria

Kinetochores must remain associated with microtubule ends, as they undergo rapid transitions between growth and shrinkage. The molecular basis for this essential activity that ensures correct chromosome segregation is unclear. In this study, we have used reconstitution of dynamic microtubules and total internal reflection fluorescence microscopy to define the functional relationship between two important budding yeast kinetochore complexes. We find that the Dam1 complex is an autonomous plus end–tracking complex. The Ndc80 complex, despite being structurally related to the general tip tracker EB1, fails to recognize growing ends efficiently. Dam1 oligomers are necessary and sufficient to recruit Ndc80 to dynamic microtubule ends, where both complexes remain continuously associated. The interaction occurs specifically in the presence of microtubules and is subject to regulation by Ipl1 phosphorylation. These findings can explain how the force harvested by Dam1 is transmitted to the rest of the kinetochore via the Ndc80 complex.

Introduction

The ability of spindle microtubules to connect to centromeric DNA is fundamental to ensure faithful transmission of the eukaryotic genome. Kinetochores, large protein complexes, physically tether chromosomes to microtubule plus ends and relay their dynamic instability into directed chromosome movement. To date, the molecular basis of how transitions between microtubule growth and shrinkage are coupled to chromosome movement remains unclear (Westermann et al., 2007; Cheeseman and Desai, 2008; Santaguida and Musacchio, 2009).

Two principal types of kinetochore complexes have been proposed to connect dynamic microtubules to chromosome motion: ring couplers and fibrillary couplers. The yeast Dam1 complex oligomerizes in vitro into a ring that encircles the microtubule plus end like a sleeve, allowing the exchange of tubulin subunits at the end while maintaining a firm grip on the polymer (Cheeseman et al., 2001b; Miranda et al., 2005; Westermann et al., 2005). Processive attachment to depolymerizing ends (Westermann et al., 2006; Gestaut et al., 2008) and force generation in the piconewton range have spotlighted the Dam1 complex as a primary coupler in budding yeast (Asbury et al., 2006; Grishchuk et al., 2008a). These features do not strictly depend on ring formation, leaving open the question of the physiologically active form of the complex in vivo. Interestingly, artificial recruitment of the Dam1 complex to DNA bypasses the requirement for inner kinetochore complexes and is sufficient to drive segregation of yeast mini- or native chromosomes (Kiermaier et al., 2009; Lacefield et al., 2009), providing strong evidence that the complex is a critical attachment factor in vivo.

A paradigm for a fibrillary coupler is the four-protein complex Ndc80, which is part of the ternary KMN network, a central component of the kinetochore–microtubule interface in all eukaryotes (Cheeseman et al., 2006). The Ndc80 complex interacts with microtubules via calponin homology domains located in the Ndc80-Nuf2 head (Wei et al., 2007; Ciferri et al., 2008), and individual Ndc80 molecules have been shown to undergo biased diffusion on depolymerizing microtubule ends, which may in principle allow them to convert microtubule depolymerization into chromosome movement (Powers et al., 2009). The respective contribution of Ndc80 and Dam1 complexes to the plus end–tracking activity of the kinetochore is unknown.

In this study, we present a minimal kinetochore plus end–tracking system. We analyzed the behavior of Dam1 and Ndc80 complexes on dynamic microtubules first individually and then in combination. We find that the Dam1 complex but not the Ndc80 complex has an intrinsic plus end–tracking ability. However, Dam1 mediates continuous Ndc80 tip association with dynamic

Correspondence to Stefan Westermann: westermann@imp.ac.at

Abbreviations used in this paper: CCD, charge-coupled device; TIRF, total internal reflection fluorescence.

The Rockefeller University Press $30.00
J. Cell Biol. Vol. 189 No. 4 641–649
www.jcb.org/cgi/doi/10.1083/jcb.200912021

microtubules, suggesting that in yeast, Dam1 complexes are the prime source of kinetochore plus end–tracking activity, whereas Ndc80 complexes structurally bridge microtubule ends with chromosomes.

Results and discussion

The Dam1 complex tracks microtubule plus ends independently of the general +TIP EB1 in vivo

To characterize the interaction of the Dam1 complex with individual microtubule plus ends in vivo, we imaged metaphase-arrested cells expressing Dam1p fused to triple GFP (Dam1-3xGFP) and Tub1p fused to mCherry (Fig. 1 A; Tanaka et al., 2005). We found that the majority of the Dam1 complex is localized at kinetochores, whereas individual signals of the complex accumulate at the tips of growing and shrinking nuclear microtubules. Furthermore, the microtubule lattice is frequently decorated by additional, well-defined Dam1 spots that are collected during microtubule shrinkage consistent with previous data (Tanaka et al., 2007). Interestingly, we observed that the complex continuously tracks microtubule ends during multiple rounds of tubulin polymerization and depolymerization (Fig. 1 B and Videos 1 and 2). Dam1 tip tracking on nuclear microtubules was reminiscent of Bim1p, the budding yeast homologue of the +TIP EB1 (Akhmanova and Steinmetz, 2008; Honnappa et al., 2009). Because interactions between the Dam1 complex and Bim1p have been reported in two-hybrid studies, we considered the possibility that Dam1 tip localization may depend on Bim1p (Cheeseman et al., 2001b; Shang et al., 2003). After 5 h in glucose, Bim1p, placed under the control of the *GAL1/10* promoter, was no longer detectable by Western blotting (Fig. 1 C), and nuclear microtubules were extremely short, which is in agreement with previous observations in *bim1Δ* or *bik1Δ* strains (Tanaka et al., 2005). However, Dam1 tip localization was retained on short nuclear microtubules, demonstrating that Dam1 plus end–tracking activity is independent of the general +TIP EB1 in vivo (Fig. 1 D and Video 3).

The Dam1 complex autonomously tracks microtubule plus ends in a minimal in vitro reconstitution system

To further establish the minimal requirements for Dam1 plus end tracking, we reconstituted interaction of the complex with dynamic microtubules in vitro using two-color total internal reflection fluorescence (TIRF) microscopy (Fig. 2 A). Previously, the behavior of the Dam1 complex had only been imaged on static or slowly depolymerizing microtubules (Westermann et al., 2006; Gestaut et al., 2008). Visualizing fully dynamic microtubules, we observed the following characteristic features of the complex: the GMPCPP-stabilized seeds were strongly decorated with Dam1 complexes, which is in agreement with previous observations (Westermann et al., 2005; Grishchuk et al., 2008b). In addition, the complex appeared in discrete foci at the plus ends of microtubule extensions, where it persisted during phases of microtubule growth and shrinkage (Fig. 2 B and Video 4). Thus, the Dam1 complex autonomously tracks growing microtubule plus ends in vitro (Fig. 2 C and Videos 5 and 6).

As the complex can exist in a variety of concentration-dependent oligomeric states, such as individual complexes, small oligomers, and full rings, we aimed to determine the nature of the tracking species in our assays. We mimicked flow cell conditions in the test tube and examined the decoration of dynamic microtubules (at 14 µM) with different concentrations of Dam1 by EM. We found that at a concentration of 100 nM Dam1, only few rings decorating the microtubules were observed by EM (Fig. S1 A). Quantitative analysis of fluorescent Dam1 signals using TIRF microscopy at the same concentration showed a distribution of various intensities on the microtubule lattice. Most Dam1 spots displayed twice the intensity of the weakest signals, whereas very few spots showed intensities that could correspond to full rings (Fig. S1 B). Thus, under our imaging conditions (100 nM Dam1), the complex predominantly exists in the form of small oligomers.

Dam1 moves continuously with growing microtubule plus ends

The Dam1 complex is only the third molecule for which autonomous tip tracking is reported in vitro. The microtubule polymerase XMAP215 is thought to be processive, persisting at the tip during multiple rounds of tubulin dimer addition (Brouhard et al., 2008), whereas EB1 rapidly turns over on a transiently existing structure at the plus end (Bieling et al., 2007). To distinguish between these possibilities and investigate the mechanism of Dam1 plus end tracking in more detail, we increased the temporal resolution of our videos by recording streaming videos. We observed that those Dam1 foci located most distal to the stable seed continuously moved outward during microtubule growth with a mean speed of $4.02 \pm 0.225\ \mu m \times min^{-1}$. This value is in agreement with the mean growth speed of microtubules in the presence of 100 nM unlabeled Dam1 and 20 µM free tubulin (Fig. 2 D). Moreover, we performed "spike" experiments by reducing the fraction of labeled Dam1 complex at least 10-fold while sustaining the total protein concentration with unlabeled complex. Under these conditions, we were able to visualize individual Dam1 signals that moved away from the stable seed (Fig. 2 E), supporting the notion that the Dam1 complex is an autonomous and continuous plus end tracker.

The Ndc80 complex interacts weakly with dynamic microtubules and is not an autonomous end-binding protein

Although a moderate affinity of oligomeric Ndc80 assemblies for depolymerizing microtubule ends has been described in vitro (Powers et al., 2009), it is at present unknown whether the complex can autonomously recognize plus ends and remain attached to them or whether this activity requires additional factors. Using reconstituted *Saccharomyces cerevisiae* Ndc80 complex with its Nuf2 subunit fused to EGFP (Ndc80–EGFP; Fig. 3 A), we performed microtubule cosedimentation assays and found that the interaction is extremely salt sensitive. Increasing the salt concentration from 25 to 100 mM NaCl lowered the binding affinity by more than one order of magnitude, leading to an apparent dissociation constant of K_D (100 mM) = 1.27 ± 0.27 µM compared with K_D (25 mM) = 0.107 ± 0.023 µM (Fig. 3 B). This implies that under physiologically relevant salt concentrations, the intrinsic microtubule-binding activity of the Ndc80 complex is significantly impaired.

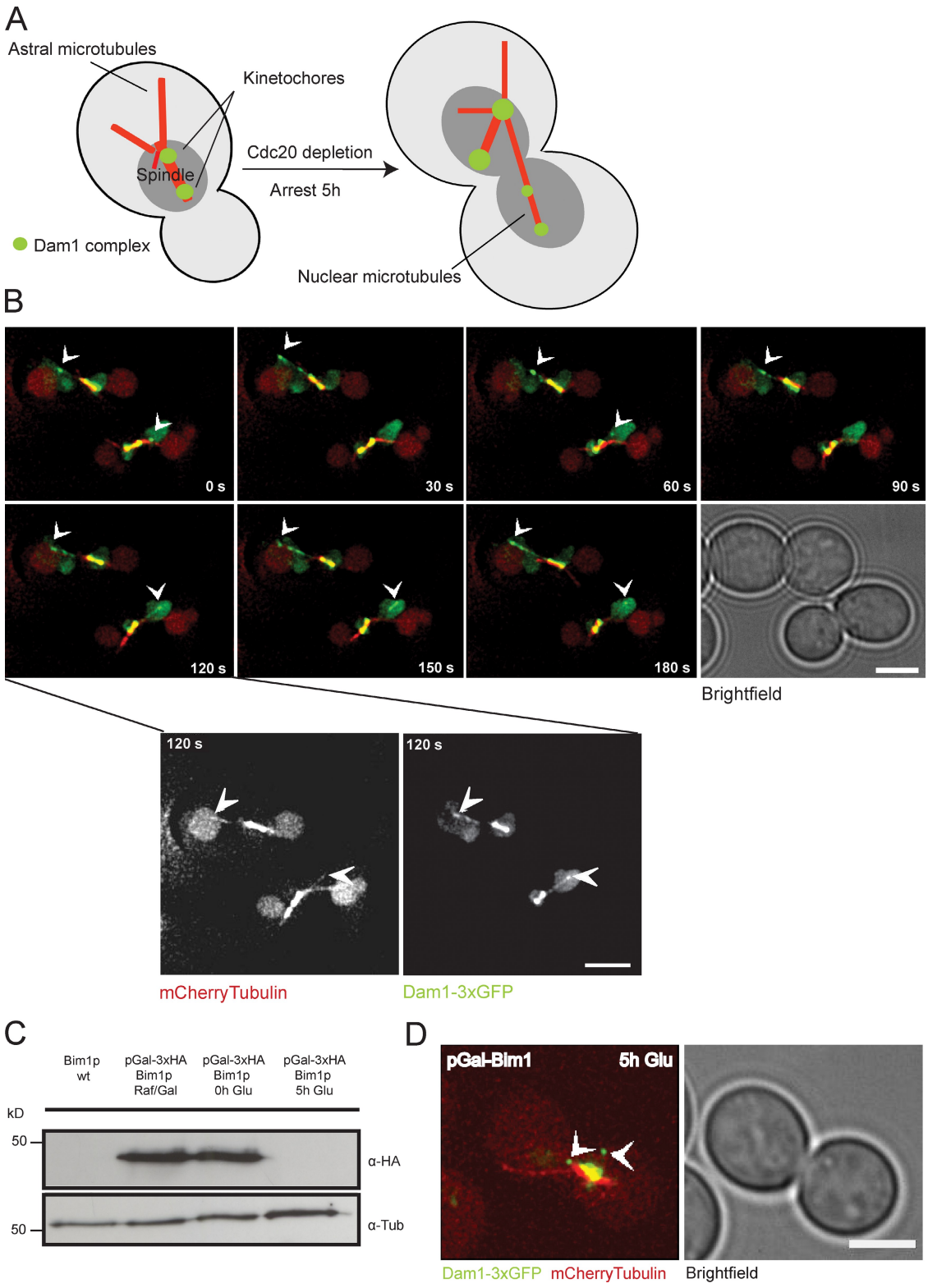

Figure 1. **The Dam1 complex tracks plus ends independently of Bim1p in vivo.** (A) Schematic illustration of the live cell imaging strategy (Tanaka et al., 2005). (B) Time-lapse live cell microscopy showing plus end tracking of the Dam1 complex (arrowheads) during phases of microtubule growth and shrinkage (Videos 1 and 2). Insets show higher magnification views of the indicated panel (120 s). (C) Western blot analysis showing depletion of Bim1p-3xHA in a Dam1-3xGFP, mCherry-tubulin background probed with an anti-HA antibody. (D) Still image from a video depicting microtubule plus end localization of the Dam1 complex (arrowheads) in the absence of the +TIP Bim1p (Video 3). Bars, 2 μm.

We next studied the interaction of the Ndc80 complex with dynamic microtubules in the TIRF assay. To establish imaging conditions that allow observation of plus end tracking, we first visualized the association of the yeast EB1 protein Bim1p with dynamic microtubules. As expected, Bim1p accumulated at the ends of growing but not shrinking microtubules

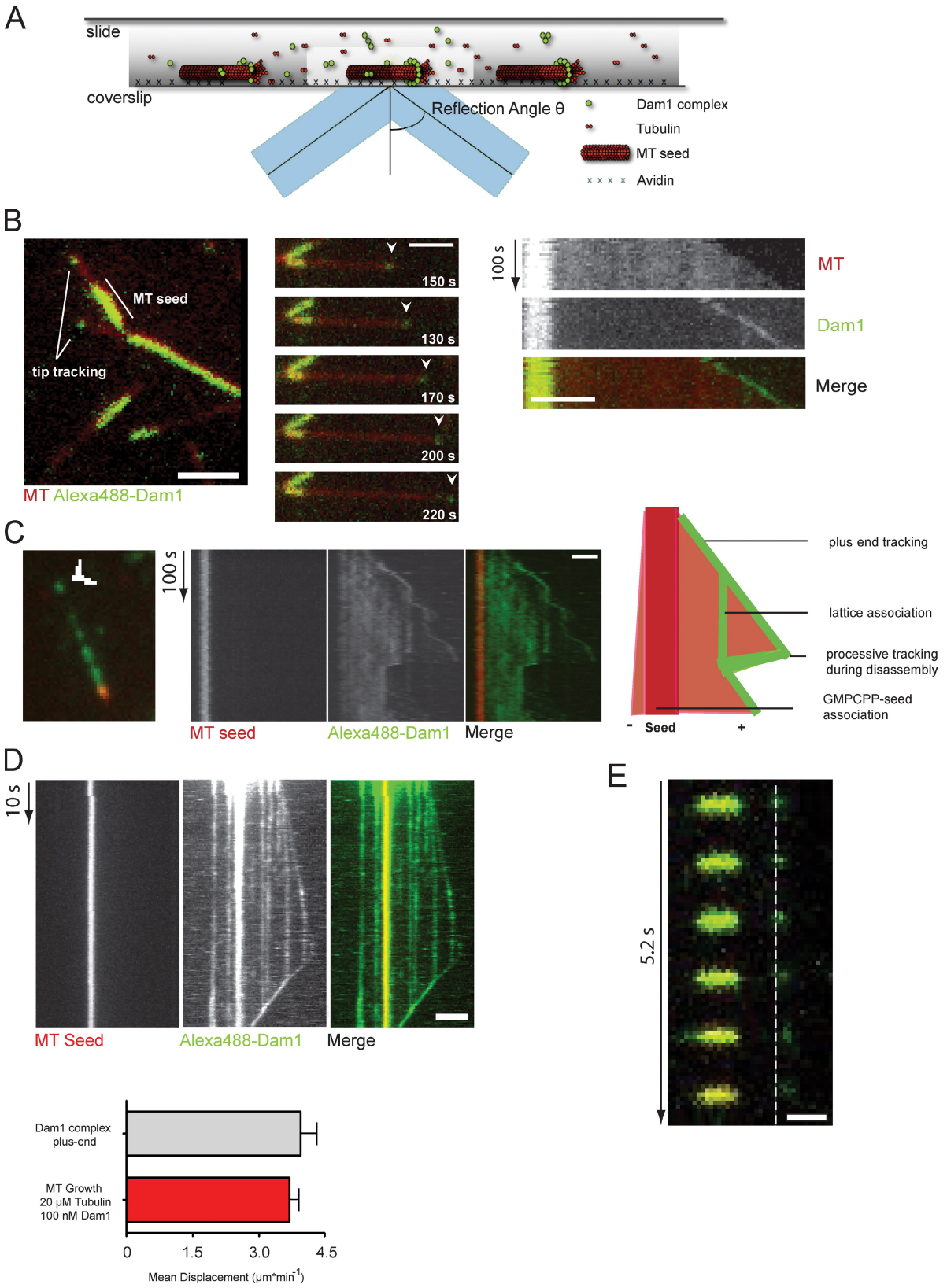

Figure 2. **Reconstitution of Dam1 plus end tracking in vitro using TIRF microscopy.** (A) Schematic illustration of the in vitro imaging setup. (B, left) Still image of the Alexa Fluor 488–labeled Dam1 complex (100 nM) on dynamic rhodamine-labeled microtubules (MT). The complex shows preferred association with the plus end and the GMPCPP seed. (middle) A time sequence of Dam1 plus end tracking. (right) Kymographs (time/space plot) of Dam1 plus end tracking are shown (Video 4). (C) Still image and kymograph of a time-lapse video showing Dam1 decoration on unlabeled tubulin extensions. Overlay and individual channels are shown. The Dam1 complex tracks plus ends during phases of growth and shrinkage. The microtubule lattice is decorated by additional Dam1 complexes, which are collected during microtubule disassembly (Videos 5 and 6). (B and C) Arrowheads indicate Dam1 localization at the tip of the

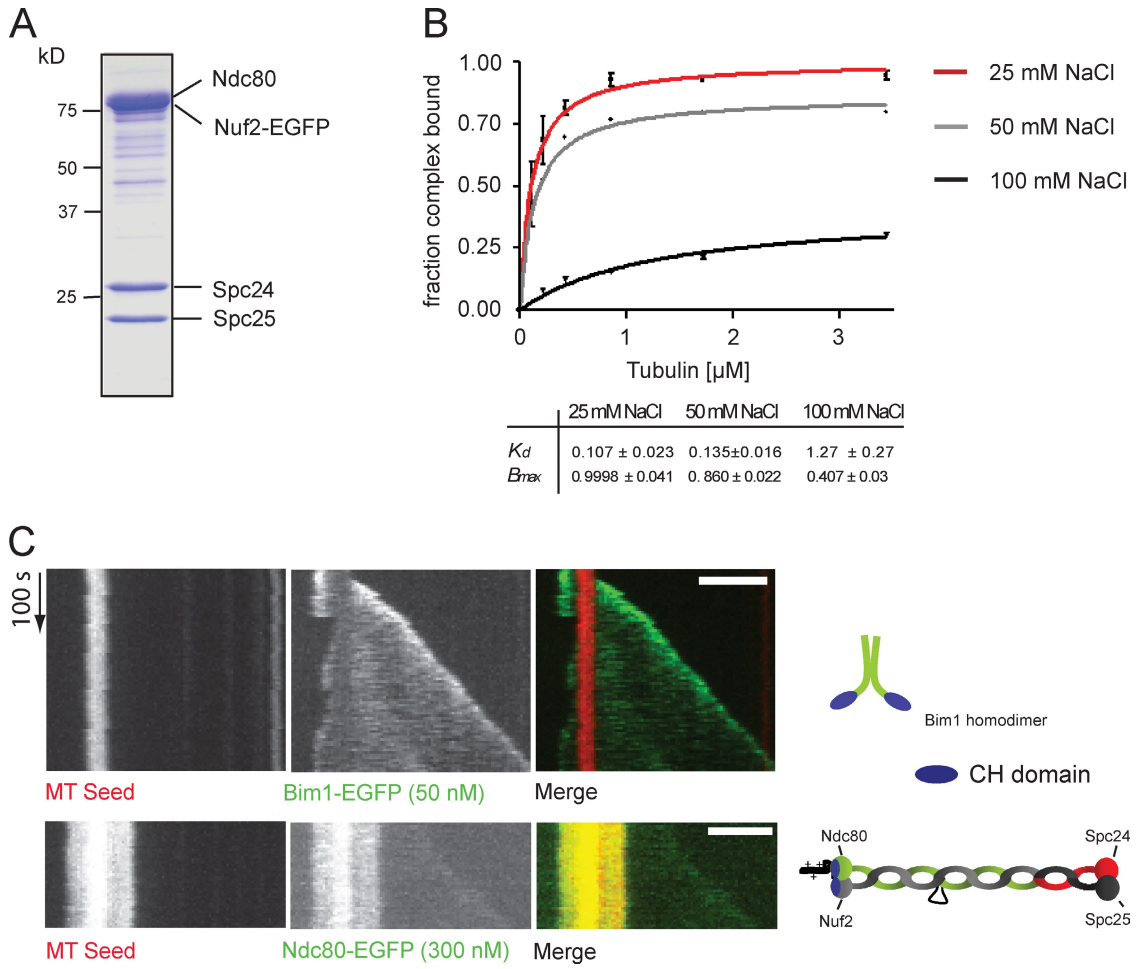

Figure 3. **Ndc80 is not an autonomous end-binding complex.** (A) Coomassie-stained SDS-PAGE showing the reconstituted *S. cerevisiae* Ndc80 complex. The Nuf2 subunit is fused to EGFP. (B) The Ndc80 complex was tested for its ability to cosediment with taxol-stabilized microtubules in the presence of increasing amounts of salt. The binding affinity curves plot averaged data from three independent experiments. Error bars represent standard error. (C) Kymographs demonstrating 50 nM Bim1-EGFP tip tracking during microtubule (MT) assembly (top) and faint association of 300 nM Ndc80–EGFP with the microtubule lattice (bottom). CH, calponin homology. Bars, 2 μm.

(Fig. 3 C; Bieling et al., 2007). However, when imaged under the same conditions, the Ndc80 complex was barely visible on the dynamic microtubule extensions, and we did not observe a substantial accumulation on growing or shrinking microtubule ends (Fig. 3 C). Thus, under experimental conditions in which yeast EB1 displays robust plus end tracking in vitro, the Ndc80 complex only weakly interacts with dynamic microtubules and does not accumulate at growing or shrinking ends.

The Dam1 complex is necessary and sufficient to recruit the Ndc80 complex to dynamic microtubule ends

We wondered whether the dynamic properties of the Ndc80 complex would be altered in the presence of the Dam1 complex, which is a tempting idea in the light of autonomous Dam1 plus end–tracking activity and reported two-hybrid interactions between the two complexes (Shang et al., 2003; Wong et al., 2007). We first asked whether inclusion of the Dam1 complex would alter the binding behavior of Ndc80 in cosedimentation assays. At salt concentrations of 100 mM NaCl that strongly impair Ndc80 binding, addition of equimolar amounts of Dam1 drastically increased the affinity of the Ndc80 complex for taxol-stabilized microtubules (Fig. 4 A). Analysis of Coomassie-stained gels revealed that a substantial portion of Ndc80 was now found along with Dam1 in the pellet fraction (Fig. 4 A). The isolated Ndc80-Nuf2 head was sufficient for recruitment (unpublished data). Furthermore, the N-terminal 116 amino acids of Ndc80, critical for the intrinsic microtubule-binding activity of Ndc80, are dispensable for Dam1-dependent recruitment (Fig. S2).

We next visualized the binding of the Ndc80 complex to rhodamine-labeled, taxol-stabilized microtubules by fluorescence microscopy. In the presence of 100 mM KCl,

microtubule. (D) Kymograph from a streaming video recording continous Dam1 tip tracking. Error bars indicate averaged Dam1 outward displacement at the tip and lattice compared with the mean growth speed of microtubules ($n \geq 20$). (E) Still series of a spike experiment depicting an individual Dam1 dot moving away from the stable seed. The dashed line indicates the position of the Dam1 signal at time 0. Bars: (B–D) 2 μm; (E) 1 μm.

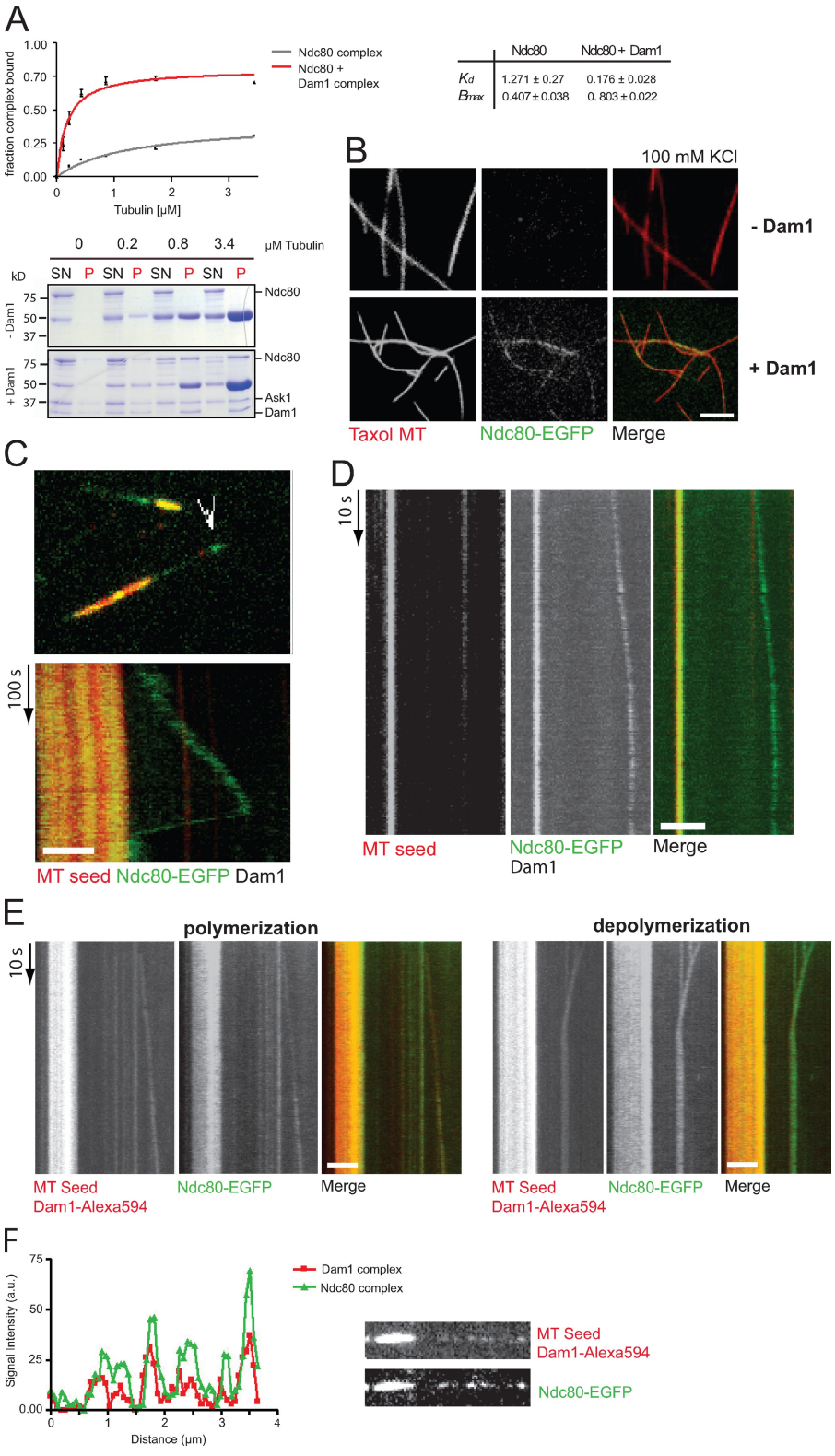

Figure 4. **The Dam1 complex recruits the Ndc80 complex to dynamic microtubule plus ends.** (A) Microtubule-binding activity of Ndc80 was tested in the absence and presence of equimolar amounts of Dam1 complex and 100 mM NaCl. (B, top) TIRF micrographs showing little microtubule (MT) decoration of the Ndc80 complex under physiological ionic strength. (bottom) The Dam1 complex efficiently recruits Ndc80 to taxol-stabilized microtubules. SN, supernatant; P, pellet. Bar, 4 μm. (C) Still image and kymograph of a time-lapse video demonstrate that in the presence of 100 nM unlabeled Dam1 complex, Ndc80–EGFP tracks microtubule plus ends (Video 7). Arrowhead indicates Ndc80–EGPF at the tip of the microtubule. (D) Streaming video showing continuous tip tracking of Ndc80–EGFP in the presence of unlabeled Dam1 (Video 8). (E) The Dam1–Alexa Fluor 594 complex and Ndc80–EGFP colocalize at microtubule plus ends during microtubule polymerization and depolymerization (Video 9). (F) Intensity scan demonstrating that Dam1 signals on the microtubule lattice correlate with the signal intensity profile of the Ndc80 complex. Bars, 2 μm.

Ndc80–EGFP was barely visible on the stable microtubules. However, upon addition of 100 nM unlabeled Dam1 complex, Ndc80–EGFP signals were readily observed on the microtubule lattice (Fig. 4 B). We conclude that the Dam1 complex enhances the affinity of the Ndc80 complex for stable microtubules in vitro.

To understand the collective behavior of the complexes on dynamic microtubules, we imaged Ndc80–EGFP in the presence of 100 nM unlabeled Dam1 complex using TIRF microscopy. Strikingly, the Ndc80 complex was now readily visible on the dynamic lattice and displayed features characteristic of Dam1 behavior: it persisted in discrete foci at the end of growing

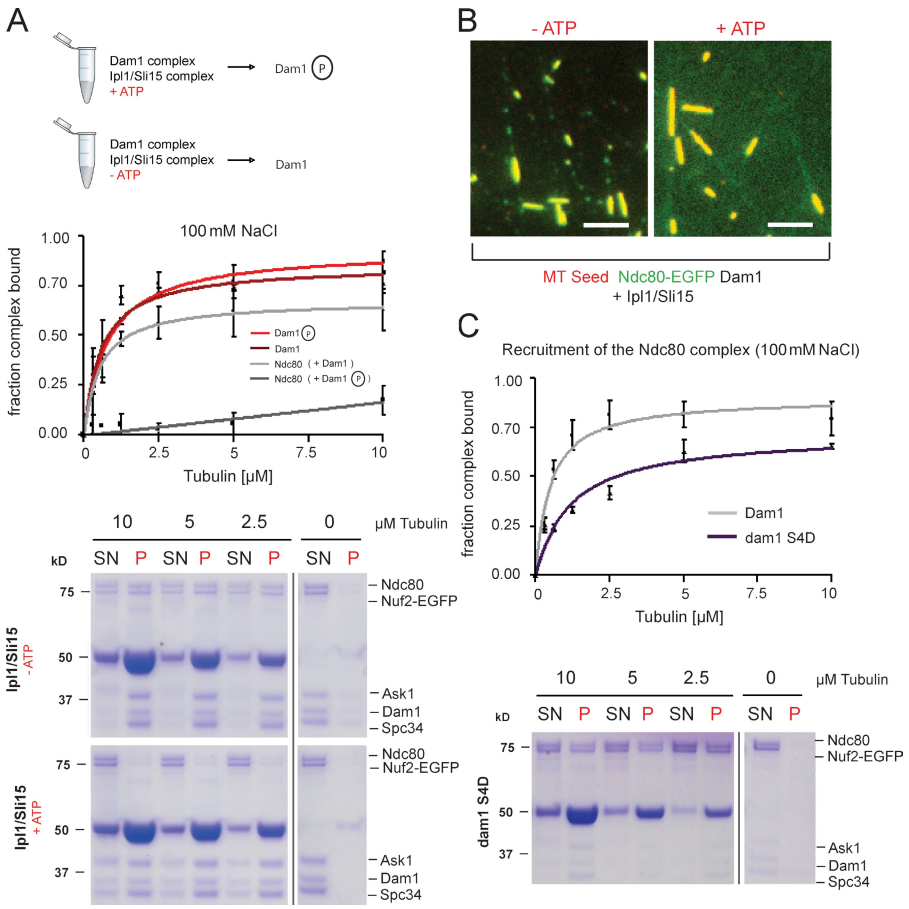

Figure 5. **Phosphorylation of Dam1 by Ipl1–Sli15 prevents Ndc80 recruitment to microtubules.** (A) The Ndc80 complex was tested for microtubule binding in the presence of phosphorylated and unphosphorylated Dam1 complex. (top) The phosphorylation experiments are outlined. The binding affinity curves plot averaged data from two independent experiments. Error bars represent SEM. (B) TIRF micrographs showing that the Dam1 complex phosphorylated by Ipl1–Sli15 fails to recruit the Ndc80 complex to dynamic microtubules (right). Bars, 2 μm. (C) The ability of the dam1 S4D (S20D, S257D, S265D, and S292) complex to recruit the Ndc80 complex to microtubules was tested in the presence of 100 mM NaCl. The dam1 S4D complex has a decreased ability to recruit Ndc80. The binding affinity curves plot averaged data from two independent experiments. SN, supernatant; P, pellet. Error bars represent SEM.

microtubules and tracked the depolymerizing ends of shrinking microtubules (Fig. 4 C and Video 7). To ask whether the association of Ndc80 with growing microtubule ends was continuous, we recorded streaming videos of Ndc80–EGFP in the presence of unlabeled Dam1 complex. We found that Ndc80 signals distal from the stable seed showed continuous outward displacement, and we did not find evidence for turnover at the temporal resolution achievable in our imaging system (Fig. 4 D and Video 8).

Dam1 and Ndc80 colocalize persistently at growing and shrinking microtubule plus ends

We considered two possibilities by which the Dam1 complex may increase the interaction of the Ndc80 complex with dynamic microtubule ends. First, the presence of Dam1 may alter properties of the microtubule lattice, thereby making it more favorable for Ndc80 association. Alternatively, the complexes may physically engage at dynamic microtubule ends. To distinguish between these possibilities, we simultaneously imaged Alexa Fluor 594–labeled Dam1 complex and Ndc80–EGFP complex on dynamic microtubules. We found that Alexa Fluor 594 and EGFP signals colocalized to lattice-associated spots that did not display movement during our observation and to distal spots that showed outward displacement (Fig. 4, E and F; and Video 9). Further experiments using FRAP will be necessary to clarify whether the complexes show turnover at the plus end.

On depolymerizing microtubule ends, Dam1 and Ndc80 spots colocalized, distal signals remained associated with depolymerizing ends, and lattice-associated signals were "picked up," increasing the fluorescence intensity of the end-tracking species. These observations support the notion that the Ndc80 and Dam1 complexes directly interact on dynamic microtubules. Interestingly, however, we were not able to detect an interaction between the complexes in solution, as they eluted independently in gel filtration experiments (Fig. S3). Thus, the presence of microtubules strongly enhances interaction between these complexes on the lattice (see Tien et al. in this issue).

Kinetochore–microtubule interactions are under the control of the aurora B kinase (Ipl1p in budding yeast), which ensures bipolar attachment of kinetochores to opposite spindle poles. We asked whether the Dam1–Ndc80 interaction is sensitive to Ipl1 phosphorylation by performing microtubule cosedimentation experiments under conditions in which Ndc80 binding to microtubules is dependent on Dam1 (100 mM NaCl). To this end, Dam1 complex and substoichiometric amounts of Ipl1–Sli15 were incubated in the presence or absence of ATP and tested for their ability to recruit Ndc80 to microtubules. Recruitment of the Ndc80 complex to microtubules was diminished in the ATP-containing sample, whereas phosphorylation had little affect on the affinity of the Dam1 complex for microtubules itself (Fig. 5 A). We next tested whether Ipl1 phosphorylation affected Ndc80 recruitment to dynamic microtubules in the TIRF assay. We found that recruitment of the Ndc80 complex to

discrete foci on the dynamic microtubule lattice was prevented by inclusion of Ipl1–Sli15 in an ATP-dependent manner (Fig. 5 B). Additionally, we found that a mutant Dam1 complex mimicking Ipl1 phosphorylation on four previously established sites (Dam1 S4D) recruited less Ndc80 than wild-type (Fig. 5 C), but was not as severely affected as the in vitro–phosphorylated complex, suggesting that additional Ipl1 phosphorylation sites on the Dam1 complex may contribute to the inhibition of Ndc80 recruitment. In summary, our results suggest that phosphorylation by Ipl1–Sli15 prevents the Dam1-dependent recruitment of the Ndc80 complex to stable and dynamic microtubules.

Conclusions

Our results reveal novel biochemical activities for the Dam1 complex and can explain how it is connected to the rest of the kinetochore. We show that the complex is an autonomous, continuous plus end tracker that recruits Ndc80 in a microtubule-dependent manner to dynamic plus ends. We speculate that the Dam1 complex may exploit its high affinity for GTP-tubulin to diffuse back to the plus end as the microtubule grows.

Furthermore, our results immediately explain several in vivo observations. First, in contrast to human cells, where deletion of the unstructured N terminus of Ndc80 leads to loss of kinetochore–microtubule attachments (Guimaraes et al., 2008; Miller et al., 2008), eliminating the corresponding part in the yeast Ndc80 complex has no effect on viability (Kemmler et al., 2009). Thus, severely crippling the microtubule-binding activity of Ndc80 does not prevent chromosome segregation, suggesting that the microtubule-binding activity provided by Dam1 is sufficient in this system. Second, localization of the Dam1 complex to centromeres, as assayed by chromatin immunoprecipitation, is both dependent on the Ndc80 complex and on microtubules (Li et al., 2002). This can be explained by the microtubule-dependent engagement that we observed in vitro. Our results support the notion that a mature kinetochore–microtubule interface is compositely formed from the centromere and the microtubule side. The role of the Dam1 complex is to provide end recognition and continued association, and the defined geometry with which the calponin homology domains of the Ndc80 complex emerge from microtubule lattice (Wilson-Kubalek et al., 2008) allows the connection to the rest of the kinetochore via the Spc24/25 heads. Future experiments include a detailed structural investigation of the Dam1–Ndc80 interface and a mechanistic understanding of the microtubule-specific interaction between these complexes.

Materials and methods

Yeast genetics

All Westermann laboratory strains are derived from strain S288C. Standard procedures were applied to genetically modify strains.

Live cell imaging

Cells expressing *Dam1-3xGFP* and *mCherry-Tub1* (FLY26: *MAT* α, *lys2-801*, *ade2-1*, *leu2*, *cdc20::TRP1::GAL1/10-CDC20*, *mCherry-tubulin::URA3*, and *Dam1-3xGFP::HIS3*; or FLY48: *MAT a*, *lys2-801*, *ade2-1*, *leu2*, *cdc20::TRP1::GAL1/10-CDC20*, *mCherry-tubulin::URA3*, *Dam1-3xGFP::HIS3*, and *pGal-3xHA-Bim1::HIS3*) were arrested in metaphase for 5 h in synthetic medium containing 2% glucose. Time-lapse images were collected at ambient temperature (21°C) using live cell microscopy (DeltaVision; Applied Precision), a UPlanSApo 100× NA 1.40 oil immersion objective lens (Olympus), and a charge-coupled device (CCD) camera (CoolSnap HQ; Photometrics). Z stacks (0.5 µm) were acquired in 20–30-s intervals, subsequently deconvoluted, projected to two-dimensional images (SoftWoRx software; Applied Precision), and further analyzed by MetaMorph (MDS Analytical Technologies) or ImageJ (National Institutes of Health) software.

Purification of recombinant complexes from bacteria

Expression, purification, and labeling of the Dam1 complex were performed as previously described (Westermann et al., 2005). The two subcomplexes of the Ndc80 complex (Ndc80p–6xHis/Nuf2p–EGFP or $_{\Delta N1\text{-}116}$–Ndc80p–6xHis/Nuf2p–EGFP, Spc24p–6xHis/Spc25p) were separately expressed from the pETDuett or pACYCDuet-1 vectors (EMD). Both plasmids were cotransfected into BL21 DE3 (EMD). Bacteria were grown to OD_{600} = 0.6 at 37°C, induced with 0.2 mM IPTG, and grown for 12–15 h at 18°C. The two subcomplexes were eluted with 150 mM NaCl, 10 mM Hepes, pH 7.0, and 250 mM imidazol from the Ni-NTA beads then subjected to in vitro reconstitution of the full-length Ndc80 complex and further purified on the Superdex 200 HiLoad 16/60 (GE Healthcare). Gel filtration was conducted in 150 mM NaCl and 10 mM Hepes, pH 7.

Microtubule-binding assays

The microtubule cosedimentation assay was performed as described previously (Cheeseman et al., 2001a). Purified Ndc80–EGFP and –Dam1 complexes were precleared and added to a final concentration of 0.4–0.5 µM to taxol-stabilized microtubules. The salt concentration was adjusted to 20, 25, 50, or 100 mM NaCl. Quantification was performed as previously described (Zimniak et al., 2009). To determine apparent K_D for Ndc80–EGFP complex binding to microtubules, data points were fitted into the equation $Y = B_{max} \times X/(K_D + X)$ using Prism (version 4.0; GraphPad Software, Inc.).

Analytical gel filtration

Ndc80 and the Dam1 complex were mixed in an equimolar ratio at 5.5 µM and incubated for 10 min at RT. 0.5 ml was loaded onto the Superdex 200 HiLoad 16/60. Proteins were eluted in buffer containing 100 mM NaCl and 10 mM Hepes, pH 7.

In vitro reconstitution of a plus end–tracking system

Flow cells were constructed using silanized glass slides, two double-sided tapes, and precleaned coverslips. Resulting chambers were blocked with 5 mg/ml biotinylated BSA (Vector Laboratories) for at least 3 h and subsequently washed with BRB80 buffer. Afterward, a solution of 0.3 mg/ml avidin DN (Vector Laboratories) in BRB80 was introduced for at least 20 min and exchanged for a blocking solution containing 0.1% pluronic F-127 (Sigma-Aldrich) in BRB80 (Westermann et al., 2006; Zimniak et al., 2009). Rhodamine-labeled short GMPCPP (2′-deoxy-guanosince-5′-[(α,β)-methyleno]triphosphate) microtubule seeds were introduced and incubated for 30 s followed by a wash with wash buffer (BRB80 supplemented with 150 mM KCl, 1 mM GTP, 0.5% [vol/vol] β-mercaptoethanol, 4.5 µg/ml glucose, 200 µg/ml glucose oxidase, and 35 µg/ml catalase). Microtubule growth was induced by introducing a reaction mix composed of 14 µM tubulin (unlabeled or 1 µM labeled with rhodamine), 150 mM KCl, 0.6 mM GTP, 0.13% (wt/vol) methylcellulose, 0.33 mg/ml casein, 0.5% (vol/vol) β-mercaptoethanol, 4.5 µg/ml glucose, 200 µg/ml glucose oxidase, 35 µg/ml catalase, and 100 nM Dam1–Alexa Fluor 488 complex. Time-lapse videos were recorded at 30°C using 4–5-s intervals between frames. Image acquisition was performed using the TIRF3 microscopy system operated with AxioVision software (Carl Zeiss, Inc.), a 100× Plan Apochromat 1.46 NA objective, and an EM CCD camera (C9100-02; Hamamatsu Photonics). For streaming videos, concentration of free tubulin was increased to 20 µM and the time resolution to 400 ms/frame. For Ndc80–EGFP (300 nM) and Dam1–Alexa Fluor 594 (10 nM labeled + 90 nM unlabeled Dam1 complex) experiments, we used coverslips grafted with polyethylene glycol biotin, 100 mM KCl, and an EM CCD camera (Cascade II; Photometrics).

In vitro phosphorylation of the Dam1 complex

0.5 µM recombinant Ipl1–Sli15 complex was incubated with 2.5 µM recombinant Dam1 wild-type complex in kinase buffer (20 mM Hepes, pH 7.5, 100 mM KCl, 10 mM $MgCl_2$, 25 mM β-glycerophosphate, and 1 mM DTT) in the presence or absence of 1 mM ATP. The reaction was performed at 30°C for 40 min.

EM

Short GMPCPP microtubule seeds were incubated for 5 min with a solution containing 14 µM tubulin, 150 mM KCl, 0.6 mM GTP, 0.33 mg/ml

casein, 0.5% (vol/vol) β-mercaptoethanol, 4.5 µg/ml glucose, 200 µg/ml glucose oxidase, 35 µg/ml catalase, and variable concentrations of the Dam1–Alexa Fluor 488 complex in BRB80 buffer. The reaction mix was placed on a carbon-coated grid, negatively stained with 2% uranyl acetate, and imaged immediately with an electron microscope operating at 80 kV (Morgagni; FEI) equipped with a CCD camera (Morada SIS; Olympus).

Online supplemental material

Fig. S1 addresses the oligomerization status of the Dam1 complex. Fig. S2 demonstrates that the N-terminal tail of Ndc80p is not essential for Dam1-dependent recruitment to microtubules. Fig. S3 shows that there is no interaction between the Ndc80 complex and the Dam1 complex in solution. Videos 1 and 2 visualize plus end tracking of the Dam1 complex in vivo. Video 3 shows that Dam1 tip localization is independent of the +TIP Bim1p. Videos 4–6 demonstrate autonomous microtubule plus end–tracking activity of the Dam1 complex in vitro. Video 7 displays plus end tracking of the Ndc80–EGFP complex in the presence of unlabeled Dam1 complex. Video 8 shows continuous tip tracking of the Ndc80–EGFP complex in the presence of unlabeled Dam1 complex. Video 9 demonstrates that the Dam1 complex and the Ndc80 complex colocalize on dynamic microtubule plus ends. Online supplemental material is available at http://www.jcb.org/cgi/content/full/jcb.200912021/DC1.

We wish to thank all members of the Westermann laboratory for discussions, Karin Aumayr and Pawel Pasierbek for help with TIRF microscopy and image analysis, and Carrie Cowan, René Ladurner, and Jan-Michael Peters for critical reading of the manuscript.

The research leading to these results has received funding from the European Research Council (ERC) under the European Community's Seventh Framework Program (grant FP7/2007-2013; ERC grant agreement 203499) and by the Austrian Science Fund (FWF; grant SFB F34-B03).

Submitted: 3 December 2009
Accepted: 16 April 2010

References

Akhmanova, A., and M.O. Steinmetz. 2008. Tracking the ends: a dynamic protein network controls the fate of microtubule tips. *Nat. Rev. Mol. Cell Biol.* 9:309–322. doi:10.1038/nrm2369

Asbury, C.L., D.R. Gestaut, A.F. Powers, A.D. Franck, and T.N. Davis. 2006. The Dam1 kinetochore complex harnesses microtubule dynamics to produce force and movement. *Proc. Natl. Acad. Sci. USA.* 103:9873–9878. doi:10.1073/pnas.0602249103

Bieling, P., L. Laan, H. Schek, E.L. Munteanu, L. Sandblad, M. Dogterom, D. Brunner, and T. Surrey. 2007. Reconstitution of a microtubule plus-end tracking system in vitro. *Nature.* 450:1100–1105. doi:10.1038/nature06386

Brouhard, G.J., J.H. Stear, T.L. Noetzel, J. Al-Bassam, K. Kinoshita, S.C. Harrison, J. Howard, and A.A. Hyman. 2008. XMAP215 is a processive microtubule polymerase. *Cell.* 132:79–88. doi:10.1016/j.cell.2007.11.043

Cheeseman, I.M., and A. Desai. 2008. Molecular architecture of the kinetochore-microtubule interface. *Nat. Rev. Mol. Cell Biol.* 9:33–46. doi:10.1038/nrm2310

Cheeseman, I.M., C. Brew, M. Wolyniak, A. Desai, S. Anderson, N. Muster, J.R. Yates, T.C. Huffaker, D.G. Drubin, and G. Barnes. 2001a. Implication of a novel multiprotein Dam1p complex in outer kinetochore function. *J. Cell Biol.* 155:1137–1145. doi:10.1083/jcb.200109063

Cheeseman, I.M., M. Enquist-Newman, T. Müller-Reichert, D.G. Drubin, and G. Barnes. 2001b. Mitotic spindle integrity and kinetochore function linked by the Duo1p/Dam1p complex. *J. Cell Biol.* 152:197–212. doi:10.1083/jcb.152.1.197

Cheeseman, I.M., J.S. Chappie, E.M. Wilson-Kubalek, and A. Desai. 2006. The conserved KMN network constitutes the core microtubule-binding site of the kinetochore. *Cell.* 127:983–997. doi:10.1016/j.cell.2006.09.039

Ciferri, C., S. Pasqualato, E. Screpanti, G. Varetti, S. Santaguida, G. Dos Reis, A. Maiolica, J. Polka, J.G. De Luca, P. De Wulf, et al. 2008. Implications for kinetochore-microtubule attachment from the structure of an engineered Ndc80 complex. *Cell.* 133:427–439. doi:10.1016/j.cell.2008.03.020

Gestaut, D.R., B. Graczyk, J. Cooper, P.O. Widlund, A. Zelter, L. Wordeman, C.L. Asbury, and T.N. Davis. 2008. Phosphoregulation and depolymerization-driven movement of the Dam1 complex do not require ring formation. *Nat. Cell Biol.* 10:407–414. doi:10.1038/ncb1702

Grishchuk, E.L., A.K. Efremov, V.A. Volkov, I.S. Spiridonov, N. Gudimchuk, S. Westermann, D. Drubin, G. Barnes, J.R. McIntosh, and F.I. Ataullakhanov. 2008a. The Dam1 ring binds microtubules strongly enough to be a processive as well as energy-efficient coupler for chromosome motion. *Proc. Natl. Acad. Sci. USA.* 105:15423–15428. doi:10.1073/pnas.0807859105

Grishchuk, E.L., I.S. Spiridonov, V.A. Volkov, A. Efremov, S. Westermann, D. Drubin, G. Barnes, F.I. Ataullakhanov, and J.R. McIntosh. 2008b. Different assemblies of the DAM1 complex follow shortening microtubules by distinct mechanisms. *Proc. Natl. Acad. Sci. USA.* 105:6918–6923. doi:10.1073/pnas.0801811105

Guimaraes, G.J., Y. Dong, B.F. McEwen, and J.G. Deluca. 2008. Kinetochore-microtubule attachment relies on the disordered N-terminal tail domain of Hec1. *Curr. Biol.* 18:1778–1784. doi:10.1016/j.cub.2008.08.012

Honnappa, S., S.M. Gouveia, A. Weisbrich, F.F. Damberger, N.S. Bhavesh, H. Jawhari, I. Grigoriev, F.J. van Rijssel, R.M. Buey, A. Lawera, et al. 2009. An EB1-binding motif acts as a microtubule tip localization signal. *Cell.* 138:366–376. doi:10.1016/j.cell.2009.04.065

Kemmler, S., M. Stach, M. Knapp, J. Ortiz, J. Pfannstiel, T. Ruppert, and J. Lechner. 2009. Mimicking Ndc80 phosphorylation triggers spindle assembly checkpoint signalling. *EMBO J.* 28:1099–1110. doi:10.1038/emboj.2009.62

Kiermaier, E., S. Woehrer, Y. Peng, K. Mechtler, and S. Westermann. 2009. A Dam1-based artificial kinetochore is sufficient to promote chromosome segregation in budding yeast. *Nat. Cell Biol.* 11:1109–1115. doi:10.1038/ncb1924

Lacefield, S., D.T. Lau, and A.W. Murray. 2009. Recruiting a microtubule-binding complex to DNA directs chromosome segregation in budding yeast. *Nat. Cell Biol.* 11:1116–1120. doi:10.1038/ncb1925

Li, Y., J. Bachant, A.A. Alcasabas, Y. Wang, J. Qin, and S.J. Elledge. 2002. The mitotic spindle is required for loading of the DASH complex onto the kinetochore. *Genes Dev.* 16:183–197. doi:10.1101/gad.959402

Miller, S.A., M.L. Johnson, and P.T. Stukenberg. 2008. Kinetochore attachments require an interaction between unstructured tails on microtubules and Ndc80(Hec1). *Curr. Biol.* 18:1785–1791. doi:10.1016/j.cub.2008.11.007

Miranda, J.J., P. De Wulf, P.K. Sorger, and S.C. Harrison. 2005. The yeast DASH complex forms closed rings on microtubules. *Nat. Struct. Mol. Biol.* 12:138–143. doi:10.1038/nsmb896

Powers, A.F., A.D. Franck, D.R. Gestaut, J. Cooper, B. Gracyzk, R.R. Wei, L. Wordeman, T.N. Davis, and C.L. Asbury. 2009. The Ndc80 kinetochore complex forms load-bearing attachments to dynamic microtubule tips via biased diffusion. *Cell.* 136:865–875. doi:10.1016/j.cell.2008.12.045

Santaguida, S., and A. Musacchio. 2009. The life and miracles of kinetochores. *EMBO J.* 28:2511–2531. doi:10.1038/emboj.2009.173

Shang, C., T.R. Hazbun, I.M. Cheeseman, J. Aranda, S. Fields, D.G. Drubin, and G. Barnes. 2003. Kinetochore protein interactions and their regulation by the Aurora kinase Ipl1p. *Mol. Biol. Cell.* 14:3342–3355. doi:10.1091/mbc.E02-11-0765

Tanaka, K., N. Mukae, H. Dewar, M. van Breugel, E.K. James, A.R. Prescott, C. Antony, and T.U. Tanaka. 2005. Molecular mechanisms of kinetochore capture by spindle microtubules. *Nature.* 434:987–994. doi:10.1038/nature03483

Tanaka, K., E. Kitamura, Y. Kitamura, and T.U. Tanaka. 2007. Molecular mechanisms of microtubule-dependent kinetochore transport toward spindle poles. *J. Cell Biol.* 178:269–281. doi:10.1083/jcb.200702141

Tien, J.F., N.T. Umbreit, D.R. Gestaut, A.D. Franck, J. Cooper, L. Wordeman, T. Gonen, C.L. Asbury, and T.N. Davis. 2010. Cooperation of the Dam1 and Ndc80 kinetochore complexes enhances microtubule coupling and is regulated by aurora B. *J. Cell Biol.* 189:713–723.

Wei, R.R., J. Al-Bassam, and S.C. Harrison. 2007. The Ndc80/HEC1 complex is a contact point for kinetochore-microtubule attachment. *Nat. Struct. Mol. Biol.* 14:54–59. doi:10.1038/nsmb1186

Westermann, S., A. Avila-Sakar, H.W. Wang, H. Niederstrasser, J. Wong, D.G. Drubin, E. Nogales, and G. Barnes. 2005. Formation of a dynamic kinetochore-microtubule interface through assembly of the Dam1 ring complex. *Mol. Cell.* 17:277–290. doi:10.1016/j.molcel.2004.12.019

Westermann, S., H.W. Wang, A. Avila-Sakar, D.G. Drubin, E. Nogales, and G. Barnes. 2006. The Dam1 kinetochore ring complex moves processively on depolymerizing microtubule ends. *Nature.* 440:565–569. doi:10.1038/nature04409

Westermann, S., D.G. Drubin, and G. Barnes. 2007. Structures and functions of yeast kinetochore complexes. *Annu. Rev. Biochem.* 76:563–591. doi:10.1146/annurev.biochem.76.052705.160607

Wilson-Kubalek, E.M., I.M. Cheeseman, C. Yoshioka, A. Desai, and R.A. Milligan. 2008. Orientation and structure of the Ndc80 complex on the microtubule lattice. *J. Cell Biol.* 182:1055–1061. doi:10.1083/jcb.200804170

Wong, J., Y. Nakajima, S. Westermann, C. Shang, J.S. Kang, C. Goodner, P. Houshmand, S. Fields, C.S. Chan, D. Drubin, et al. 2007. A protein interaction map of the mitotic spindle. *Mol. Biol. Cell.* 18:3800–3809. doi:10.1091/mbc.E07-06-0536

Zimniak, T., K. Stengl, K. Mechtler, and S. Westermann. 2009. Phosphoregulation of the budding yeast EB1 homologue Bim1p by Aurora/Ipl1p. *J. Cell Biol.* 186:379–391. doi:10.1083/jcb.200901036